International Journal of
Molecular Sciences

MDPI

Review

Unsaturated Macrolactones from Renewable Feedstocks: Synthesis, Ring-Opening Polymerization and Application Prospects

Ilya Nifant'ev [1,2,*], Anna Afanaseva [1,3], Alexander Vinogradov [1] and Pavel Ivchenko [1,2,*]

[1] A.V. Topchiev Institute of Petrochemical Synthesis RAS, 29 Leninsky Pr., 119991 Moscow, Russia; aan.naa00@mail.ru (A.A.); amvvin@mail.ru (A.V.)
[2] Chemistry Department, M.V. Lomonosov Moscow State University, 1 Leninskie Gory Str., Building 3, 119991 Moscow, Russia
[3] Faculty of Chemistry, National Research University Higher School of Economics, Myasnitskaya Str. 20, 101100 Moscow, Russia
* Correspondence: ilnif@yahoo.com or inif@org.chem.msu.ru (I.N.); phpasha1@yandex.ru or inpv@org.chem.nsu.ru (P.I.); Tel.: +7-495-939-4098 (P.I.)

Abstract: Unsaturated macrolactones (UMs) have long attracted researchers' attention due to a combination of a reactive ester fragment and C=C bond in their structures. UMs of natural origin are comparatively few in number, and the task of developing synthetic approaches to new UMs is relevant. Recent advances in the synthesis of UMs cannot be dissociated from the progress in design of metathesis catalysts, since this catalytic approach is an atom-economy alternative to conventional organochemical methods. In the present review, we summarized and discussed the use of ring-closing metathesis, catalyzed by Ru and Group 6 metal complexes, in the synthesis of Ums and the advantages and shortcomings of the catalytic approach to UMs in comparison with organochemical methods. In a separate section, the use of UMs in the synthesis of unsaturated polyesters, the functionalization of these (co)polymers, and the prospects for practical use of the material obtained are also presented. It is essential that the actual approaches to UMs are often based on the use of renewable feedstocks, thereby meeting Green Chemistry principles.

Keywords: carbene complexes; grafted polymers; metathesis; metathesis polymerization; molybdenum catalysts; polyesters; ring-opening polymerization; ruthenium catalysts; unsaturated macrolactones

Academic Editor: Haiyang Gao

Received: 7 April 2025
Revised: 13 May 2025
Accepted: 21 May 2025
Published: 23 May 2025

Citation: Nifant'ev, I.; Afanaseva, A.; Vinogradov, A.; Ivchenko, P. Unsaturated Macrolactones from Renewable Feedstocks: Synthesis, Ring-Opening Polymerization and Application Prospects. *Int. J. Mol. Sci.* **2025**, *26*, 5039. https://doi.org/10.3390/ijms26115039

1. Introduction

Unsaturated macrocyclic lactones (macrolactones, UMs) have long attracted the attention of researchers. As such, UMs are widely used as a components of perfume and cosmetic compositions [1]. At the same time, in recent years UMs are actively studied as (co)monomers in catalytic ring-opening transesterification polymerization (ROTEP) in order to obtain polyesters containing reactive C=C bonds in the main chain of (co)polymers [1,2]. Some UMs occur naturally in plants and animal organs [1]; however, further expansion of the range of similar compounds requires the development of new, atom-efficient and versatile synthetic approaches to these compounds.

Common organochemical approaches to UMs primarily use a lactonization reaction, intramolecular (trans)esterification with the formation of unsaturated cyclic esters (Scheme 1a) [3–5]. The ring-closing metathesis (RCM) of alkenyl alkenoates (Scheme 1b) represents an obvious alternative to macrolactonization [6–8], and that is the direction

that is being actively developed in recent years [7]. It is quite obvious that the metathesis of alkenyl alkenoates at high substrate concentrations mainly results in the formation of polymeric acyclic diene metathesis (ADMET) products (Scheme 1c), which in turn can be transformed into UMs by shifting the ring–chain equilibrium [9].

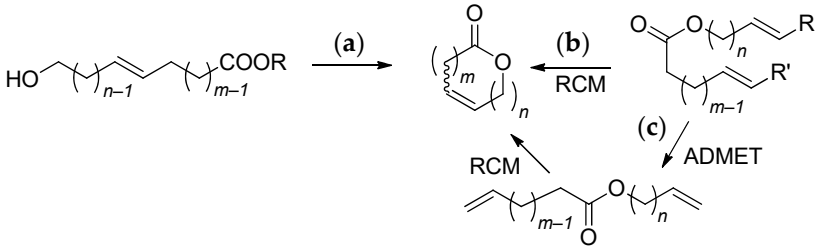

Scheme 1. Common synthetic approaches to unsaturated macrolactones: (**a**) intramolecular (trans)esterification and (**b**) ring-closing metathesis (RCM) of alkenyl alkenoates, including RCM of acyclic diene metathesis products (**c**).

In our review, we describe and discuss synthetic approaches to UMs, focusing on the preparation of natural macrolactones and the RCM of alkenyl alkenoates based on renewable feedstocks. To complete the picture, actual data on the RCM of other alkenyl alkenoates are summarized to reveal key patterns and prospects for this catalytic process. Particular attention is paid to the results of recent studies aimed at the design of new Ru-, Mo- and W-based RCM catalysts and the development of efficient preparative-scale RCM reactions. The use of UMs in cosmetics and perfumery is beyond the scope of our review, and the last part of the manuscript is devoted to the use of UMs in the synthesis of unsaturated polyesters and the applications of the (co)polymers obtained.

2. Synthesis of Unsaturated Macrolactones

The main problem for the further use of UMs, directly isolated from natural feedstocks, results from the variability in composition and structure of similar products. So, for example, commercial macrolactone globalide (formally corresponding to an oxacyclohexadec-12-en-2-one structure) is actually a mixture of positional and configurational isomers (Scheme 2) [10]. The use of other commercial names (e.g., habanolide) for the same product did not add clarity. First isolated in 1927 by M. Kerschbaum from ambrette (*Hibiscus abelmoschus*) seeds [11], ambrettolide (16-hexadec-7-enolide) was contained in the monoester fraction of ambrette seeds in an amount of 11 wt% (3.8‰ in dried seeds) along with 14-tetradec-5-enolide (0.5 wt%) and 18-octadec-9-enolide (7 wt%) [12], which makes them difficult to separate.

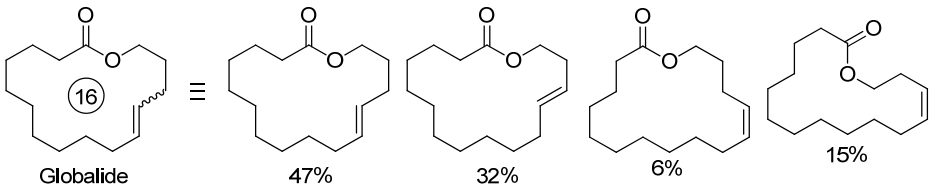

Scheme 2. The real composition of commercial UM globalide (habanolide) [10].

It is therefore apparent that the search for synthetic approaches to UMs has drawn researchers' attention. An additional incentive for studies in this field is the possibility of obtaining new, previously unknown substances. To date, a number of conventional organochemical approaches to macrolactones have been developed [3–5]; however, in recent years more and more attention has been given to the catalytic ring-closing metathesis (RCM) of alkenyl alkenoates [7,8].

2.1. Organochemical Approaches to Unsaturated Macrolactones

A detailed discussion of organochemical approaches to UMs is not a subject for the present review. Below, we consider some particular examples of the preparation of Ums, with their advantages, disadvantages and limitations.

The methods and approaches of classical organic chemistry are not always able to provide the required structural homogeneity. For instance, cyclohexadeca-1,8-diene was converted via the intermediate formation of the corresponding unsaturated ketones and subsequent Baeyer–Villiger oxidation (8 stages) to a mixture of 17-membered unsaturated lactones (total yield 9.5%) [13]. Back in 1980, the WCl_6/Me_4Sn-catalyzed cross-metathesis of methyl undec-10-enoate and $CH_2{=}CH(CH_2)_4OAc$, followed by hydrolysis and intramolecular esterification, was used in the synthesis of 15-membered unsaturated lactone; the yields of the reaction intermediates and final product were not reported [14]. Taking into account the statistical nature of cross-metathesis, this approach appears to be too costly.

The synthesis of Yuzu lactone was based on the product of the ozonolysis of methyl oleate (MO); its interaction with phosphonium salt and $KN(SiMe_3)_2$ resulted in the formation of a pure (*Z*)-isomer of O-protected unsaturated ester (Scheme 3a). Its saponification, bromination and cyclization led to the formation of the target product (total yield 34%, *Z*:*E* ratio 80:1) [15]. A number of (*Z*)-unsaturated lactones were prepared from tetrahydropyranyl derivatives of ω-hydroxy keto esters via the intermediate formation of macrolactones with an internal C≡C bond (Scheme 3b) [16]. ω-Hydroxyalkynyl carboxylic acid intermediate (n = 5, m = 8) can be used in the synthesis of ambrettolide, first performed in 1983 [17]. An alternative approach to ambrettolide was based on the Wittig reaction between ^{t}BuMe$_2$SiO(CH$_2$)$_8$CHO and [Ph$_3$P(CH$_2$)$_6$COOMe]Br, followed by the deprotection and intramolecular esterification of ω-hydroxyalkenyl acid (1 mM in cyclohexane) using lipase B (*Cattleya aurantiaca*) acrylic resin as a catalyst; after 3 h at 40 °C, the yield was 40% [18]. In a recent study of Guerrero-Morales and Collins, a preference for the biocatalytic route to macrolactones was demonstrated [19]. Although high yields in the macrolactonization of ω-hydroxyacids can be provided by the use of C_6F_5COCl via the intermediate formation of mixed anhydrides, high dilutions (~1.5 mM) are still needed [20].

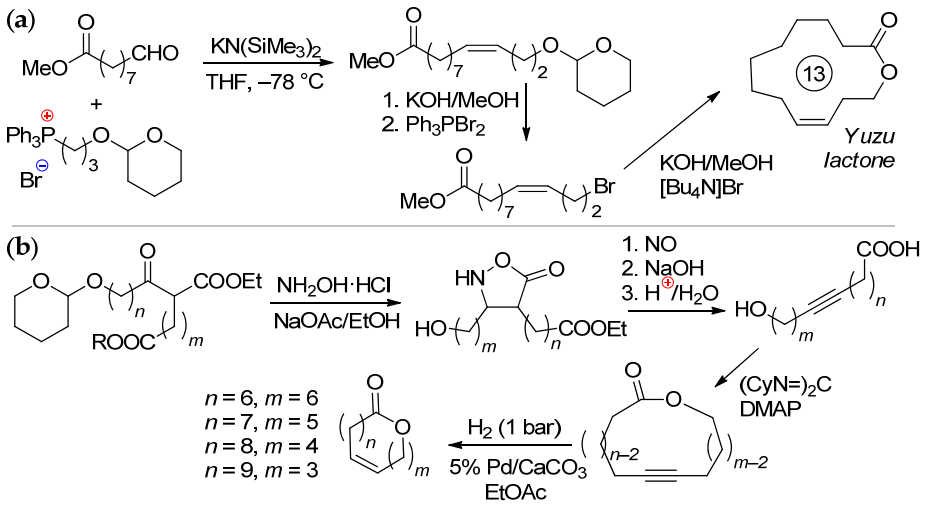

Scheme 3. Organochemical approaches to unsaturated macrolactones. (**a**) Preparation of the Yuzu lactone [15]. (**b**) (*Z*)-selective synthesis of 10-membered lactones [16].

Based on *threo*-aleuritic acid, a major ingredient of the *Laccifer lacca* natural shellac, (9*E*)-isoambrettolide was synthesized (total yield 72%, Scheme 4) [21].

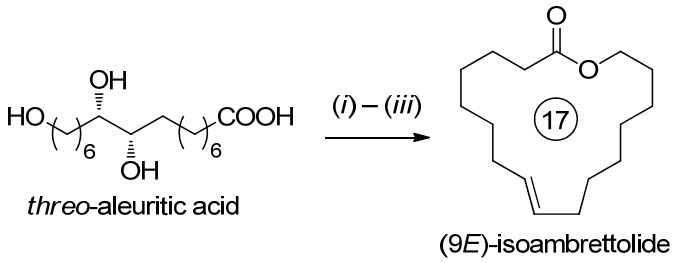

Scheme 4. Synthesis of (9*E*)-isoambrettolide. Reagents and conditions: (*i*) 2-methyl-6-nitrobenzoic anhydride, *N*,*N*-dimethylaminopytidine *N*-oxide/Et_3N in THF/CH_2Cl_2, 83%; (*ii*) 1,10-thiocarbonyldiimidazole/*N*,*N*-dimethylaminopytidine, toluene, 110 °C, 91%; (*iii*) $P(OMe)_3$, 140 °C, 87% [21].

Among other organochemical approaches to different UMs, the synthesis of 16-membered macrolactone impresses with its simplicity and the availability of the starting compound, dodecahydro-2*H*-cyclododeca[*b*]pyran [22]. The corresponding hydroperoxide was converted into corresponding UMs with high yields (Scheme 5) [23,24].

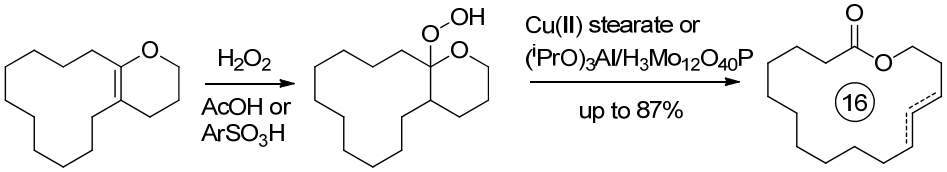

Scheme 5. Synthesis of 16-membered UMs from dodecahydro-2*H*-cyclododeca[*b*]pyran [23,24].

Except for the last approach, which has severe limitations on the substrate and corresponding product, organochemical methods of the synthesis of UMs are complex, have a low atom efficiency and are unable to provide preparations of the wide spectrum of macrolactones. At first glance, the ring-closing metathesis of alkenyl alkenoates appears to be more convenient and versatile, but certain difficulties arise when using RCM for macrolactonization.

2.2. The Basic Patterns of Ring-Closing Metathesis

Scheme 6 reflects the main processes involving alkenyl alkenoates in the presence of metathesis catalysts, metal carbene complexes. The substrates can react with a formation of UMs (RCM, intramolecular process) or oligomers/polymers, the products of acyclic diene metathesis polymerization (ADMET, intermolecular process). To minimize the formation of oligomers, the reaction should be conducted according to the Ruggli–Ziegler high dilution principle, with a substrate concentration ~1 $mmol \cdot L^{-1}$ (mM). The nature of the catalyst is essential for achieving the high productivity and selectivity of the process. The nature of the substrate is also important; however, alkenyl esters of both oleic acid and ω-unsaturated acids (dec-9-enoic, undec-10-enoic, etc.) are very attractive for using in RCM due to the high synthetic availability of these substrates. In particular, methyl oleate (MO) is the main component of fatty acid methyl esters (FAMEs) obtained by the methanolysis of high-oleic plant oils [8], undec-10-enoic acid is produced industrially from castor oil [25], and methyl dec-9-enoate can be obtained by the ethenolysis of MO [26–28]. It is these alkenyl esters that are of the greatest interest as a part of this review.

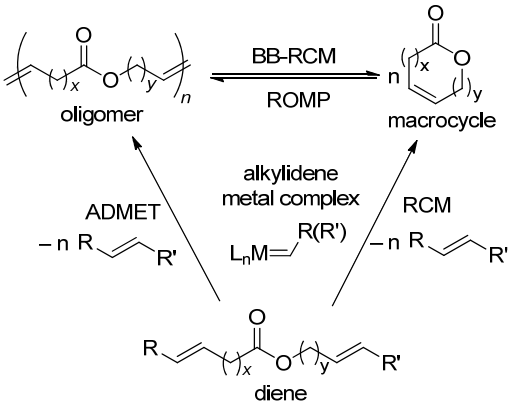

Scheme 6. Transformations of alkenyl alkenoates in the presence of metathesis catalysts.

In contrast to the industrially implemented cross-metathesis of ethylene and α-olefins, based on the use of moderately active catalysts under harsh conditions [29], the RCM of alkenyl alkenoates requires the use of active catalysts, carbene complexes of Ru and Mo. It should be noted though that Ru- and Mo-catalyzed RCM at elevated temperatures, with the distillation of the reaction products, was developed in recent years (see Section 2.4).

The high catalytic activity of Ru and Mo carbene complexes also has a reverse side, which is that the active catalysts have increased sensitivity to substrate impurities, moisture and air, and the progress in RCM was inextricably linked with the common progress in the design of chemically stable metathesis catalysts. The structural formulas of Ru complexes, studied in the RCM of alkenyl alkenoates and related substrates, are presented in Scheme 7. The first-generation Grubbs catalysts **Ru1**–**Ru4** (Grubbs I, G-I) turned out to be relatively unstable; the Grubbs II (G-II) catalysts **Ru6**–**Ru8** and **Ru10**, as well as the Hoveyda–Grubbs II (HG-II) catalyst **Ru14**, showed better results (see Section 2.3.1). Even more efficient RCM catalysts have been synthesized and studied in recent years (see Sections 2.3 and 2.4). The Group 6 metal (Mo, W)-catalyzed RCM of alkenyl alkenoates was the subject of a few studies (see Section 2.5).

The presence of the ester group in the substrate molecule could help to promote or hinder RCM. For example, in the presence of **Ru2** (4 mol%), hex-5-enyl undec-10-enoate formed 16-membered lactone with a 79% yield, whereas octadeca-1,17-diene formed oligomers (Scheme 8a) [30]. This observation can be explained by the additional coordination of >C=O at the Ru center, which creates a 'template' for cyclization [31]. At the same time, the presence of a relatively short $(CH_2)_n$ fragment between the ester group and double bond may result in catalyst inhibition due to the formation of stable chelates (Scheme 8b) [31–33]. A partial solution to the problem was the addition of $Ti(O^iPr)_4$ that degrades chelate by the formation of the more stable >C=O···Ti bond [32]. In this way, the lengths of hydrocarbon spacers between ester group and C=C bonds affect the yield and selectivity of the RCM, and the synthetic availability of the UMs depends largely on the ring size (see Section 2.3.3).

Another important aspect of RCM is regio- and stereoselectivity [34]. The migration of the C=C bond during the reaction is caused by decomposition of the catalyst, with the formation of low-valent species capable of activating C–H bonds. The stereoselectivity ((*Z*)-/(*E*)- ratio) depends on the relative stability of the diastereomers; for lengthy Ums, (*Z*)-isomers are thermodynamically less stable than the corresponding (*E*)-isomers [34]. The nature of the catalyst can also affect the stereoselectivity, and studies in this area were actively carried out in 2000s [35] and are continuing at present (see Section 2.4).

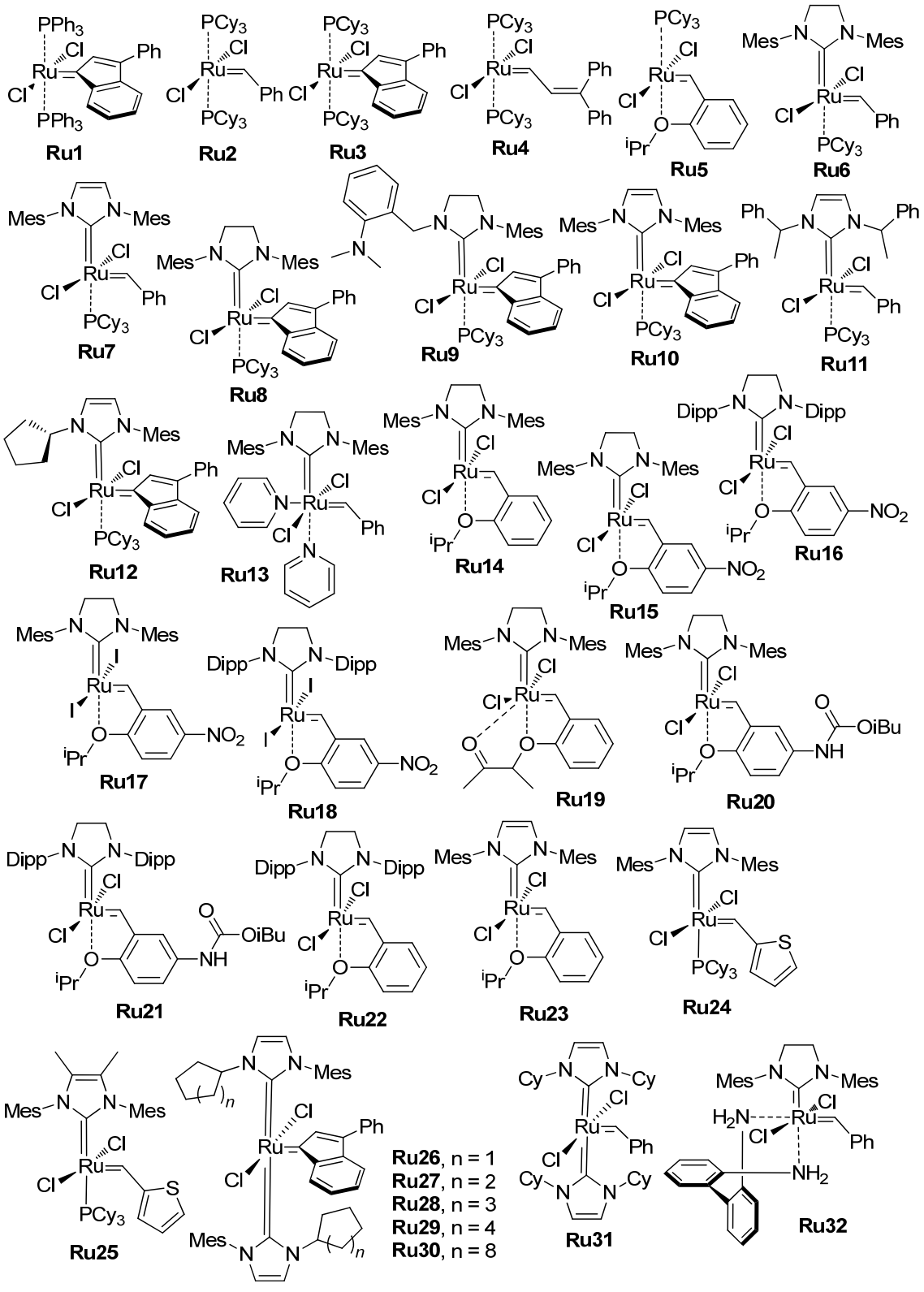

Scheme 7. *Cont.*

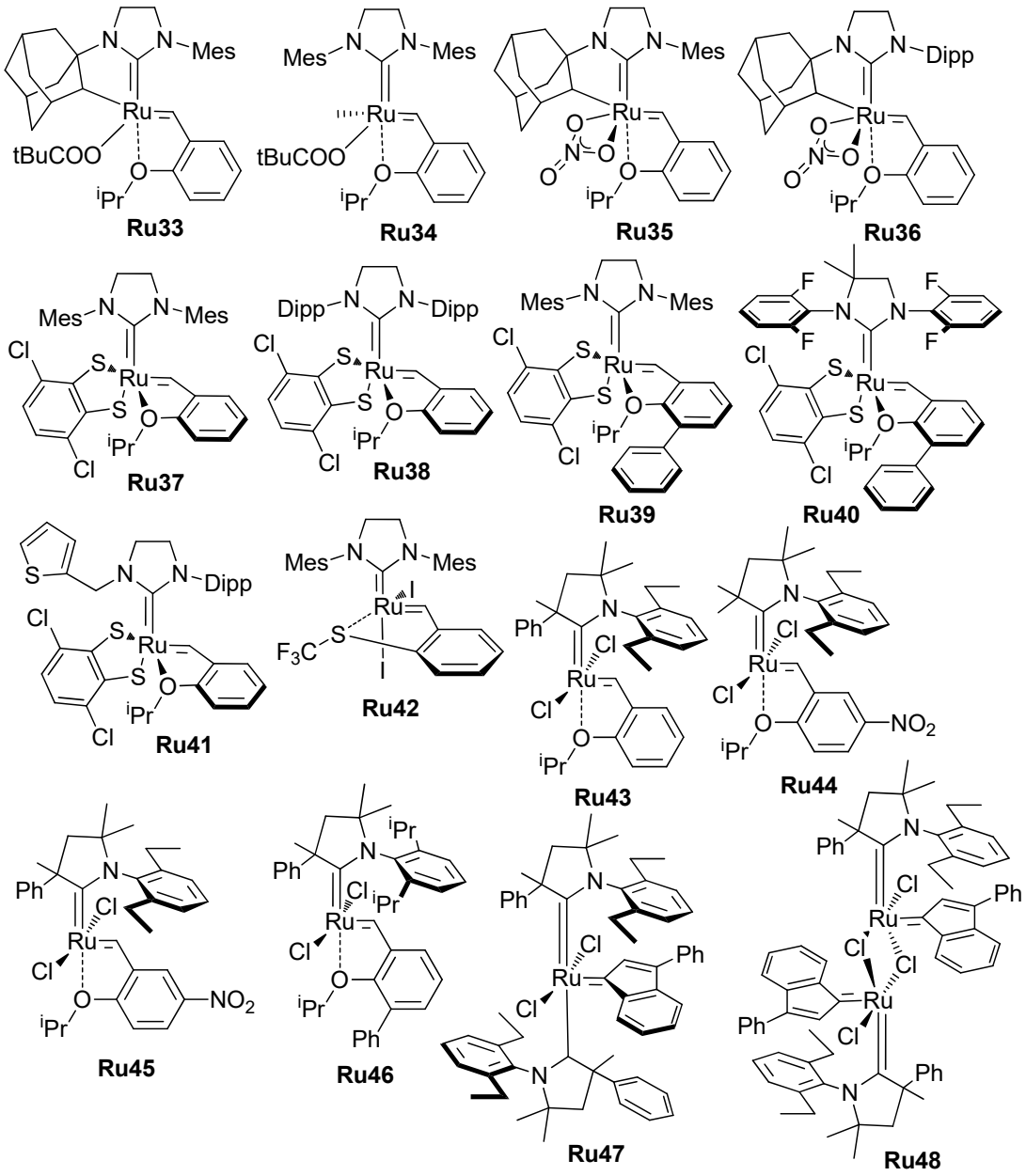

Scheme 7. Ru catalysts studied in RCM of alkenyl alkenoates.

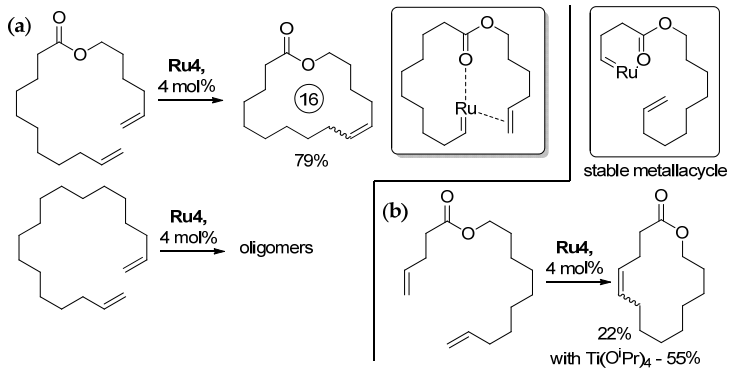

Scheme 8. (**a**) Successful RCM of hex-5-enyl undec-10-enoate due to the presence of the ester group and intermediate >C=O···Ru coordination [30]. (**b**) Formation of stable chelate that hinders RCM and the positive effect of the addition of $Ti(O^iPr)_4$ [32].

In addition to spacing between the ester fragment and C=C bonds, the type of the alkenyl fragments in the substrate is important: when alkenyl alkenoate represents α,ω-diene, ethylene is a product of the RCM process. The formation of ethylene, with its subsequent elimination from the reaction mixture, would favor the RCM process. On the other hand, the intermediate formation of $L_nRu{=}CH_2$ species can promote decomposition of Ru-based catalysts [36]. Generally, decomposition of Ru-based catalysts [37] can occur in two pathways, via bimolecular decomposition involving $L_nRu{=}CH_2$ species and bimolecular coupling (Scheme 9a) or via β-hydride elimination (Scheme 9b), and the rate of decomposition directly depends on the ligand environment of the Ru center. Ru hydride complexes can also be formed during decomposition of the catalysts; similar species are also considered as C–H activation and C=C bond isomerization catalysts [38]. Combined experimental and theoretical studies of different Ru complexes revealed the lower stability of cyclic alkyl amino carbene (CAAC) complexes (for example, **Ru43**) in comparison with *N*-heterocyclic carbene (NHC) derivatives (HG-II complex **Ru14** and its analogs) in bimolecular decomposition. On the other side, CAAC-Ru complexes turned out to be more resistant to β-H elimination in comparison with NHC-Ru catalysts [39]. The influence of the nature of alkenyl fragments in substrate (terminal or not) on the yield of the UMs and reaction selectivity is discussed in Section 2.3.2.

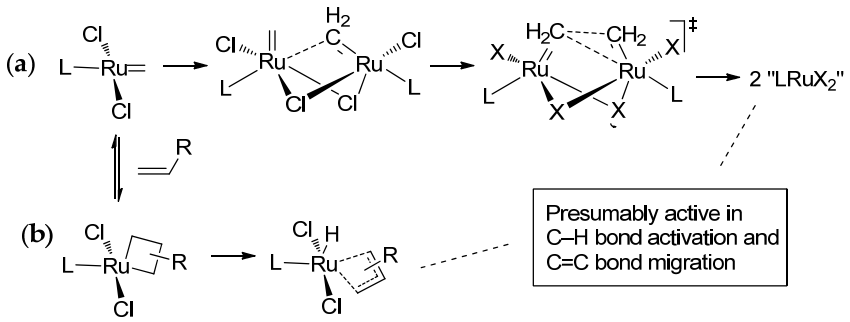

Scheme 9. Mechanisms of decomposition of Ru metathesis catalysts, (**a**) via formation of $L_nRu{=}CH_2$ species and (**b**) via β-hydride elimination [36,39].

To prevent isomerization, the use of different additives, e.g., chlorinated solvents [40], Brønsted acids [41] and substituted benzoquinones (for example, 2,3,5,6-tetrafluorocyclohexa-2,5-diene-1,4-dione, TFQ) [42,43], was proposed.

Numerous studies, aimed at the development of highly active and/or highly selective metathesis catalysts bearing in mind the mechanistic features of the process, have been conducted. A number of key patterns have been identified for simpler substrates, e.g., olefins. In particular, even in 2009 Schrock, Hoveyda and coll. revealed the impact of the bulky phenolate fragment in Mo carbene complexes on (*Z*)-selectivity in the homocoupling of α-olefins, attributed to the preference of the formation of less sterically hindered metallacyclic intermediates with *syn*-configuration than that form (*Z*)-alkene [44]. The appplicability of this approach to the synthesis of (*Z*)-UMs using Mo and W catalysts was demonstrated in later studies [45,46]. $M{=}CH_2$ species promote secondary (*Z*)-alkene isomerization, and the elimination of ethylene is crucial for the high (*Z*)-stereoselectivity of RCM [46].

For Ru-based catalysts, the formation of constrained geometry centers with an unequal ligand environment provided a higher (*Z*)-selectivity. Examples of (*Z*)-selective Ru catalysts include **Ru35** and **Ru36** [47,48]; the further studies of (*Z*)-selective catalytic systems are discussed in Section 2.3.4.

It should be noted that, according to reference [49], the formation of UMs may be preceded by the formation of oligomeric ADMET products that will subsequently form macrocycles via backbiting RCM. As can be seen in Figure 1, in the presence of **Ru7** (5 mol%), a reduction in the concentration of oligomer is accompanied by a proportional increase in the concentration of 16-membered unsaturated lactone. This transformation takes place in time, making it important to increase the stability of the catalysts.

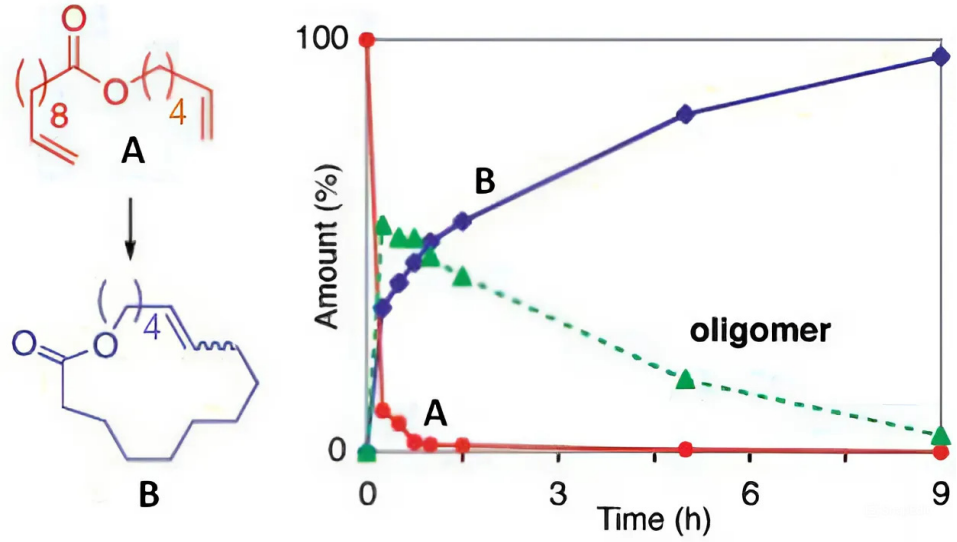

Figure 1. Metathesis of CH_2=CH$(CH_2)_8$COO$(CH_2)_4$CH=CH_2 (5 mol% **Ru7**): substrate conversion (A, red) and the content of oligomers (green) and RCM product (B, blue) in the reaction mixture over time. Adopted with permission from [49]. Copyright (2007) American Chemical Society.

2.3. Ru-Catalyzed Ring-Closing Metathesis of Alkenyl Alkenoates at High Dilution Ratios

2.3.1. Early Studies of Ru-Catalyzed RCM

During the late 1990s, some Ru-based catalysts were investigated. In 1996, Fürstner and Langemann synthesized isomeric 16-membered lactones from CH_2=CH$(CH_2)_8$COO$(CH_2)_4$CH=CH_2 and CH_2=CH$(CH_2)_4$COO$(CH_2)_8$CH=CH_2, in the presence of **Ru4** (4 mol%), with yields of 79 and 62%, respectively [50]. The same authors a year later showed that corresponding α,ω-dienes under similar conditions formed oligomers [30]. The cyclization of CH_2=CH$(CH_2)_2$COO$(CH_2)_8$CH=CH_2 (5 mol% of **Ru4**) proceeded with a 22% yield that was increased to 55% when Ti(O^iPr)$_4$ (5 mol%) was added (Scheme 8b) [32].

The RCM of CH_2=CH$(CH_2)_n$COO$(CH_2)_9$CH=CH_2 (n = 7, 8), catalyzed by **Ru4** (1 mol%, C_6H_6, 60 °C), resulted in the formation of 20-membered (Z/E 57:43) and 21-membered (Z/E 60:40) macrolactones; the yields were 83 and 82%, respectively. ω-Alkenyl oleates gave 19- and 20-membered (Z/E 71:29) lactones with 65 and 63% yields. The concentrations of substrates were 5–7 mM [51]. Of undoubted interest are the results of comparative studies of the RCM of CH_2=CH$(CH_2)_n$COO$(CH_2)_{10-n}$CH=CH_2 (2 mM in CH_2Cl_2, 2 mol% **Ru4**), with the formation of 14-membered lactones [52]. As indicated in Table 1, maximum yields were achieved when using alkenyl alkenoate with C=C fragments equidistant from the ester group. Calculations of the relative strain of diastereomers using the MicroModel 4.5 program [53] showed that the (Z)/(E) ratio in most cases is determined by the relative stability of isomers. It should also be noted that allyl ester turned out to be inert in RCM.

Table 1. Formation of 14-membered MLs via RCM of CH_2=CH$(CH_2)_n$COO$(CH_2)_{10-n}$CH=CH_2 (2 mM in CH_2Cl_2) catalyzed by **Ru4** (2 mol%) [52].

n	Time, h	Yield (Recovered Substrate), %	(*Z*)/(*E*) Ratio	Calc. (*Z*)/(*E*) Ratio [1]
1	30	11 (41)	50:50	4:96
2	31	45 (13)	18:82	1:99
3	20	47 (26)	77:23	65:35
4	6	75 (5)	44:56	35:65
5	30	62 (11)	1:99	4:96
6	20	31 (28)	41:59	36:64
7	1.5	63 (9)	27:73	41:59
8	31	70 (5)	13:87	5:95
9	30	0 (66)	–	35:65

[1] Calculated using MicroModel 4.5 [53].

The RCM of CH_2=CH$(CH_2)_8$COO$(CH_2)_n$CH=CH_2 (n = 4, 9) revealed the difference between **Ru11** and **Ru31**: the former was more efficient in the synthesis of 21-membered lactone, whereas the latter catalyzed cyclization to 16-membered lactone with a higher yield [54]. Double-bond isomerization with the formation of 20-membered lactone was detected back in 2000 in the example of CH_2=CH$(CH_2)_8$COO$(CH_2)_9$CH=CH_2 and **Ru7** [**40**]. A study of the influence of the type of alkenyl fragment (terminal or internal) in CH_2=CH$(CH_2)_8$COO$(CH_2)_2$CH=CHR (3 mM in CH_2Cl_2) on conversion and the (*Z*)/(*E*) ratio was also carried out in 2000 with the use of **Ru2** and **Ru6** (0.5–5 mol%); near quantitative yields were reported for **Ru6** without kinetic selectivity control [55]. At early stages of the studies, the use of supercritical CO_2 was proposed for the RCM of CH_2=CH$(CH_2)_8$COO$(CH_2)_4$CH=CH_2 (2.7 mM); in the presence of **Ru4** (1 mol%) an 88% yield was achieved after 72 h at 40 °C [56].

In the 2000s, there was a decline in researchers' interest in the RCM of alkenyl alkenoates; the only article [57] was devoted to the synthesis of alkenyl alkenoates CH_2=CH$(CH_2)_n$COO$(CH_2)_{n+1}$CH=CH_2 (n = 3–16) from CH_2=CH$(CH_2)_n$CHO by the Tishchenko reaction (^{i}Bu$_2$AlH), followed by G-I (10 mol%)-catalyzed RCM. An increasing interest in RCM was observed in the 2010s and in recent years, with the development of new types of metathesis catalysts (see below).

2.3.2. Different Ru Catalysts in RCM of Hex-5-en-1-yl Undec-10-enoate

Since the yield and selectivity of RCM depend not only on catalysts but also on the type of substrate (the length of $(CH_2)_n$ spacers between the ester group and C=C fragment, terminal or internal C=C bond), comparison of the catalysts makes sense when the same substrate is used in different experiments. Due to the high availability of undec-10-enoic acid, a large number of works were devoted to the study of the RCM of CH_2=CH$(CH_2)_8$COO$(CH_2)_4$CH=CH_2 [33,41,49,50,54,58–66]. The results of these studies are summarized in Table 2.

Table 2. Experimental data on ring-closing metathesis of CH_2=CH$(CH_2)_8$COO$(CH_2)_4$CH=CH_2.

Catalyst	Substr. Conc., mM	Catalyst, mol%	Solvent	Time, h	T, °C	Conv., %	Yield, %	(*Z*)/(*E*) Ratio	Ref.
Ru2	10	1	EtOAc	4	70	– [1]	<5	20:80	[41]
Ru3	10	1	EtOAc	4	70	–	<5	20:80	[41]
Ru4	4.8	4	CH_2Cl_2	24	20	–	79	–	[50]
Ru4	2.7	1	supercritical CO_2, d = 0.62 g·mL^{-1}	72	40	–	88	–	[56]
Ru5	5	0.05	C_6H_6	1; 4	40	12; 31	5; 21	–	[58]
Ru6	10	1	EtOAc	4	70	–	83	20:80	[41]

Table 2. *Cont.*

Catalyst	Substr. Conc., mM	Catalyst, mol%	Solvent	Time, h	T, °C	Conv., %	Yield, %	(*Z*)/(*E*) Ratio	Ref.
Ru6	5	0.003; 0.03	toluene	40 min	70	17; 99	12; 98	–; 24:76	[59]
Ru7	100; 5	5	CH_2Cl_2	0.25; 5	40	85; 99	10; 99	28:72	[49]
Ru8	10	1	EtOAc	4	70	–	79	20:80	[41]
Ru9	10	3	toluene (in air)	1.5	50	–	72	23:77	[60]
Ru10	8	0.0075	toluene	–	80	100	83	24:76	[61]
Ru11	--	2	CH_2Cl_2	19	40	–	72	24:76	[54]
Ru12	10	1	EtOAc	4	70	–	31	20:80	[41]
Ru13	5	5	CH_2Cl_2	1	22	–	–	–	[49]
Ru14	5	0.05	C_6H_6	1; 4	40	48	24; 33	–	[58]
Ru14	10	1	EtOAc	4	70	–	79	20:80	[41]
Ru15	10	1	EtOAc	4	70	–	42	20:80	[41]
Ru15	5	0.05	toluene; toluene 0.1% H_2O	2	20	93; 43	87; 30	22:78	[62]
Ru15	5	1; 0.1	C_6H_6	1	20	100; 91	92; 80	22:78	[33]
Ru15	5	0.3	toluene with C_2H_4 rem.; toluene	2	70	77; 5	54; 4	26:74	[63]
Ru15	5	0.3	toluene	0.7	70	10	7	–	[59]
Ru16	5	0.3	toluene with C_2H_4 rem.; toluene	2	70	77; 8	69; 7	29:71	[63]
Ru16	5	0.3	toluene	20 min	70	5 ± 2	5 ± 2	–	[59]
Ru16	5	2.5	EtOAc	5	80	99	17	–	[67]
Ru17	5	0.05	toluene; toluene 0.1% H_2O	2	20	92; 72	85; 62	28:72; 30:70	[62]
Ru17	5	0.3	toluene with C_2H_4 rem.; toluene	2	70	98; 87	91; 77	24:76; 73:27	[63]
Ru18	5	0.3	toluene with C_2H_4 rem.; toluene	2	70	90	85; 7	30:70	[63]
Ru19	10	1	EtOAc	4	70	–	43	20:80	[41]
Ru20	10	1	EtOAc	4	70	–	70	20:80	[41]
Ru21	10	1	EtOAc	4	70	–	76	20:80	[41]
Ru23	5	0.05	C_6H_6	1; 4	40	39; 56	29; 40	–	[58]
Ru24	8	0.0075	toluene with C_2H_4 rem.	–	80	100	88	25:75	[61]
Ru24	5	0.003	toluene	20 min	70	<1	<0.5	–	[59]
Ru25	8	0.005	toluene with C_2H_4 rem.	–	80	92	80	24:76	[61]
Ru26	10	1	EtOAc	29	70	–	<5		[41]
Ru26	10	1	EtOAc	4	100	–	8	20:80	[41]
Ru26	10	1	EtOAc; 20 mol% 1 M HCl	4	100	–	88/80 [2]	20:80	[41]
Ru26	10	1	EtOAc; 10 mol% 1 M HCl	4	100	–	90/76	30:70	[41]
Ru26	10	0.1	EtOAc; 5 mol% 1 M HCl	4	100	–	88/76	20:80	[41]
Ru26	10	0.05	EtOAc; 2.5 mol% 1 M HCl	4	100	–	90/78	20:80	[41]
Ru26	20	0.05	EtOAc; 2.5 mol% 1 M HCl	4	100	–	76/67	20:80	[41]
Ru26	10	0.05	Me-THF; 2.5 mol% 1 M HCl	4	100	–	91/73	20:80	[41]
Ru26	10	0.05	$(EtO)_2CO$; 2.5 mol% 1 M HCl	4	100	–	13/7	20:80	[41]
Ru26	10	0.05	iPrOH; 2.5 mol% 1 M HCl	4	100	–	26/20	20:80	[41]
Ru27	10	1	EtOAc; 2.5 mol% 1 M HCl	4	100	–	95/72	30:70	[41]
Ru28	10	1	EtOAc; 2.5 mol% 1 M HCl	1	100	–	93/73	40:60	[41]
Ru29	10	1	EtOAc; 2.5 mol% 1 M HCl	1	100	–	90/70	30:70	[41]
Ru30	10	1	EtOAc; 2.5 mol% 1 M HCl	4	100	–	93/73	30:70	[41]

Table 2. *Cont.*

Catalyst	Substr. Conc., mM	Catalyst, mol%	Solvent	Time, h	T, °C	Conv., %	Yield, %	(*Z*)/(*E*) Ratio	Ref.
Ru31	--	4	CH_2C1_2	55	40	–	81	24:76	[54]
Ru32	5	0.05	toluene 0; 0.01; 0.1 vol.% H_2O	2	20	91; 49; 3	86; 36; 3	22:78–33:63	[62]
Ru32	5	1; 0.1	C_6H_6	1	20	100; 95	100; 85	22:78	[33]
Ru32	5	0.1	C_6H_6	0.25	60	99	66	24:76	[33]
Ru32	5	0.05	C_6H_6	2	23	75	72	–	[64]
Ru35	5	0.5	toluene 0; 0.1 vol.% H_2O 0.01 bar	2	60	68; 31	64; 25	83:17; 85:15	[62]
Ru37	5	5	toluene 0; 0.1 vol.% H_2O 0.01 bar	2	60	44; 52	17; 17	75:25; 70:30	[62]
Ru43	5	0.05	C_6H_6	1; 4	40	86; 94	80; 90	–	[58]
Ru43	5	0.003	toluene	20 min	70	10	10	–	[59]
Ru43	5	0.05	toluene	2	80	100	87	–	[68]
Ru43	20	0.05	toluene	2	80	100	68	–	[68]
Ru44	5	0.003	toluene	20 min	70	6	4	–	[59]
Ru45	5	0.0045	toluene	20 min	70	99	98	34:66	[59]
Ru45	10	0.0015	toluene	20 min	70	94	85	34:66	[59]
Ru45	20	0.002	toluene	20 min	70	94	62	36:64	[59]
Ru45	5	0.01; 0.0045	C_6H_6	2	40; 70	100; 99	94; 98	–	[64]
Ru46	5; 10	0.1; 0.05	toluene	6	80	99; 85	87; 81	30:70	[65]
Ru46	10; 25	0.01	toluene	6	80	55; 49	55; 45	30:70	[65]
Ru46	50; 100	0.01	toluene	6	80	50; 49	25; 25	30:70	[65]
Ru47	5	0.005	toluene	20 min	70	8	8	–	[59]
Ru47	5	0.025; 0.025	C_6H_6	2	70; 80	95; >99	91; 83	–	[64]
Ru47	5	0.025	toluene	1	75	95	91	35:65	[66]
Ru48	5	0.01; 0.002	C_6H_6	2	40	100; 56	92; 55	–	[64]

[1] No data. [2] GC data or GC data/isolated yield.

As can be seen in Table 2, G-I catalysts (**Ru2**, **Ru3**) were virtually inactive in the RCM of CH_2=CH$(CH_2)_8$COO$(CH_2)_4$CH=CH_2 [41], whereas the close analog **Ru4** provided relatively high yields of the UM but for a long reaction time [50]. G-II and HG catalysts containing saturated (e.g., **Ru6**, **Ru8**, **Ru14**–**Ru18**) and unsaturated (**Ru7**, **Ru23**–**Ru25**) NHC fragments turned out to be more active. The HG-II catalyst **Ru15**, containing an acceptor–NO_2 group in the benzene ring, showed a higher productivity in comparison with **Ru14**; an 87% yield of the UM was achieved when using 0.05 mol% of the catalyst [62]. It was also reported that the use of R_2SO as an additional ligand in G-II type catalysts, instead of PCy_3, increases RCM productivity and selectivity [69]. The catalytic activity and thermal stability of the NHC-type catalysts were improved by the coordination of bidentate (N,N)-ligand at the Ru center (**Ru32** [33,62]). Among NHC Ru complexes, **Ru24** and **Ru25** have demonstrated the highest activities when ethylene was removed from the reaction mixture [61].

The first attempts to optimize the process parameters (reactor configuration) for the **Ru6**-catalyzed RCM of CH_2=CH$(CH_2)_8$COO$(CH_2)_4$CH=CH_2 were made in 2010 by Fogg and coll. [70]. The use of a continuous stirred-tank reactor with an efficient elimination of ethylene afforded an order-of-magnitude increase in TON and reduced the catalyst loadings to 0.2 mol%, thus providing near quantitative levels of yield and selectivity. The use of a continuous-flow reactor allowed the substrate concentration to be increased to 20 mM ($C_2H_4Cl_2$); after 3 h at 70 °C in the presence of **Ru35** (7.5 mol%) the yield of UM was 70% ((*Z*)/(*E*) ratio 86:14) [71].

In recent years, CAAC Ru complexes have attracted researchers' attention, demonstrating high activities in the cross-metathesis of oleates [26–28]. In the RCM of CH_2=CH$(CH_2)_8$COO$(CH_2)_4$CH=CH_2 the complexes **Ru43**–**Ru45** showed high activities; a 98% yield of UM was obtained when using 45 ppm of **Ru45**; a record TON of 62,000 was achieved at a 10 ppm loading of **Ru45** [59]. However, the bis-CAAC complex **Ru47**

was inferior to **Ru45** in catalytic activity [65]. The preference of CAAC complexes in RCM was confirmed by a mechanistic point of view in a recent study of Fogg and coll. [58]. Note that in 2019, the scientific group of Fogg reported that the dimeric CAAC complex **Ru48** is highly active in RCM (a 56% conversion after 2 h at 40 °C at a 20 ppm loading of the catalyst) [64]. Also note that the replacement of Cl by I in **Ru44** and other CAAC Ru complexes resulted in an increase in the yield of UM [68].

In most RCM experiments, the (*Z*)/(*E*) ratio was 1:2 to 1:4, reflecting the relative thermodynamic stability of diastereomers of 16-membered unsaturated lactone. However, the sterically hindered complexes **Ru35** and **Ru37** containing acceptor bidentate ligands (NO_3^-, 3,6-dichlorobenzene-1,2-ditiolate) showed a high (*Z*)-selectivity [62] (the stereoselectivity of RCM is discussed in more detail in Section 2.3.4)

As was mentioned in Section 2.2, the selectivity of RCM (the formation of the cycle with a given number of atoms) may be quite different from 100%: C=C bond migration during the RCM process may result in the formation of UMs with a smaller ring size. For example, the selectivities of the RCM of CH_2=CH$(CH_2)_8$COO$(CH_2)_4$CH=CH_2 (10 mM in EtOAc, 1 mol% of the catalyst) were 95% (**Ru6**), 98% (**Ru8**), 93% (**Ru14**), 77% (**Ru15**), 67% (**Ru19**), 96% (**Ru21**) and >99% (**Ru12**) [41]; isomerization was suppressed by the addition of 2–20 mol% HCl.

2.3.3. Ru-Catalyzed RCM of Other Alkenyl Alkenoates

To date, a wide range of alkenyl alkenoates have been studied in Ru-catalyzed RCM. The diversity of the types of substrates and reaction products required the development of reliable methods for the analysis of reaction mixtures. The most common methods of analysis have been and remain GC (e.g., [41,70]) and GC/MS (e.g., [31,72]); ^{1}H NMR diffusion-ordered spectroscopy (DOSY) can also be applied for the detection of the characteristic signals of RCM products and oligomers (Figure 2); these data can be used for the fast monitoring of the reaction mixtures [73].

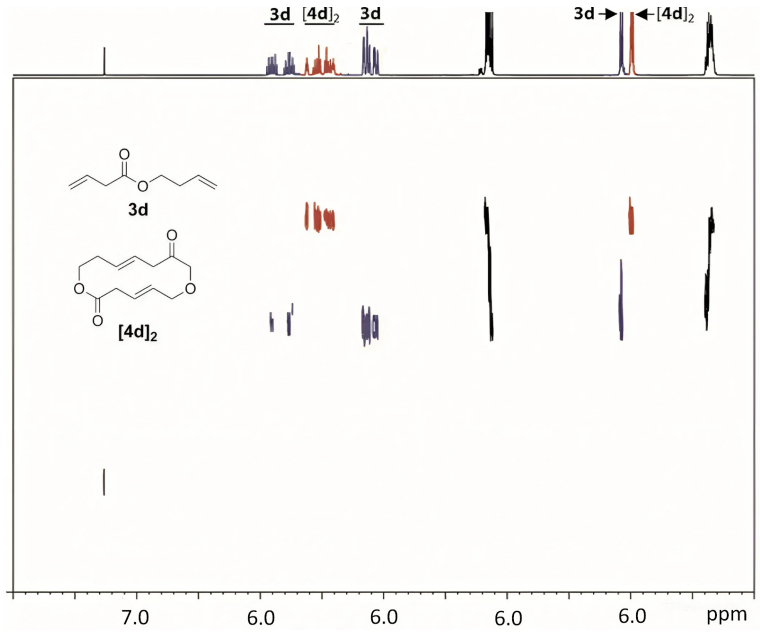

Figure 2. ^{1}H DOSY NMR spectrum of a 1:1 mixture of but-3-enyl but-3-enoate (**3d**) and its cyclic dimer, (4*E*,11*E*)-1,7-dioxacyclotetradeca-4,11-diene-2,9-dione (**[4d]$_2$**) (500 MHz, $CDCl_3$). The signals of **3d** and **[4d]$_2$** are shown in blue and in red, respectively. Reprinted with permission from [73]. Copyright (2010) Elsevier B. V.

The results of the studies of different catalysts and substrates are summarized in Table 3. The data presented do not include the results of the studies with the use of clearly unacceptable catalyst's loadings and conditions (e.g., 20 mol% in [74], 10 mol% and 5 days of the reaction in [75]), without correctly specifying the catalysts [76] and suspect reports [77] (see the more detailed comment at the end of this section). As can be seen in Table 3, the yields and configurations of UMs depend on the lengths of alkenyl fragments and positions of C=C bonds and their configurations.

Table 3. Experimental data on ring-closing metathesis of $R^1CH=CH(CH_2)_nCOO(CH_2)_mCH=CHR^2$.

R^1	n	m	R^2	Cat.	Sub. Conc., mM	Cat., mol%	Solvent	Time, h	T, °C	Yield, %	(*Z*)/(*E*) Ratio	Ref.
H	3	9	H	**Ru4**	4.8	4	CH_2Cl_2	23	20	62	– [1]	[50]
H	2	8	H	**Ru4**	–	–	–	72	25	22	–	[32]
H	8	2	H	**Ru6**	3	–	CH_2Cl_2	40 min	40	>99	8:92	[55]
H	8	2	Et	**Ru6**	3	–	CH_2Cl_2	30 min	40	>99	9:91	[55]
H	3	9	H	**Ru6**	5	5	CH_2Cl_2	1	40	61	21:79	[45]
H	1	2	H	**Ru7**	5; 0.5	5	CH_2Cl_2	1	40	29; 78	0:100	[49]
H	4	2	H	**Ru7**	5; 0.5	5	CH_2Cl_2	0.5; 0.75	40	41; 95	41:59	[49]
H	8	2	H	**Ru7**	5	5	CH_2Cl_2	3	40	94	89:11	[49]
H	1	2	H	**Ru7**	5	5	CH_2Cl_2	30 min	40	~30	–	[73]
H	8	2	H	**Ru10**	40	0.005	toluene	–	80	30	9:91	[61]
H	2	9	H	**Ru10**	10	0.0075	toluene	–	80	50	10:90	[61]
H	0	10	H	**Ru14**	1	5	CH_2Cl_2	12	22	87	5:95	[78]
H	7	–(*R*)-CH(Me)$(CH_2)_2CH=CH_2$		**Ru14**	–	–	toluene, C_6F_6	–	–	27	–	[79]
H	7	5	Et (*Z*-)	**Ru15**	1.5	2	toluene	5	50	87 [3]	18:82	[42]
n-C_8H_{17} (*Z*-)	7	5	Et (*Z*-)	**Ru15**	1.5	2	toluene	5	50	91 [3]	22:78	[42]
n-C_8H_{17} (*Z*-)	7	5	Et (*Z*-)	**Ru15**	1.5	2	EtOAc	5	77	91 [3]	19:81	[42]
n-C_8H_{17} (*Z*-)	7	5	Et (*Z*-)	**Ru15**	5	1	EtOAc	5	77	90 [3]	19:81	[42]
n-C_8H_{17} (*Z*-)	7	5	Et (*Z*-)	**Ru15**	10	1	EtOAc	24	77	81 [3]	19:81	[42]
n-C_8H_{17} (*Z*-)	7	5	Et (*Z*-)	**Ru15**	15	1	EtOAc	24	77	48 [3]	20:80	[42]
n-C_8H_{17} (*Z*-)	7	5	Et (*Z*-)	**Ru15**	21	0.5	EtOAc	24	77	43 [3]	17:83	[42]
n-C_8H_{17} (*Z*-)	7	5	Et (*Z*-)	**Ru15**	29	0.3	EtOAc	24	77	40 [3]	17:83	[42]
n-C_8H_{17} (*Z*-)	7	5	Et (*Z*-)	**Ru15**	40	0.1	EtOAc	24	77	35 [3]	20:80	[42]
n-C_8H_{17} (*Z*-)	7	5	Et (*Z*-)	**Ru15**	50	0.1	EtOAc	24	77	36 [3]	17:83	[42]
n-C_8H_{17} (*Z*-)	7	5	Et (*Z*-)	**Ru15**	100	0.1	EtOAc	24	77	16 [3]	18:82	[42]
H	7	6	H	**Ru15**	1.5	2	toluene	5	50	77	31:69	[42]
H	7	–$(CH_2)_2CHMe(CH_2)_2C=CMe_2$		**Ru15**	1.5	2	toluene	5	50	88	15:85	[42]
H	7	–(*Z*)-$CH_2C=C(Me)(CH_2)_2C=CMe_2$		**Ru15**	1.5	2	toluene	5	50	80	24:76	[42]
H	7	–(*E*)-$CH_2C=C(Me)(CH_2)_2C=CMe_2$		**Ru15**	1.5	2	toluene	5	50	87	13:87	[42]
H	7	–(*Z*)-$(CH_2)_5CH=CHEt$		**Ru15**	1.5	2	toluene	5	50	87	18:82	[42]
H	7	4	H	**Ru15**	1.5	2	toluene	5	50	71	48:52	[42]
Oleyl (*n* = 7)		6	H	**Ru15**	1.5	2	toluene	5	50	90	31:69	[42]
Oleyl (*n* = 7)		–$(CH_2)_2CHMe(CH_2)_2C=CMe_2$		**Ru15**	1.5	2	toluene	5	50	48	18:82	[42]
Oleyl (*n* = 7)		–(*Z*)-$CH_2C=C(Me)(CH_2)_2C=CMe_2$		**Ru15**	1.5	2	toluene	5	50	48	25:75	[42]
Oleyl (*n* = 7)		–(*E*)-$CH_2C=C(Me)(CH_2)_2C=CMe_2$		**Ru15**	1.5	2	toluene	5	50	40	16:84	[42]

Table 3. *Cont.*

R^1	n	m	R^2	Cat.	Sub. Conc., mM	Cat., mol%	Solvent	Time, h	T, °C	Yield, %	(*Z*)/(*E*) Ratio	Ref.
Oleyl (*n* = 7)		–(*Z*)-$(CH_2)_5$ CH=CHEt		**Ru15**	1.5	2	toluene[2]	5	50	91	22:78	[42]
Oleyl (*n* = 7)		4	H	**Ru15**	1.5	2	toluene[2]	5	50	62	48:52	[42]
Me (*E*-)	6	6	H	**Ru15**	1.5	2	toluene[2]	5	50	84	43:57	[43]
H	7	5	Me (*E*)-	**Ru15**	1.5	2	toluene[2]	5	50	85	18:82	[43]
H	3	9	H	**Ru16**	5	0.5	AcOEt	70 min	70	99	25:75	[80]
Oleyl (*n* = 7)		5	Et (*Z*-)	**Ru17**	5	1	toluene	5	50	80	18:82	[81]
Me (*E*-)	6	7	Me (*E*-)	**Ru17**	1.5	2	toluene[2]	5	50	84	–	[82]
Me (*E*-)	6	5	Et (*Z*-)	**Ru17**	1.5	2	toluene[2]	5	50	84	–	[82]
Me (*E*-)	6	8	H	**Ru17**	1.5	2	toluene[2]	5	50	86	–	[82]
H	7	5	Me (*E*-)	**Ru17**	1.5	2	toluene[2]	5	50	85	–	[82]
H	8	2	H	**Ru24**	40	0.005	toluene	–	80	25	9:91	[61]
H	8	3	H	**Ru24**	8	0.01	toluene	–	80	12	–	[61]
H	2	9	H	**Ru24**	10	0.0075	toluene	–	80	56	9:91	[61]
H	8	2	H	**Ru25**	40	0.005	toluene	–	80	26	9:91	[61]
H	2	9	H	**Ru25**	10	0.0075	toluene	–	80	56	9:91	[61]
H	7	6	H	**Ru26**	10	1	EtOAc[4]	4	77	70	–	[41]
H	8	6	H	**Ru26**	10	1	EtOAc[4]	4	77	76	–	[41]
H	8	3	H	**Ru26**	10	1	EtOAc[4]	4	77	39	–	[41]
H	8	9	H	**Ru31**	–	4	CH_2Cl_2	20	40	73	–	[54]
H	7	2	H	**Ru35**	3	7.5	$C_2H_4Cl_2$	24	60	40	86:14	[48]
H	8	2	H	**Ru35**	3	7.5	$C_2H_4Cl_2$	24	60	58	85:15	[48]
H	5	8	H	**Ru35**	3	7.5	$C_2H_4Cl_2$	24	60	71	89:11	[48]
H	3	9	H	**Ru35**	3	7.5	$C_2H_4Cl_2$	24	60	72	84:16	[48]
H	8	8	H	**Ru35**	3	7.5	$C_2H_4Cl_2$	24	60	75	94:6	[48]
H	7	–(*R*)-CH(Me) $(CH_2)_2CH=CH_2$		**Ru35**	–	–	toluene, C_6F_6	–	–	38	95:5	[79]
H	5	8	H	**Ru36**	3	7	$C_2H_4Cl_2$	24	60	64	95:5	[47]
H	7	5	Et	**Ru37**	3	6	CH_2Cl_2	1	40	–	95:5	[83]
H	5	3	Me (*Z*-)	**Ru38**	3	6	CH_2Cl_2	1	40	70	>99:1	[84]
H	7	2	Et (*Z*-)	**Ru38**	3	6	CH_2Cl_2	1	40	98	95:5	[84]
H	8	2	Et (*Z*-)	**Ru38**	3	6	CH_2Cl_2	1	40	67	95:5	[84]
H	7	3	Me (*Z*-)	**Ru38**	3	6	CH_2Cl_2	1	40	72	98:2	[84]
H	8	3	Et (*Z*-)	**Ru38**	3	6	CH_2Cl_2	1	40	74	99:1	[84]
H	8	5	Et (*Z*-)	**Ru38**	3	6	CH_2Cl_2	1	40	75	95:5	[84]
Me (*E*-)	8	4	Me (*E*-)	**Ru39**	5	7.5	THF	24	35	66[3]	1:99	[85]
Me (*E*-)	5	3	Me (*E*-)	**Ru40**	5	7.5	THF	5	35	60[3]	1:99	[85]
Me (*E*-)	7	2	Me (*E*-)	**Ru40**	5	7.5	THF	5	35	75[3]	1:99	[85]
Me (*E*-)	8	2	Me (*E*-)	**Ru40**	5	7.5	THF	5	35	65[3]	1:99	[85]
Me (*E*-)	8	3	Me (*E*-)	**Ru40**	5	7.5	THF	5	35	70[3]	1:99	[85]
Me (*E*-)	7	3	Me (*E*-)	**Ru40**	5	7.5	THF	5	35	67[3]	1:99	[85]
Me (*E*-)	8	4	Me (*E*-)	**Ru40**	5	7.5	THF	5	35	70[3]	1:99	[85]
Me (*E*-)	8	6	Me (*E*-)	**Ru40**	5	7.5	THF	5	35	63[3]	1:99	[85]
H	3	9	H	**Ru40**	100/5[5]	4	THF	12	35	56	96:4	[86]
H	6	4	H	**Ru40**	100/5[5]	4	THF	12	35	67	98:2	[86]
H	4	7	H	**Ru40**	100/5[5]	4	THF	12	35	86	98:2	[86]
H	4	8	H	**Ru40**	100/5[5]	4	THF	12	35	70	98:2	[86]
H	6	9	H	**Ru40**	100/5[5]	4	THF	12	35	65	98:2	[86]
H	8	9	H	**Ru40**	100/5[5]	4	THF	12	35	60	96:4	[86]
H	7	5	Et (*Z*-)	**Ru41**	3	6	CH_2Cl_2	1	40	<5	–	[83]
H	7	8	Me	**Ru42**	20	2	toluene	1	100	83	9:91	[72]
H	2	7	Me	**Ru42**	20	2	toluene	1	100	32	24:76	[72]
H	2	8	Me	**Ru42**	20	2	toluene	1	100	40	10:90	[72]
H	3	8	Me	**Ru42**	20	2	toluene	1	100	48	34:66	[72]
H	4	8	Me	**Ru42**	20	2	toluene	1	100	52	14:86	[72]
H	7	5	Me	**Ru42**	20	2	toluene	1	100	55	24:76	[72]

Table 3. *Cont.*

R^1	n	m	R^2	Cat.	Sub. Conc., mM	Cat., mol%	Solvent	Time, h	T, °C	Yield, %	(*Z*)/(*E*) Ratio	Ref.
H	3	10	Me	**Ru42**	20	2	toluene	1	100	71	14:86	[72]
H	4	10	Me	**Ru42**	20	2	toluene	1	100	68	17:83	[72]
H	7	7	Me	**Ru42**	20	2	toluene	1	100	75	15:85	[72]
H	4	11	Me	**Ru42**	20	2	toluene	1	100	81	6:94	[72]
H	5	11	Me	**Ru42**	20	2	toluene	1	100	78	28:72	[72]
H	7	10	Me	**Ru42**	20	2	toluene	1	100	62	19:81	[72]
H	7	11	Me	**Ru42**	20	2	toluene	1	100	59	27:73	[72]

[1] No data. [2] 4 mol% TFQ. [3] Isolated yield. [4] 2.5 mol% HCl. [5] 20 equiv. of (*Z*)-but-2-ene was added at the first stage; after elimination of the excess of (*Z*)-but-2-ene, the mixture was diluted to 5 mM.

In general, the yields of 10–13-membered UMs are lower; the optimum ring size is 15–20. Note that six-membered unsaturated UM can be obtained via RCM, in contrast to seven-membered [49]. Undoubtedly of interest is the study of the RCM of dodec-11-en-1-yl acrylate (1 mM in C_6H_6): **Ru14** and **Ru35** (10 mol%) catalyzed the formation of 14-membered lactone with 87 and 5% yields, respectively [78]. The common patterns of the formation of UMs match those of the cyclization of bifunctional substrates [87], manifested in lower yields of 7–13-membered cyclic products. Back in 2007 [49], Fogg formulated recommendations for the optimal concentrations of α,ω-dienes in RCM: 100 mM for 5–6-membered rings, 5 mM for 7-membered, 0.5 mM for 8–13-membered, and 5 mM for 14+ macrocycles. With regard to unsaturated lactones, these recommendations apply only to 6-membered and 10+ macrocycles. The yields of UMs in some cases are relatively low, but in some cases RCM seems to be better than separation from the natural sources: for example, the content of 13-membered unsaturated lactone, derivative of dec-9-enoic acid, in *Medicago rugosa* amounted to ~8 mg·kg^{-1} [88].

The type of the alkenyl alkenoate (terminal or internal C=C fragment) can also affect the product yield and selectivity (the configuration of the C=C bond is also important, see Section 2.3.4). During a comparative study of four substrates, derivatives of oleic acid in **Ru15**-catalyzed RCM (Scheme 10), Grela and coll. showed the preference of the use of alkenyl alkenoates containing one terminal and one internal C=C bond [42]. In the synthesis of 16-membered UM, the type of C=C bond had little effect on the yield of the product [42].

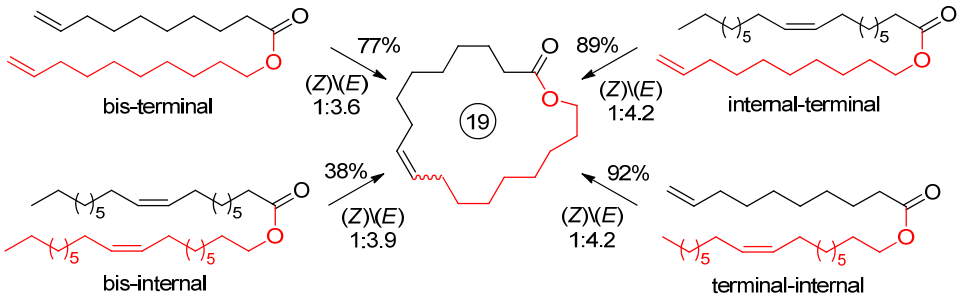

Scheme 10. Influence of the substituents at the C=C bond on the yield of 19-membered UM [42].

In 2020, Jamison, Bio and coll. proposed the use of a membrane sheet-in-frame pervaporation module reactor (Figure 3) for the RCM of CH_2=CH$(CH_2)_8$COO$(CH_2)_2$CH=CH_2; under optimized conditions (5 mM in toluene, 1.5 mol% **Ru17**, 10.5 min at 100 °C), the yield of UM was 95.4% [89].

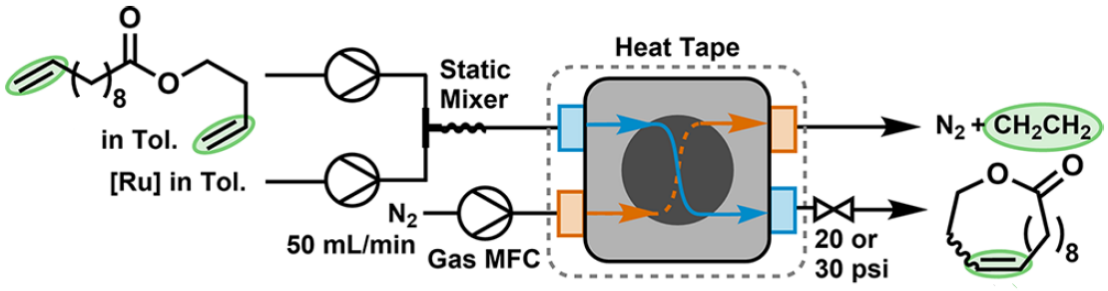

Figure 3. Continuous RCM of CH_2=CH(CH_2)$_8$COO(CH_2)$_2$CH=CH_2 using the membrane sheet-in-frame reactor. Reprinted with permission from [89]. Copyright (2020) American Chemical Society.

At the conclusion of this section, the results of the catalytic experiments on the RCM of different alkenyl alkenoates, including allyl esters (50 mM in CH_2Cl_2), catalyzed by **Ru6** [77] should be mentioned. The reported isolated yields of unsaturated 11–23-membered lactones amounted to 72–85% which is contrary to the results of early and recent studies, and these data were not included in Table 3.

2.3.4. Stereoselectivity of Ru-Catalyzed Ring-Closing Metathesis

Besides the macrolactone yield and selectivity of RCM (the absence of C=C bond migration), the (*E*)/(*Z*) ratio is also important. In 2000, Lee and Grubbs showed that the formation of 14-membered lactone occurs with a high (*E*)-selectivity due to the higher thermodynamic stability of the (*E*)-isomer [55] (Scheme 11).

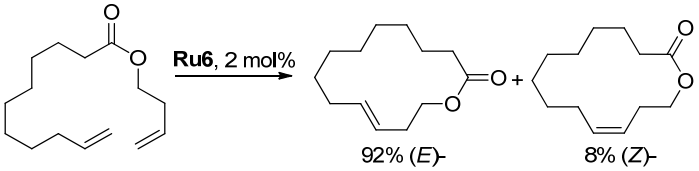

Scheme 11. Stereoselective cyclization of but-3-enyl undec-10-enoate [55].

In the case of lactones with larger rings, the relative stability of (*Z*)-isomers increases, setting the stage for the development of stereoselective metathesis catalysts. The (*Z*)-selectivity of NHC Ru catalysts in the RCM of model substrates was increased by the coordination of the –$OCMe_3$ ligand (**Ru33**, **Ru34**) [90,91]. Further studies [47,92] revealed cyclometallated catalysts with high (*Z*)-selectivity (**Ru35**, **Ru36**); the complex **Ru35** showed a high (*Z*)-selectivity in the formation of 16-membered UM [62] and other lactones [48].

In 2013, Hoveyda proposed the use of dithiolate ligands to improve the (*Z*)-selectivity of RCM catalysts [93]; this work initiated the development of (*Z*)-selective catalysts of the formation of UMs. The Ru complexes containing the dithiocatechol fragment **Ru37** showed very low activity but unprecedented (*Z*)-selectivity in the RCM of CH_2=CH(CH_2)$_7$COO(CH_2)$_5$CH=CH_2 at high substrate concentrations (200 mM instead of the typically used 5 mM) [83]. When using dithiolate NHC catalysts (e.g., **Ru38**), the configuration of the C=C bond in UMs depends on the configurations of C=C bonds in starting alkenyl alkenoates; (*Z*)-isomers of 12–17-membered UMs were obtained from (*Z*)-alkenyl ω-alkenoates with a >95% stereoselectivity [84,94]. However, the presence of two (*E*)-alkenyl fragments in the substrates resulted in the formation of (*E*)-UMs during RCM catalyzed by **Ru39** and **Ru40** [85]. For the synthesis of (*Z*)-UMs using **Ru37**–**Ru40,** Hoveyda and coll. proposed an in situ methylene capping approach based on the addition of (*Z*)-but-2-ene to α,ω-dienyl substrate, with the formation of (*Z*)-MeCH=CH-terminated alkenyl alkenoate that was subsequently subjected to cyclization with high stereoselectivity;

when (*E*)-but-2-ene was used, (*E*)-UMs were formed [86]. Among dithiolate Ru catalysts, the complex **Ru40** demonstrated the highest activity and stereoselectivity.

Note that the content of (*E*)-isomer in RCM products can be increased by (*Z*)-selective ethenolysis (Scheme 12) [48], but a similar approach cannot be considered as atom-efficient.

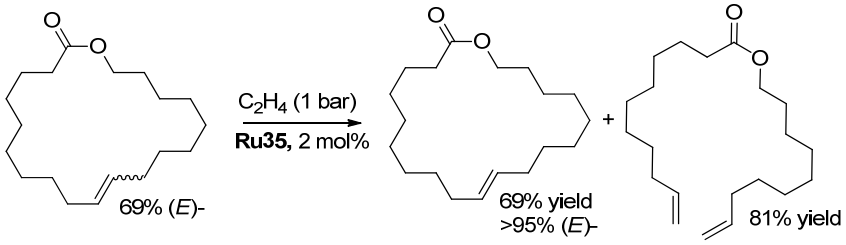

Scheme 12. (*E*)-enrichment of the RCM products by (*Z*)-selective ethenolysis [48].

An alternative approach to the pure (*Z*)-isomers of unsaturated macrolactones was proposed by Fürstner and coll. [95]: the RCM of alkynyl alkynoates (20 mM in C_6H_5Cl) with the formation of 13- and 17-membered lactones (5 mol% $Mo(CO)_6$/*p*-chlorophenol, 140 °C), with subsequent hydrogenation over Lindlar catalyst, resulted in the formation of Yuzu lactone and ambrettolide with high *Z*-selectivity.

At the end of this part of the review, mainly devoted to kinetically controlled RCM with the formation of UMs, some generalizations and conclusions are worth drawing.

First, the common dilution principle in the RCM of alkenyl alkenoates cannot be ignored. The rational design of metathesis catalysts allow one to obtain UMs with high isolated yields, but compliance with the dilution principle actualizes the problem of the use and utilization of the solvents. In most of earlier and even recent works, CH_2Cl_2 [30,40,49,50,52,54,55,83,84] or $ClCH_2CH_2Cl$ [47,48,71] were used. However, because of the environmental issues, less toxic and dangerous solvents have been applied for RCM. In particular, relatively high conversions and yields were achieved in toluene [42,45,59–61,66,68,70,74,75,81,89], ethyl acetate [41,43,65,67,72,76,96], THF [85,86] and dimethyl carbonate [96]. The use of benzene as a solvent for RCM was proposed in a number of works [33,51,58,64,78] but seems not suitable for scaling due to the high toxicity of benzene. The traces of water deactivate catalysts [62], thus creating additional requirements for the solvent purity. Supercritical CO_2, a popular green solvent, was also studied as a reaction medium for RCM [56], but the catalyst's activities and UM yields were moderate. The problems of high dilution and solvent utilization in the synthesis of UMs have been solved by the use of high-boiling non-toxic hydrocarbons at elevated temperatures—but only for thermodynamically driven processes [31] (see Section 2.4.1 below).

Second, the availability of the catalytic component is critical in light of the possible application of RCM in the production of UMs. Even the use of a low catalyst loading does not remove the problem of the recycling, especially for more expensive Ru-based catalysts. The problems of the separation and recycling of Ru were discussed in an early review [97]; however, these problems are still relevant. Attempts to prepare heterogeneous recyclable catalysts for the RCM of alkenyl alkenoates have already been made (see Section 2.4.2 below), but the problem is far from being solved.

2.4. Ru-Catalyzed Ring-Closing Metathesis of Alkenyl Alkenoates at High Concentrations

2.4.1. Ring-Closing Metathesis with Distillation of the Products

The key problems in RCM are related to the unfavorable entropic effect that makes the oligomerization (ADMET) dominate over the desired formation of Ums; moreover, the initial formation of oligomers was detected during RCM [49]. The ring–chain equilibrium is complicated by the formation of larger macrocycles (di-, tri-, tetramers, etc.) [98]. The

desired shift of the UM/cyclic oligomer/polymer equilibrium can be achieved by the elimination of the UM from the reaction mixture. In 2018, Grela and coll. carried out the study of RCM at concentrations much higher than commonly used [31]. They proposed that the UMs can be removed from the reaction mixture by distillation in vacuo. The ADMET of hex-5-en-1-yl undec-10-enoate and subsequent depolymerization in the presence of **Ru16** (1 mol%) resulted in the formation of (*Z*/*E*) mixtures of 11–21-membered macrocycles with a maximum yield of 24% (Figure 4). The yields were increased after the addition of TFQ, but C=C bond migration and the formation of MUs of different sizes were still observed.

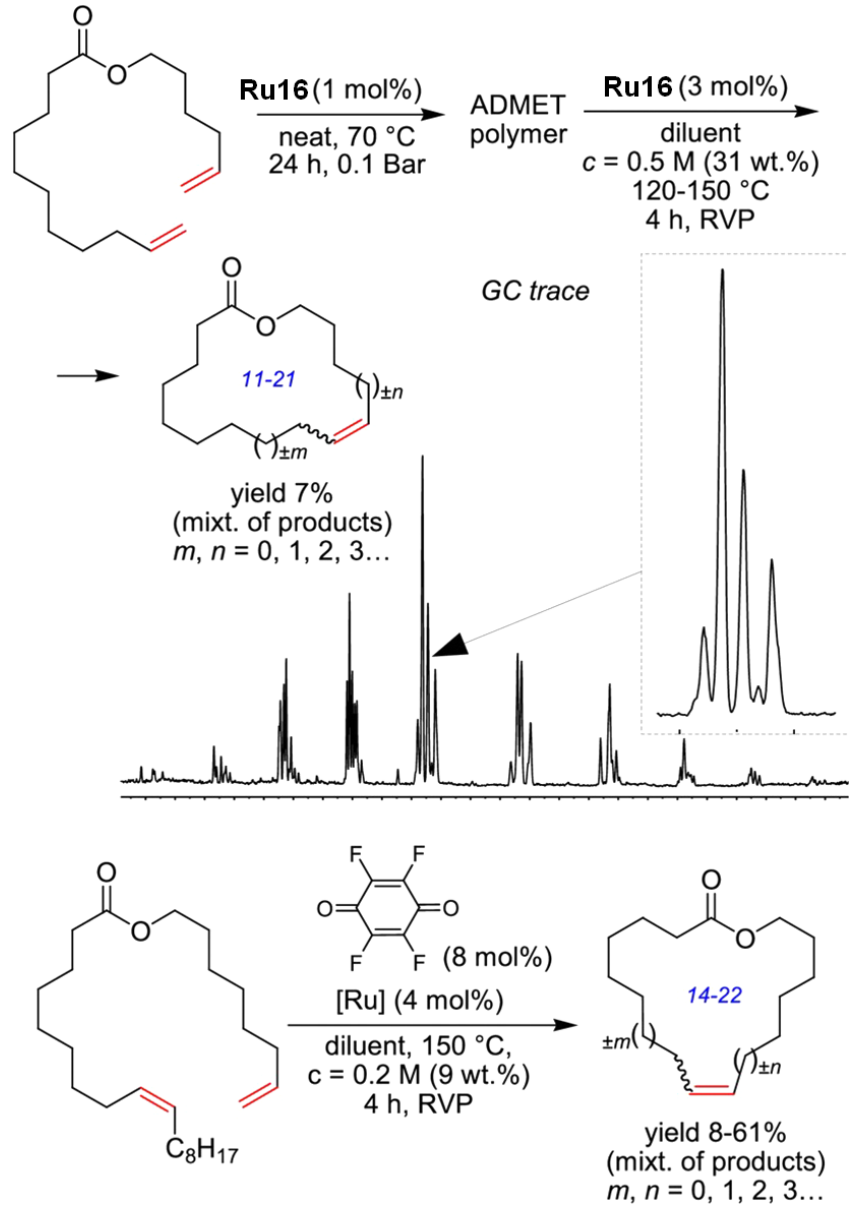

Figure 4. ADMET and then RCM depolymerization approach to macrolactones and GC trace of product. Reprinted with permission from [31]. Copyright (2018) American Chemical Society.

A comparative study of Ru complexes **Ru6**, **Ru14**, **Ru16**, **Ru19**, **Ru22** (Scheme 6) and **Ru49**–**Ru54** (Scheme 13) was conducted in experiments in paraffin oil at 110 °C (10^{-6} mBar); the substrate concentration was 0.2 M. The results of the experiments were qualitatively dependent on the type of the catalyst used (Figure 5) [31].

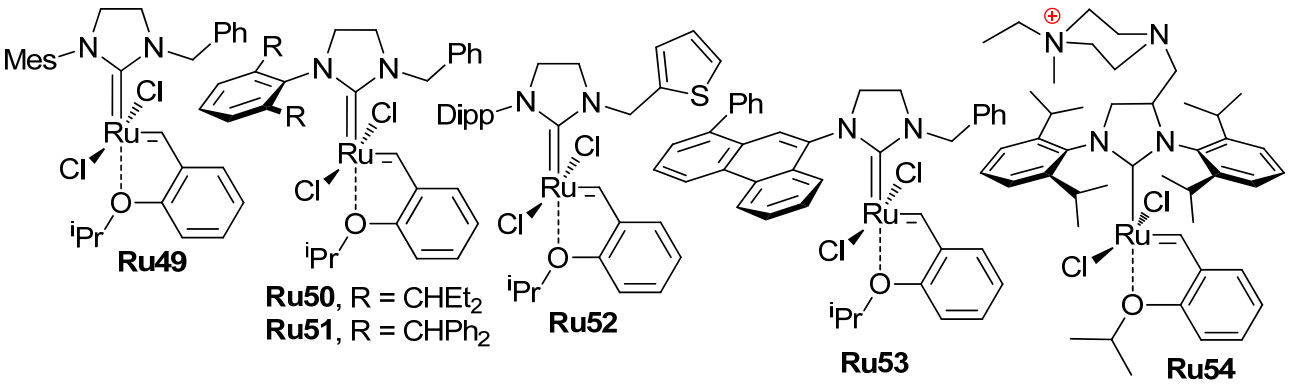

Scheme 13. NHC Ru catalysts studied in RCM of alkenyl alkenoates with distillation of UMs [31].

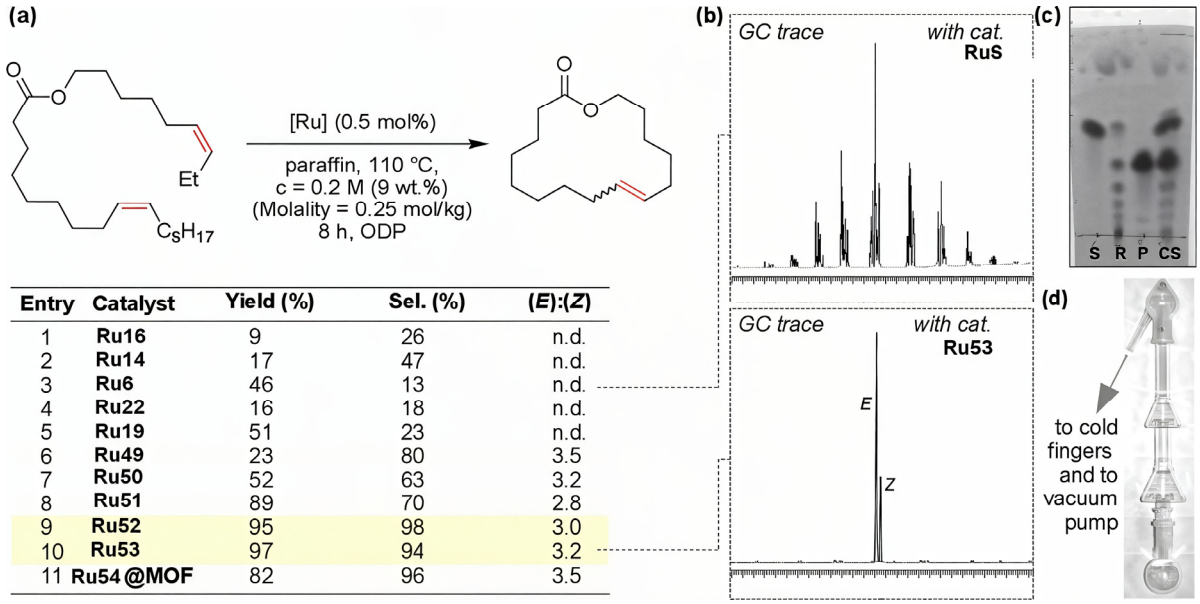

Entry	Catalyst	Yield (%)	Sel. (%)	(*E*):(*Z*)
1	**Ru16**	9	26	n.d.
2	**Ru14**	17	47	n.d.
3	**Ru6**	46	13	n.d.
4	**Ru22**	16	18	n.d.
5	**Ru19**	51	23	n.d.
6	**Ru49**	23	80	3.5
7	**Ru50**	52	63	3.2
8	**Ru51**	89	70	2.8
9	**Ru52**	95	98	3.0
10	**Ru53**	97	94	3.2
11	**Ru54@MOF**	82	96	3.5

Figure 5. RCM experiments: (**a**) Yield and selectivity of the formation of macrolactone (Selectivity = (Int. of *E* + *Z*)/(Int. of all products); the most efficient catalysts are marked in yellow. (**b**) GC traces of products obtained using complexes **Ru6** and **Ru53**. (**c**) TLC analyses of reaction mixture from experiment ceased after 20 min. S—standard of the substrate, R—sample of reaction mixture, P—standard of the product, CS—all three together. (**d**) Example of a reaction/distillation Hickman glass apparatus. Reprinted with permission from [31]. Copyright (2018) American Chemical Society.

Note that under homogeneous conditions, **Ru54** showed a low selectivity in the cyclization of CH_2=CH$(CH_2)_8$COO$(CH_2)_4$CH=CH_2 that was substantially improved when this catalyst was immobilized on a metal–organic framework (MOF) [67]. This heterogeneous catalyst was used in experiments with the distillation of the UMs in [31].

A number of alkenyl oleates were transformed to 13-, 16-, 17- and 19-membered unsaturated lactones; the yields were 60–93%, and the (*E*)/(*Z*) ratio was 2.1–4.9 depending on the ring size (Table 4); the esters of dec-9-enoic acid demonstrated similar results.

Another example of the synthesis of UM with its distillation is presented in [83]: in the presence of **Ru38** (10 mol%), the cyclization of (*Z*)-non-6-enyl oleate (200 mM in PAO6, 130 °C, 8 h) resulted in the formation of 16-membered UM with an 80% yield and 78% selectivity and a (*Z*)/(*E*) ratio of 74:26; **Ru41** under similar conditions catalyzed the formation of UM with a 31% yield and >99% (*Z*)-selectivity.

Table 4. Synthesis of UMs via ring-closing depolymerization of products of ADMET polymerization of $CH_3(CH_2)_7CH=CH(CH_2)_7COO(CH_2)_nCH=CHR$ (200 mM, 110 °C, 8 h) [31].

n	R	Cat	Cat. mol%	Diluent	Yield, %	Sel., %	(*Z*)/(*E*) Ratio
5	Et	**Ru53**	0.5	paraffin oil	97	94	24/66
5	Et	**Ru53**	0.5	paraffin wax	91	86	24/66
5	Et	**Ru53**	0.5	polyethylene	26	92	22/78
5	Et	**Ru53**	0.5	ionic liquid [1]	33	77	23/77
5	Et	**Ru53**	0.5	PAO4 [2]	97	96	23/77
5	Et	**Ru53**	0.5	PAO6 [3]	99	95	23/77
2	H	**Ru52**	2	PAO6	73	96	22/78
$-CH_2CHMe(CH_2)_2C=CMe_2$		**Ru53**	2	paraffin	56	92	19/81
5	H	**Ru53**	0.5	paraffin	60	93	24/66
6	H	**Ru52**	1	PAO6	86	94	32/68
8	n-C_8H_{17}	**Ru53**	2	paraffin	55	81	23/77

[1] 1-butyl-2,3-dimethylimidazolium hexafluorophosphate. [2] Hydrogenated dec-9-ene trimer. [3] Hydrogenated dec-9-ene tetramer.

Very recently, Grela and coll. synthesized the highly prospective catalyst **Ru55** for high-temperature RCM [99]. The synthesis of **Ru55** was based on a cheap ligand precursor, prepared from benzene-1,2-diamine in five simple steps, and **Ru22** (Scheme 14). The high efficiency of **Ru55** in (*Z*)-selective RCM with distillation of the reaction products was demonstrated in examples of the synthesis of 16- and 13-membered UMs (Figure 6).

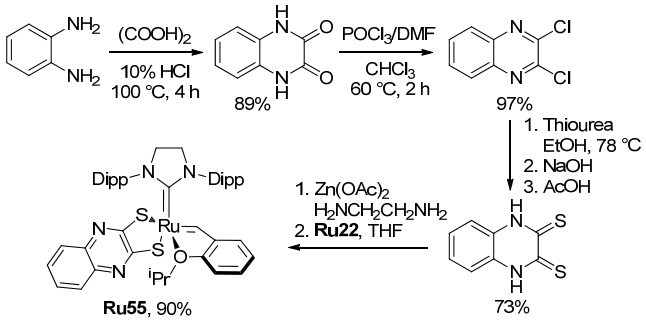

Scheme 14. Preparation of the catalyst **Ru55** [99].

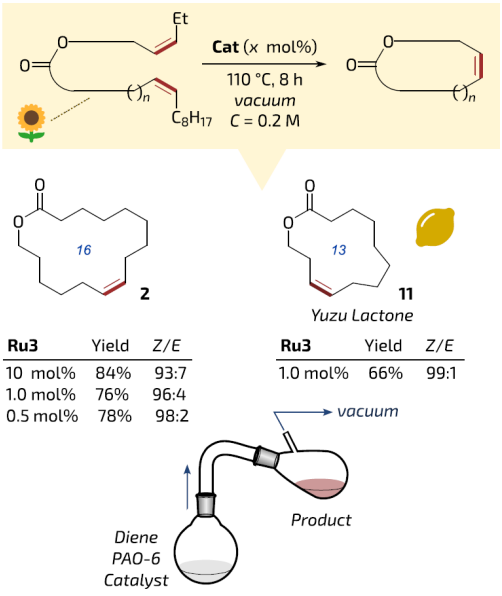

Figure 6. Examples of bio-based (partially or fully derived from oleic acid, which is symbolized by sunflower icon) macrocycles obtained in reactive vacuum distillation at high concentration. Yields of isolated pure products. Reprinted with permission from [99]. Copyright (2024) Springer Nature.

2.4.2. Ring-Closing Metathesis Under Spatial Confinement Conditions

In 2013, Lee, Hong and co-workers reported the results of their study of the HG-II-type catalyst **Ru56** immobilized on mesocellular siliceous foam (MCF) bearing large nanopores (Scheme 15). A comparative study of **Ru14** and **Ru56a**–**Ru56c** (**Ru56** immobilized on MCF with average pore diameters of 24.1 nm (**a**) and 20.6 nm (**b**) or on non-porous SiO_2 (**c**)) revealed the higher activity of the MCF-immobilized catalysts **Ru56a** and **Ru56b** in the RCM of CH_2=CH$(CH_2)_8$COO$(CH_2)_n$CH=CH_2 (n = 2, 4, 8, 9) in comparison with **Ru14** [100] (Table 5). And most importantly, when concentrations of the substrates were increased to 50 mM, the yields of UMs amounted to 4–7% when using **Ru14** and 42–55% in the presence of **Ru56a**. In 2019, Grela and coll. studied the RCM of hex-5-en-1-yl undec-10-enoate in the presence of **Ru54**, noncovalently immobilized in sulfated MOF; a yield of 72% was achieved at a 5 mM concentration of the substrate [96].

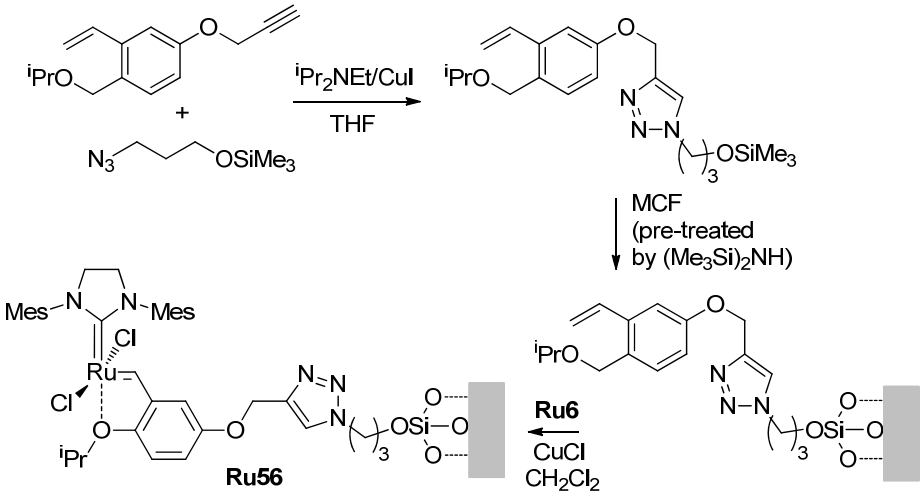

Scheme 15. Synthesis of silica-immobilized catalyst **Ru56** [101].

Table 5. RCM of CH_2=CH$(CH_2)_8$COO$(CH_2)_n$CH=CH_2 (5 mM in CH_2Cl_2, 40 °C, 5 mol% of the catalysts) [100].

n	Ring Size	Catalyst	Time, h	Yield, %	(*Z*)/(*E*) Ratio
2	14	**Ru14**	6	74	9:91
		Ru56a		83	7:93
		Ru56b		79	8:92
		Ru56c		61	8:92
4	16	**Ru14**	5	53	22:78
		Ru56a		96	23:77
		Ru56b		89	23:77
		Ru56c		77	22.78:
8	20	**Ru14**	6	29	32:68
		Ru56a		62	30:70
		Ru56b		55	29:71
		Ru56c		28	28:72
9	21	**Ru14**	8	19	31:69
		Ru56a		68	30:70
		Ru56b		62	30:70
		Ru56c		28	30:70

In 2019, Buchmeiser and coll. proposed an alternative route to solve the problem of the substrate concentration by RCM in confined geometries, using an olefin metathesis catalyst (**Ru57**, Scheme 16a) selectively immobilized inside ordered mesoporous silicas SBA-15 (Figure 7) with pore diameters *d* of 50 and 62 Å [102]. It was shown that the selectivity of macrocyclization substantially increases with an increase in the hydrodynamic diameter of the substrate (Scheme 16b) when using an SBA-15_{50}-based catalyst: e.g., dodecane-1,12-diol-based diester formed up to 60% of the RCM product at a 25 mM concentration. For dec-9-en-1-yl undec-10-enoate (25 mM in C_6D_6) in the presence of 0.1 mol% of the catalyst, the MU/oligomer ratio doubled in comparison with the MU/oligomer ratio achieved under homogeneous conditions.

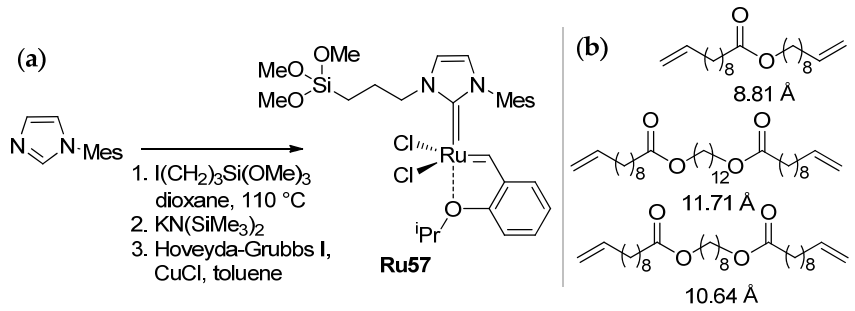

Scheme 16. (**a**) Synthesis of **Ru57** catalyst capable of immobilization on silica. (**b**) Structures and hydrodynamic diameters (DOSY-NMR data) of RCM substrates [102].

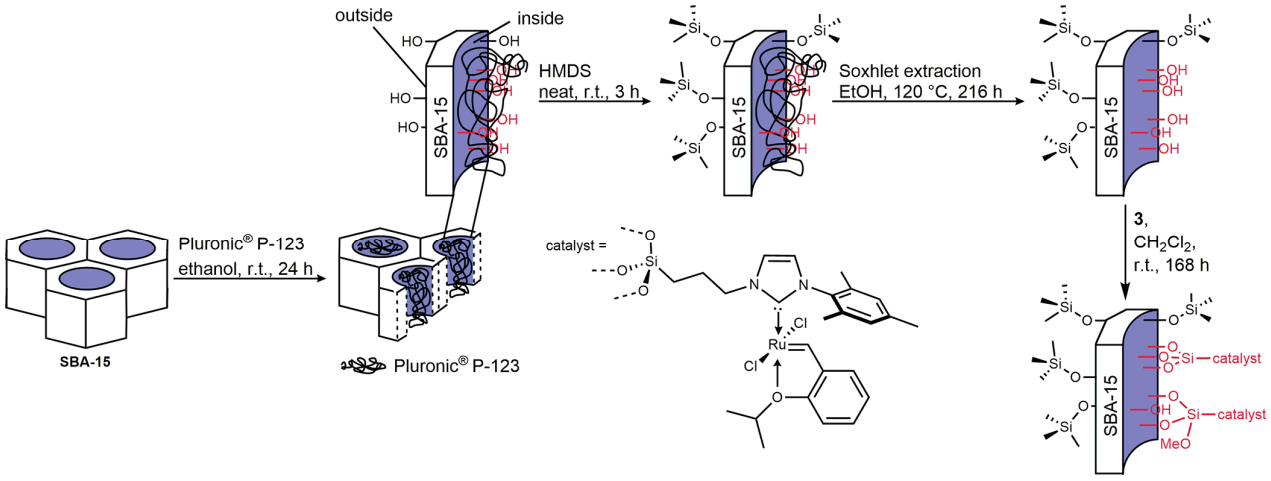

Figure 7. Multistep modification of SBA-15 for pore-selective immobilization of **Ru57** inside mesopores [102]. Copyright (2019) American Chemical Society.

The further studies of **Ru57**, immobilized on mesoporous silica, in the RCM of CH_2=CH$(CH_2)_8$COO$(CH_2)_8$CH=CH_2 (25 mM in toluene) [103,104] showed that, during macrocyclization under confinement, ADMET processes are limited by the formation of short-chain oligomers (dimers and trimers), which in turn shifts the overall ring–chain equilibrium towards the desired direction and thus increases the selectivity of UM formation.

In 2022, Lotsch, Buchmeiser and coll. developed **Ru57**, immobilized on a covalent organic framework (COF, Figure 8) [105]. For CH_2=CH$(CH_2)_8$COO$(CH_2)_8$CH=CH_2, an increase of 51% in the UM/oligomers ratio from 0.90 for **Ru57** to 1.35 for immobilized **Ru57**/COF was found, corresponding to a 59% increase in selectivity compared to the homogeneous catalyst.

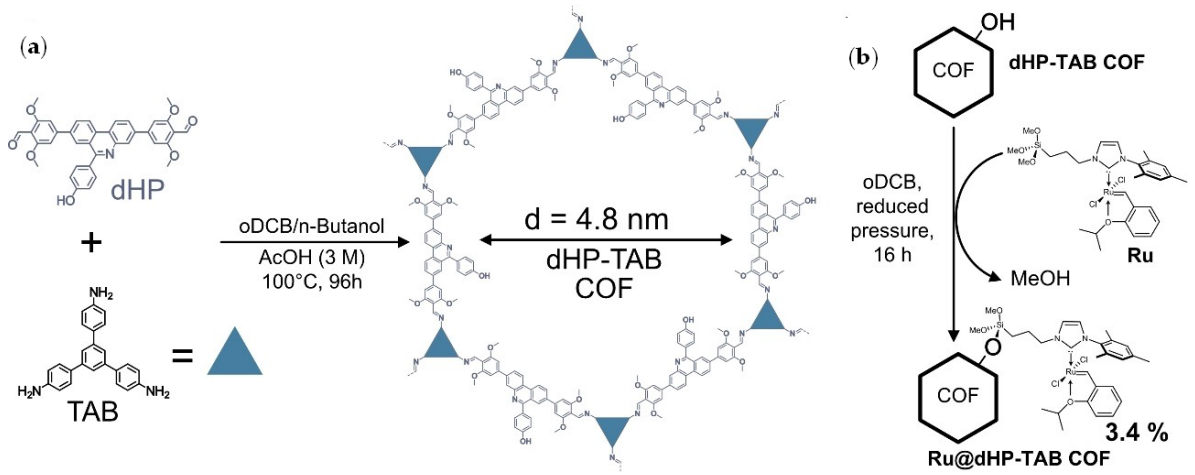

Figure 8. (**a**) Synthesis of covalent organic framework (COF). (**b**) Immobilization of **Ru57** on COF by silylation. Reprinted with permission from [105]. Copyright (2022) Wiley-VCH Verlag GmbH and Co.

2.5. Ring-Closing Metathesis Using Group 6 Metal Complexes

Historically, the first publication devoted to the use of RCM in the synthesis of unsaturated macrolactones (Villemin, 1980) describes experiments on the cyclization of CH_2=$CH(CH_2)_8COO(CH_2)_nCH$=CH_2 (n = 3, 4; 15 mM in C_6H_5Cl at 75 °C) in which WCl_6/Me_4Sn (5 mol%) was used as a catalyst; the yields of 15- and 16-membered lactones were 60 and 65%, respectively [14]. One year later, Tsuji and Hashiguchi studied the RCM of oleyl oleate and CH_2=$CH(CH_2)_8COO(CH_2)_9CH$=CH_2, catalyzed by WCl_6 (or $WOCl_2$)/(η^5-$C_5H_5)_2TiMe_2$; the yields did not exceed 18% [106].

Highly active Shrock catalysts, which represent Mo and W carbene complexes supported with imido and alkoxy (aryloxy) ligands [107] (see Scheme 17), were studied in the RCM of alkenyl alkenoates in the 2010–2020s.

In 2011, Hoveyda and coll. reported the results of comparative studies of **Ru6** and Group 6 metal complexes **Mo1**, **Mo4**, **Mo5**, **Mo6**, **W1** and **W4** (Scheme 17) in the RCM of CH_2=$CH(CH_2)_3COO(CH_2)_9CH$=CH_2 with the formation of 16-membered UM [45]. As can be seen in Table 6, **Ru6**, **Mo1** and **Mo4** showed moderate activity and stereoselectivity, whereas **Mo5**, **W1** and **W4** turned out to be (*Z*)-selective catalysts. The complexes **Mo2** and **Mo3** showed moderate activities in the RCM of alkenyl alkenoates containing trisubstituted olefinic fragments [108].

Table 6. RCM of CH_2=$CH(CH_2)_3COO(CH_2)_9CH$=CH_2 catalyzed by **Ru6** and Croup 6 metal catalysts (5 mM in toluene, 22 °C) [45].

Catalyst	Cat. Loading, mol%	Pressure, Torr	Conv., %	Yield, %	(*Z*)/(*E*) Ratio
Ru6 [1]	5	760	75	61	21:79
Mo1	5	760	85	60	22:78
Mo1	5	7	96	58	21:79
Mo4	5	760	56	45	70:30
Mo4	5	7	97	56	77:23
Mo5	5	7	91	55	72:28
Mo6	3	7	80	62	85:15
Mo6	1.2	7	75	56	92:8
W1	5	7	80	62	91:9
W4	5	7	14	10	95:5

[1] The reaction was carried out in CH_2Cl_2 at 40 °C.

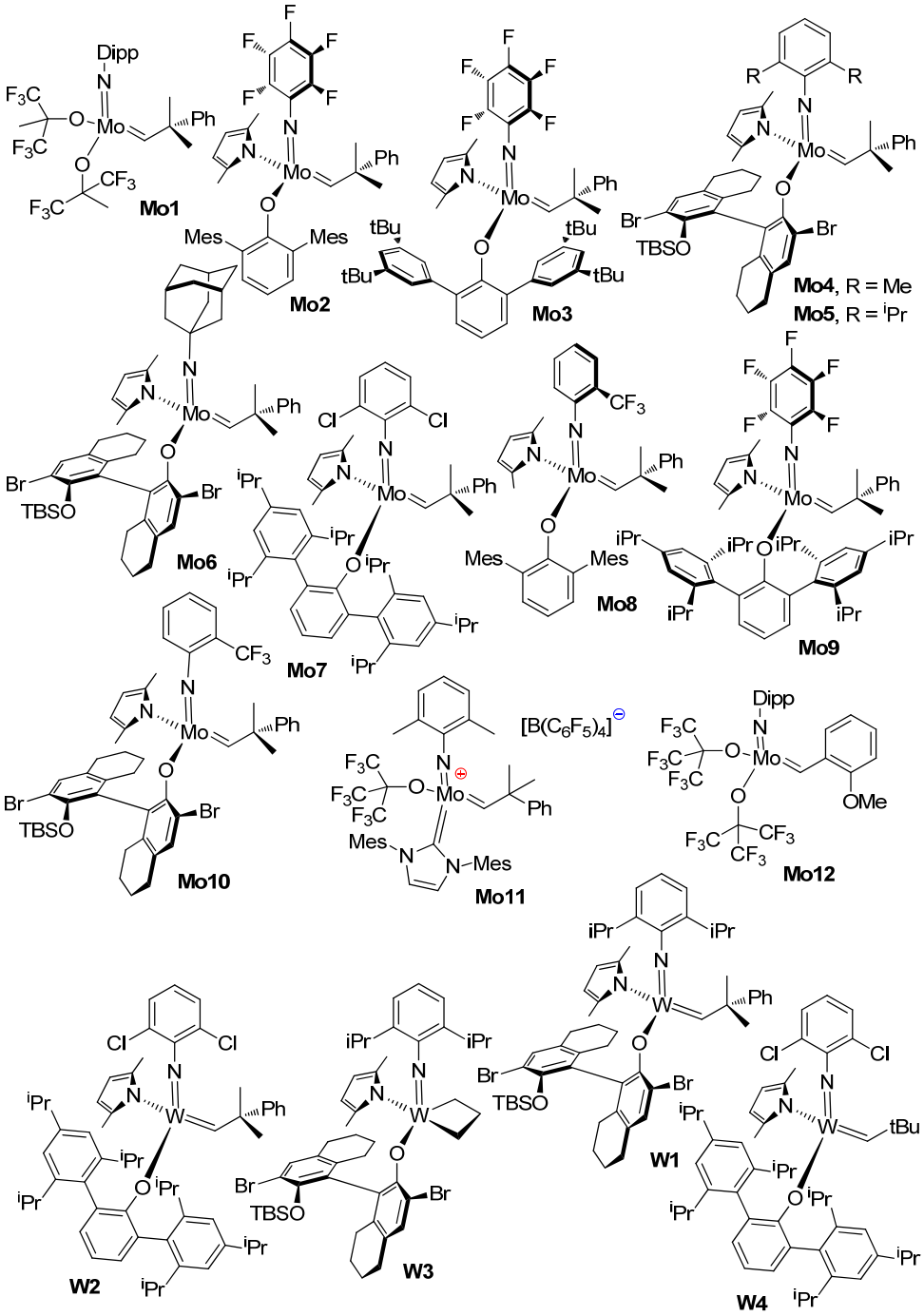

Scheme 17. Group 6 metal complexes studied in RCM of alkenyl alkenoates.

The stereoselectivity of **Mo6** depended on the size of the UM: for 5 mM substrate solutions in toluene at 22 °C with a 3 mol% catalyst loading, the (*Z*)-selectivity was 69, 80, 85 and 91% for 13-, 14-, 16- and 17-membered macrolactones, respectively [46]. The complex **W3** (5 mol%) showed a similar productivity and 73, 82 and 88% (*Z*)-selectivities for 13, 14 and 17-membered UMs. The isolated yields of Yuzu lactone (13-membered) and ambrettolide (17-membered) were ~50 and 80%, respectively. It was also demonstrated that W catalysts are less sensitive to oxygen and moisture in comparison with Mo complexes [46].

In 2014, Schrock and Hoveyda for the first time successfully carried out the RCM of ω-alkenyl acrylates [78]. In the RCM of CH_2=CHCOO(CH_2)$_{10}$CH=CH_2 **Ru14** showed moderate activity (see Table 3); **Mo4**, **Mo8**, **Mo9** and **W4** showed low conversions (<10%

after 2 h at 10 mol% catalyst loading); **Mo1** and **Mo10** were moderately active (30 and 61%, respectively); and the complex **Mo2** showed a 60% yield and 89% (*Z*)-selectivity. Other ω-alkenyl acrylates and unsaturated esters, containing a conjugated diene fragment, were also converted to UMs using **Mo2** (Scheme 18).

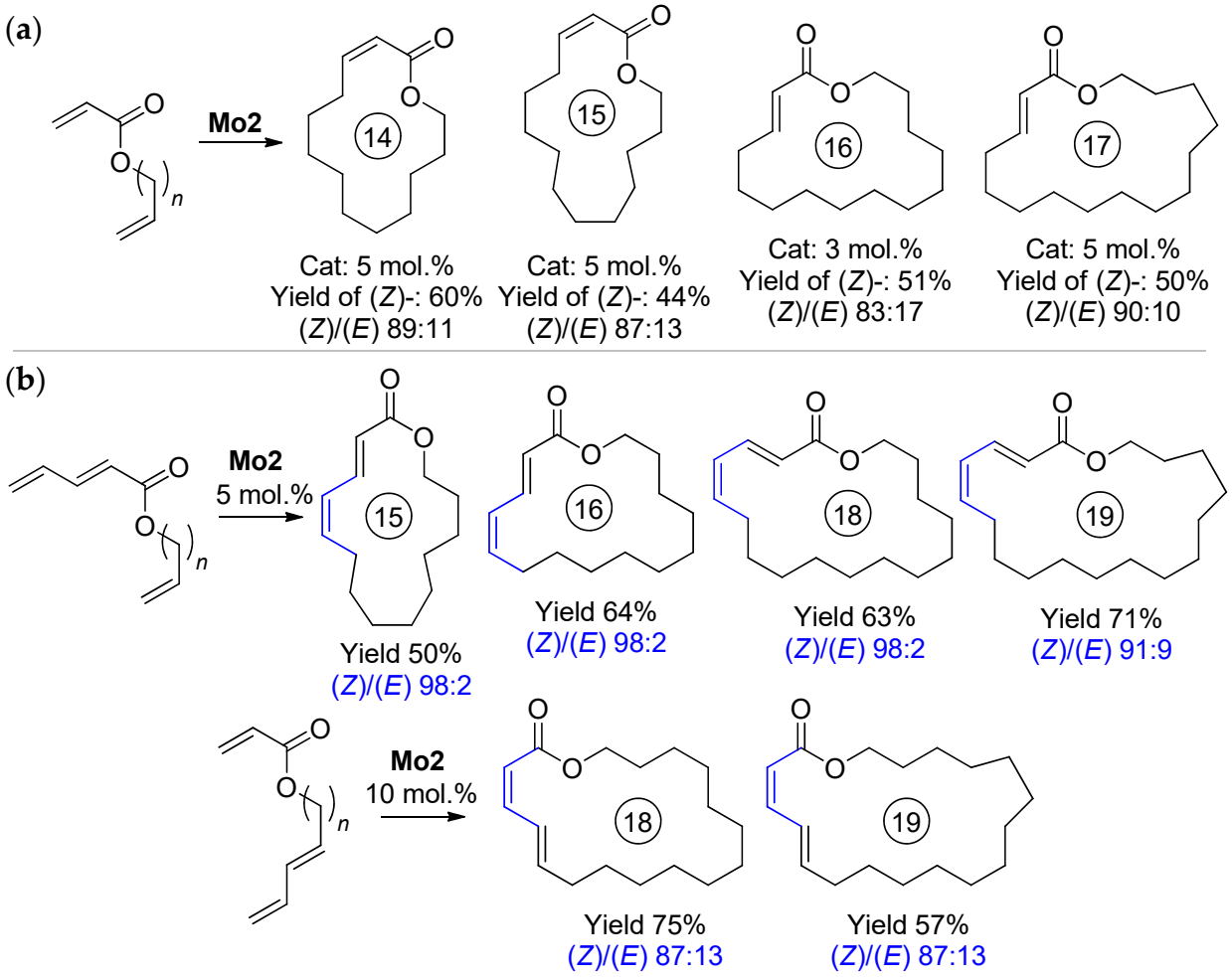

Scheme 18. (*Z*)-selective RCM, catalyzed by **Mo2**: (**a**) Cycllization of acrylates. (**b**) Cyclization affording (*E*,*Z*)- and (*Z*,*E*)-dienoates. Substrate concentration 2 mM in C_6H_6, 22 °C, 100 torr [78].

The results of DFT calculations of the relative stability of (*Z*)- and (*E*)-isomers of MUs with one C=C bond conjugated with a C=O group (macrocyclic enoates) and conjugated isomeric dienoates are presented in Figure 9 [78]. For enoates and dienoates, the thermodynamic preference for the (*E*)-isomer is reached at large (14+) ring sizes; therefore, the composition of the reaction mixtures, formed with the use of the **Mo2** catalyst, is determined by kinetic control—in other words, by the (*Z*)-stereoselectivity of the **Mo2** catalyst. The kinetically controlled (*E*)-selective synthesis of UMs can be provided by the use of diene substrates with (*E*)-configurations of C=C bonds. In 2017, Hoveyda and coll. investigated the catalytic behavior of **Mo3** (5 mol.%, 22 °C, 2 h at 28 torr) in the RCM of (*E*)-CH_2=$CH(CH_2)_3COO(CH_2)_9CH$=CHX (1 mM in toluene) [109]. High (*E*)-selectivities (96 and 93%) were achieved when using substrates containing X = –B($OCMe_2CMe_2O$) (B(pin)) and –B($OCMe_2CH_2CHMeO$), respectively. The RCM of functionalized substrates (*E*)-CH_2=$CH(CH_2)_nCOO(CH_2)_mCH$=CHB(pin) under the same conditions resulted in the formation of cyclic lactones; the yields and (*Z*)/(*E*) ratios were 60% and 4:96 (*n* = 3, *m* = 9), 57% and 4:96 (*n* = 5, *m* = 3), 40% and 9:91 (*n* = 6, *m* = 3), 40% and 6:94 (*n* = 6, *m* = 4), 59% and 2:98 (*n* = 8, *m* = 4) and 40% and 9:91 (*n* = 6, *m* = 9). A 21-membered lactone (2:98 (*Z*)/(*E*)

ratio) was synthesized with a 51% yield from a B(pin)-functionalized derivative of unced-10-enoic acid B(pin)CH=CH9CH_2)$_8$COO(CH_2)$_9$CH=CH_2. The synthesis of 12-membered UM from CH_2=CH(CH_2)$_6$COO(CH_2)$_2$CH=CHB(pin) deserves special mention: a 48% yield of pure (*E*)-isomer was achieved (when using an **Ru2** catalyst, the maximum yield was 29% with a (*Z*)/(*E*) ratio of 21:79).

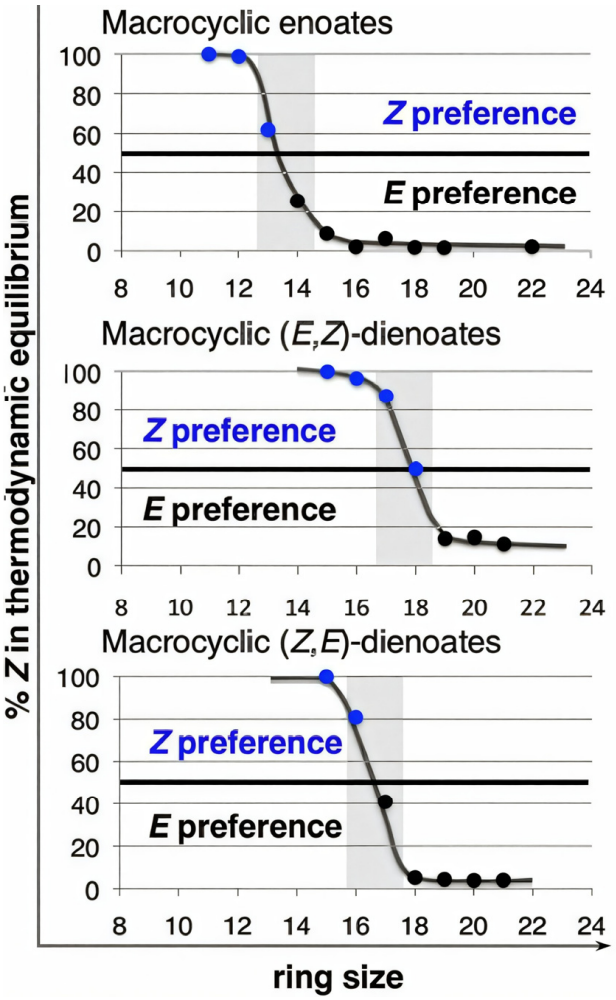

Figure 9. Variations in the thermodynamic preferences of different unsaturated macrocyclic alkenes. Reprinted with permission from [78]. Copyright (2014) American Chemical Society.

The idea of the use of the ordered mesoporous support SBA-15 (RCM in confined geometries) was also implemented for Mo complexes of *N*-heterocyclic carbenes, e.g., **Mo11** [110]. Up to 98% RCM selectivities were achieved at a 1 mol% loading of the catalyst and up to a 100 mM concentration of the substrates. However, **Mo11** is cationic, which imposes certain restrictions on its use due to a lower chemical stability and higher sensitivity to catalytic poisons.

Perhaps the most interesting actual study in the field of the RCM of alkenyl alkenoates, catalyzed by Mo complexes, was performed by Grela and coll. [111]. The high thermal stability of metathesis catalyst **Mo1** was successfully implemented in the vacuum distillation RCM of (*Z*)-non-6-en-1-yl oleate (Figure 10).

Since molybdenum alkylidenes did not cause a C=C migration even at 100–120 °C, the reaction proceeded with high selectivity, leading to well-defined UMs (Scheme 19).

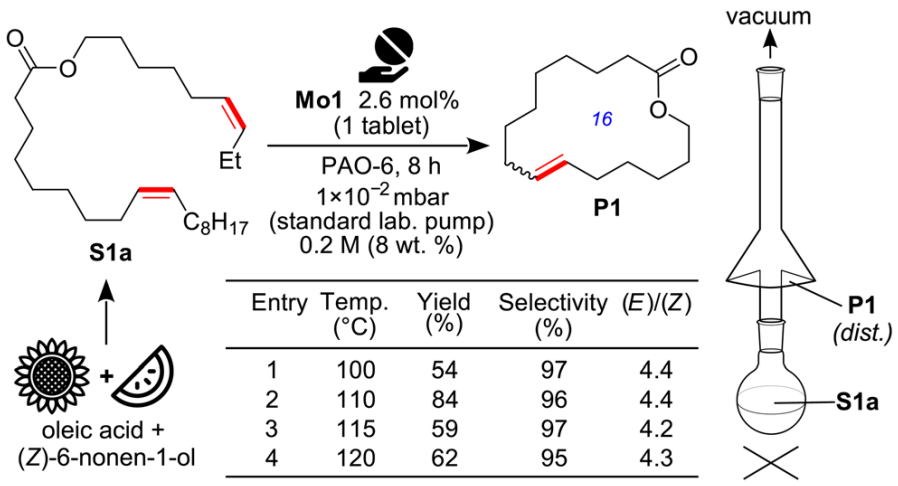

Entry	Temp. (°C)	Yield (%)	Selectivity (%)	(*E*)/(*Z*)
1	100	54	97	4.4
2	110	84	96	4.4
3	115	59	97	4.2
4	120	62	95	4.3

Figure 10. Practical promise of high-concentration RCM promoted by **Mo1** in synthesis of 16-membered UM. Reprinted with permission from [111]. Copyright (2023) Royal Society of Chemistry.

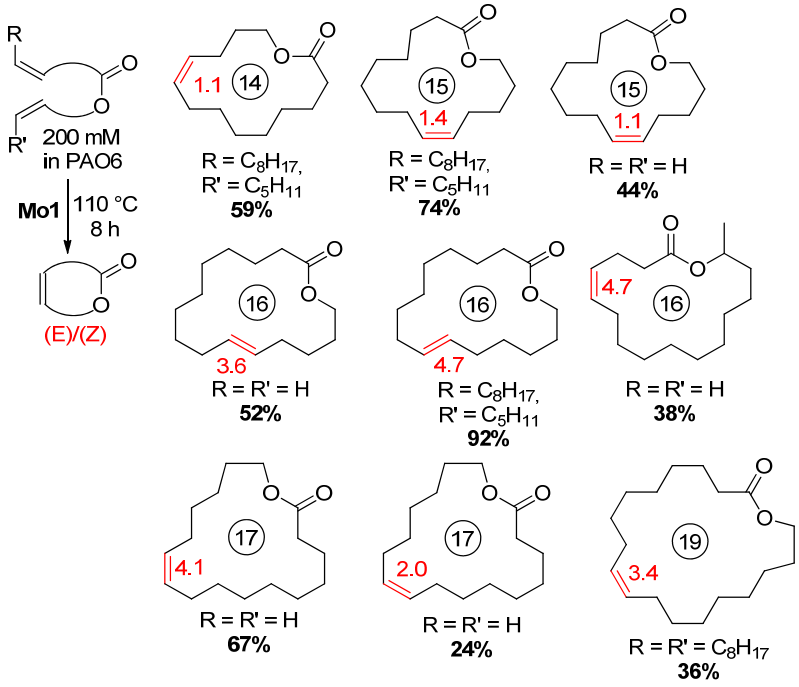

Scheme 19. Scope and limitations of high-concentration RCM promoted by **Mo1** [111].

2.6. Ring-Closing Depolymerization of Unsaturated Polyesters

The results of a number of the above-mentioned works can be considered as examples of the depolymerization approach to UMs—the actual processes of the RCM of alkenyl alkenoates [31,83,99,111], based on the distillation of low-MW UMs, involve the intermediate formation of the unsaturated oligo-/polyesters. Ring-closing depolymerization (cyclodepolymerization, CDP) deserves special consideration in view of the actual trends in polymer chemistry, focused on polymer recycling and/or upcycling [112–114], in the framework of the circular plastics economy concept [115,116]. CDP with the formation of UMs is a special case of metathesis polymer deconstruction described in a recent review of Wang and coll. [117].

Metathesis CDP, as well as the RCM of alkenyl alkenoates, requires high dilutions (mM concentrations of the macrocycles formed) and near quantitative conversions [9]. As mentioned above, thermodynamically controlled CDP may be implemented via the

elimination of the low-MW UMs from the reaction mixtures at elevated temperatures. However, biasing the kinetic product distribution toward the formation of macrocycles can also be realized, in particular by the development of new catalysts [118].

The synthesis of UMs via kinetically controlled CDP has not been sufficiently examined so far. Some key patterns of similar processes were revealed very recently by Foster and coll. by an example of isomeric bis(ω-alkenyl) phthalates and the corresponding ADMET and RCM products with the use of **Ru2**, **Ru6**, **Ru13**–**Ru15** and **Ru17** [119]. The catalyst **Ru17** showed the most promising characteristics, enabling the reaching of high conversions of polymers to RCM products at substrate concentrations up to 0.1 M. Further studies as applied to the synthesis of aliphatic UMs hold promise.

2.7. Transesterification Depolymerization of Unsaturated Polyesters

As was mentioned above, it has been proven in a number of cases [33,49] that UMs are formed from low-MW oligomers, the products of the ADMET of alkenyl alkenoates via metathesis backbiting. However, the backbiting of ADMET products can also be carried out through transesterification, via the intramolecular cleavage of C(O)–O bonds in copolymer. The natural limitation of this alternative approach is the statistical nature of the ADMET products that evidently include head-to-tail, head-to-head and tail-to-tail units in their structures (Scheme 20). A similar statisticity does not matter for RCM, but it complicates ring-closing transesterification significantly.

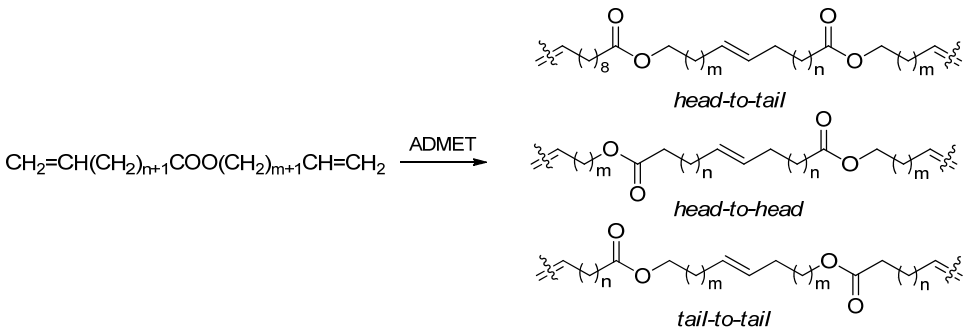

Scheme 20. The structural fragments in the products of the ADMET of alkenyl alkenoates.

During the transesterification of CH_2=CH(CH_2)$_7$COO(CH_2)$_6$CH=CH_2 polymer with the distillation of the reaction products (PEG200 as a solvent, 190–200 °C, 10 mbar, 40 h, Ti(O^{i}Pr)$_4$), a 75% yield of ambrettolide was achieved (43 g of the product of 87% purity from 100 g of polymer) [120]. The yield in the experiment on metathesis depolymerization with distillation, catalyzed by **Mo12**, was 60% [120]. The depolymerization of polyester, obtained by the ROTEP of ω-6-hexadecenlactone (see Section 3.1), with the use of $ZnCl_2$/PEG600, recovered 40% of the starting monomer [121].

Summarizing the information presented in Section 2 in view of the potential industrial scalability and sustainability of the RCM of alkenyl alkenoates, let us dare to propose most promising directions for the further development of this catalytic process according to Green Chemistry principles [122] and actual standards for advanced chemical technologies.

- To avoid the problems associated with the use of large volumes of solvents (and related problems of toxicity, recycling, etc.), the further development of the Grela approach, based on the distillation of low-MW target products, appears to be a promising technical solution. The use of non-toxic [123] hydrogenated dec-1-ene oligomers as a reaction medium is an added benefit of this approach;
- It makes sense to guide the further design and development of the catalysts toward thermally stable heterogeneous systems. It is not obvious that Ru-based catalysts are

out of the competition: Mo-based catalysts also demonstrated promising results [111]; further studies make perfect sense;

- In terms of circular economy, the RCM or ring-closing transesterification of unsaturated polyesters might be a substantial source of UMs and related cyclic substrates for subsequent polymerization (see Section 3).

However, these efforts are meaningful if the UMs will be in demand and cannot be considered without taking into account the prospects of the use of UMs for the development of new materials (see Section 3 below).

3. Polyesters Based on Unsaturated Macrolactones

In Section 2, the preparation of a wide range of unsaturated macrolactones was described. Many of these compounds—at least in theory—can be considered as a substrates for the synthesis of unsaturated polyesters. Evidently, there are two different catalytic approaches to similar polymers [2].

The first is based on ring-opening metathesis polymerization (Scheme 21a). The significant drawbacks of this approach are as follows:

- Low regioselectivity: formation of head-to-tail, head-to-head and tail-to-tail fragments (see Scheme 20);
- Excessive complexity: the same polymers can be obtained by the ADMET of alkenyl alkenoates, avoiding the labor-intensive stage of the synthesis of UMs.

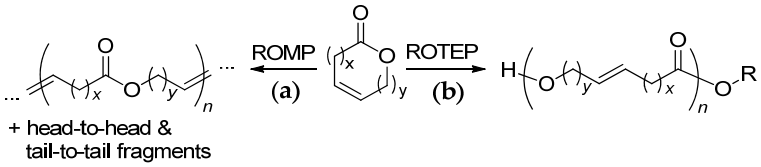

Scheme 21. Two main synthetic approaches to unsaturated polyesters: (**a**) ring-opening metathesis polymerization and (**b**) ring-opening transesterification polymerization.

The second approach is ring-opening transesterification polymerization (ROTEP, Scheme 21b). Being initiated by ROH in the presence of the catalyst of complex metal alkoxide L_nMOR, ROTEP results in the formation of polyesters containing only head-to-tail fragments. The polycondensation of ω-hydroxyalkenoic acids results in similar products, but ROTEP is usually preferred as a less energy-consuming method that provides a higher level of chain control (the degree of polymerization and dispersity $Đ_M$).

Polymers based on macrolactones were the subject of the brief review of Dove, Heise and coll., published in 2019 [2]. In this review, significant attention has been given to (co)polymers of saturated macrolactones; however, the main features and specifics of the synthesis of polyesters and the prospects of their applications have been insufficiently addressed. In this section, we tried to summarize all the information concerning UM-based (co)polymers, which has not been done previously.

3.1. Ring-Opening Transesterification Polymerization of Unsaturated Macrolactones

As mentioned above (and widely accepted in the scientific community [124,125]), the ROTEP of lactones provides excellent control over the polymerization process to produce high-MW products with a sharp molecular weight distribution under relatively mild reaction conditions. There is a qualitative difference between the ROTEP of medium ring-sized cyclic esters (6-membered δ-valerolactone δVL, lactides LA, 1,4-dioxan-2-one PDO, 1,3-dioxan-2-one (trimethylene carbonate) TMC, 7-membered ε-caprolactone εCL, 1,4-dioxepan-5-one, etc., see Scheme 22) and macrolactones (including saturated monomers,

see Schemes 22 and 23). In the first case, the process is driven by ring strain, but in the latter case ROTEP is more entropically driven [126]. For entropically driven polymerization, the advantages of enzymatic catalysis are long known [127], and it was this type of catalyst that was used for the ROTEP of UMs in most works (Section 3.1.1). In addition, the use of coordination catalysts in the ROTEP of UMs is also known and presented in a number of examples (Section 3.1.2).

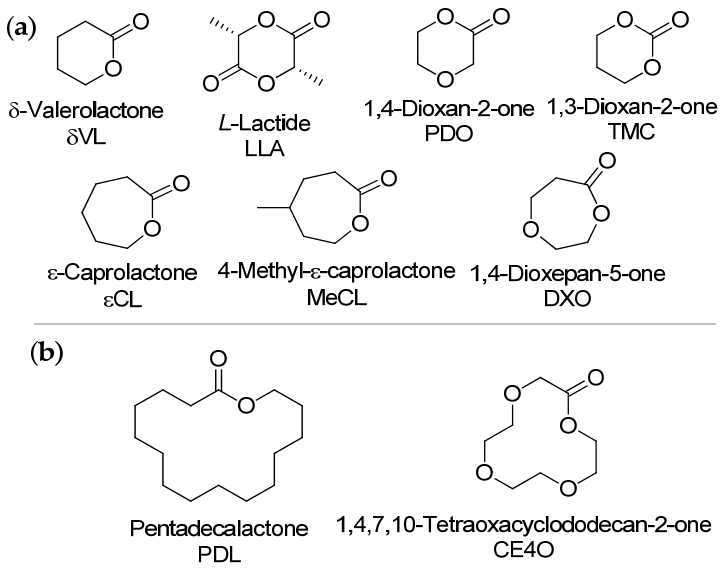

Scheme 22. Conventional ROTEP substrates: (**a**) Strained cyclic esters. (**b**) Saturated macrolactones.

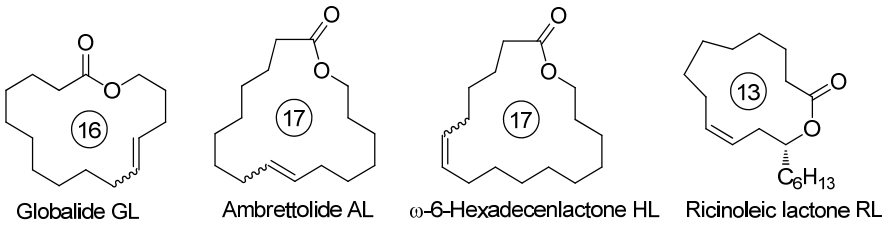

Scheme 23. Unsaturated macrolactones used in ROTEP as cyclic monomers.

In this part of the review, we tried to summarize and discuss all the published information related to the ROTEP of UMs. Surprising but true: despite the diversity of UMs separated and/or synthesized to date, only four UMs have been investigated as a ROTEP substrate, namely globalide (GL), ambrettolide (AL), isomeric to the latter ω-6-hexadecenlactone (HL), and the product of the intramolecular esterification of ricinoleic acid (RA), the corresponding 13-membered substituted lactone (RL, Scheme 23).

3.1.1. Enzyme-Catalyzed ROTEP and Copolymerization of UMs

Certain aspects of the lipase-catalyzed ROTEP of UMs were discussed in a recent review (2023) devoted to the polymerization of natural compound-based cyclic monomers [128]. Below, we summarized the results of the studies of the (co)polymerization of UMs with the use of enzymatic catalysis. To date, lipase family enzymes (mainly *Candida antarctica* Lipase B) have been investigated in the ROTEP of Ums; the polymer yield and characteristics were significantly dependent on the type of cyclic substrate, the presence and amount of comonomer and catalyst and reaction conditions [129–145] (Table 7).

Table 7. Enzyme-catalyzed ROTEP and copolymerization of UMs. For comonomer abbreviations, see Schemes 21 and 22.

UM	Comon. (C)	[UM]/[C] Ratio [1,2]	Catalyst (Loading, mg·g^{-1})	Reaction Medium	Time, h	T, °C	Yield, %	M_n, kDa	$Đ_M$	Ref.
GL	–	–	Novozym 435 [3] (21)	toluene	4	60	~70	24.2	1.92	[129]
GL	–	–	Novozym 435 (40)	toluene	24	60	80–90	24	1.9	[130,131]
GL	–	–	Novozym 435 (40)	toluene	24	60	~70	15	2.8	[132]
GL	–	–	Novozym 435 (210)	toluene	4	60	~60	16	2.5	[133]
GL	–	–	Novozym 435 (40)	toluene	4	60	~60	25	–	[134]
GL	–	–	free *Candida antarctica* B in sorbitol	$C_{16}H_{34}/H_2O$/em. [4]	5	60	–	3.6	2.1	[135]
GL	–	–	Novozym 435	bulk	–	–	–	6.35	3.4	[136]
GL	–	–	NS 88011 (20)	toluene	2	60	–	20.9	4.7	[137]
GL	–	–	NS 88011 (100)	toluene	2	60	–	31.7	3.8	[137]
GL	–	–	Novozym 435 (60)	toluene	4	60	80	20	3.5	[138]
GL	–	–	Novozym 435 (210)	toluene	4	60	97	4.7	–	[139]
GL	–	–	*Candida antarctica* B on Immobead 150 [5]	toluene	4	60	69	30.7	1.38	[140]
GL	–	–	Novozym 435 (60)	sc CO_2 [6]	2	65	85	15.2	1.66	[141]
GL	–	–	Novozym 435 (60)	sc propane [6]	2	65	72	16.6	2.41	[141]
AL	–	–	Novozym 435 (21)	toluene	4	60	~70	18.5	1.94	[129]
AL	–	–	Novozym 435 (40)	toluene	24	60	80–90	24	1.9	[130,131]
GL	DXO	9–0.4 wt [1]	Novozym 435 (40)	toluene	24	60	80–90	11–44	1.8–2.5	[130,131]
GL	MeCL	9–0.4 wt [1]	Novozym 435 (40)	toluene	24	60	80–90	6–18	2.0–2.5	[130,131]
GL	εCL	0.89–0.11 [2]	Novozym 435 (40)	toluene	24	60	~70	15–23	2.4–3.3	[132]
GL	εCL	0.05–4.3 [1]	Novozym 435 (50)	sc CO_2 [6]	–	65	–	up to 25	–	[142]
GL	εCL	1 [1]	Novozym 435 (50)	sc CO_2	2	65	–	–	–	[143]
GL	εCL	0.1–9 wt [1]	Novozym 435 (50)	sc CO_2	2	65	–	–	–	[144]
AL	CE4O	3–0.4 wt [1]	Novozym 435 (40)	toluene	24	60	80–90	8–14	1.4–2.0	[130]
AL	PDL	1:1 [1,2]	Novozym 435 (100)	toluene	24	70	–	8.2	–	[145]

[1] In feed. [2] In copolymer. [3] Novozym 435—*Candida antarctica* Lipase B immobilized on cross-linked polyacrylate beads. [4] Lutensol AT50 emulsifier was used. [5] Immobead 150—epoxy-containing methacrylate polymer. [6] Supercritical CO_2.

The homopolymerization of AL and HL, catalyzed by Novozym 435 (the commercially available catalyst, *Candida antarctica* Lipase B, immobilized on cross-linked polyacrylate) was first performed in 2008 [129]; the semicrystalline polymers had T_m = 58.8 and 96.2 °C (first heating run) and crystallization temperatures T_c = 37.7 and 76.6 °C, respectively. Over the years, the methods of the (co)polymerization of UMs have been worked out (Table 7); copolymers with εCL, MeCL, DXO, CE4O and PDL were prepared. Ther mini-emulsion polymerization of GL using pure lipase resulted in the formation of nanoparticles with an average diameter d = 80–280 nm [135]. In 2018 [137], it was shown that the commercial catalyst NS 88011 demonstrates higher activities in the ROTEP of GL in comparison

with Novozym 435. The Novozym 435-catalyzed ROTEP of GL and GL/PDL copolymerization were optimized recently with the use of supercritical CO_2 or propane reaction medium [141,146–148]. The reversibility of the enzyme-catalyzed ROTEP of GL and HL was demonstrated recently by Martínez de Ilarduya and coll., setting the stage for the further development of the enzymatic recycling of similar polymers [149].

The Novozym 435-catalyzed ROTEP of GL, initiated by $HO(CH_2)_4OH$, resulted in the obtaining of well-defined macroinitiator that was used in the synthesis of a triblock copolymer with LLA, using $Sn(Oct)_2$ as a catalyst [150].

3.1.2. ROTEP and Copolymerization of UMs, Catalyzed by Acids and Metal Complexes

The examples of the non-enzymatic ROTEP of UMs reported in scientific periodicals are relatively few in number [151–157] (Table 8); the structures of the catalysts are presented in Scheme 24.

Table 8. Synthesis of UM (co)polymers using non-enzymatic catalysis.

UM	Comon. (C)	[UM]/[C] Ratio [1,2]	Catalyst (Loading)	Reaction Medium	Time, h	T, °C	Yield, %	M_n^{SEC}, kDa	$Đ_M$	Ref.
GL	–	–	DBSA [3] (2 mol%)	in bulk	72	80	>98	7.8	2.55	[151]
GL	–	–	CF_3SO_3H (10 mol%)	in bulk	7	80	>98	n.d. [4]	n.d.	[151]
GL	–	–	DBSA (10 mol%)	$H_2O/C_{16}H_{34}$/em. [5]	24	80	88	1.4	–	[151]
AL	–	–	DBSA (10 mol%)	in bulk	24	80	>98	6.3	2.94	[151]
AL	–	–	CF_3SO_3H (10 mol%)	in bulk	7	80	>98	n.d.	n.d.	[151]
AL	–	–	DBSA (10 mol%)	$H_2O/C_{16}H_{34}$/em.	24	80	85	1.66	–	[151]
AL	–	–	**Al1** (1 mol%)	1 M in toluene	140	100	>98	12.1	6.7	[152]
AL	–	–	**Al1** (0.2 mol%)	in bulk	16	100	–	49	2.7	[153]
HL	–	–	**Al2** (1 mol%)	xylenes	27	100	60	15.4 [6]	1.6	[154]
HL	–	–	**Al2** (0.4 mol%)	xylenes	27	130	60	36.3 [6]	1.6	[154]
HL	–	–	**Al2** (0.4 mol%)	xylenes	27	130	45	12.6 [6]	1.8	[155]
HL	–	–	**Zn1** (0.5 mol%)	toluene	24	100	70	12.6 [6]	1.7	[156]
RL	–	–	Me_3SiONa (2 mol%)	THF	114	40	–	1.4	1.1	[157]
HL	εCL	1	**Al2** (1 mol%)	xylenes	29	100	75	15.8 [6]	1.6	[154]
HL	εCL	0.33	**Al2** (1 mol%)	xylenes	29	100	60	39.2	1.8	[155]
HL	εCL	0.1–1	**Zn1** (0.5 mol%)	toluene	24	100	50–70	14.7–18.2	1.5–1.6	[156]
HL	PDL	0.1–1	**Zn1** (0.5 mol%)	toluene	24	100	42–63	12.3–21.4	1.5–1.6	[156]
AL	PDL	0.05–1	**Al1** (0.2 mol%)	in bulk	16	100	–	48–87	2.2–2.6	[153]
RL	LLA	0.07–0.2	$Sn(Oct)_2$ (1.5 wt%)	toluene	4	135	–	4.7–9.9	1.3–1.5	[157]

[1] In reaction mixture. [2] In copolymer. [3] Dodecylbenzene sulfonic acid. [4] Not determined, high-MW polymer. [5] A3065 emulsifier was used. [6] Determined by ^1H NMR.

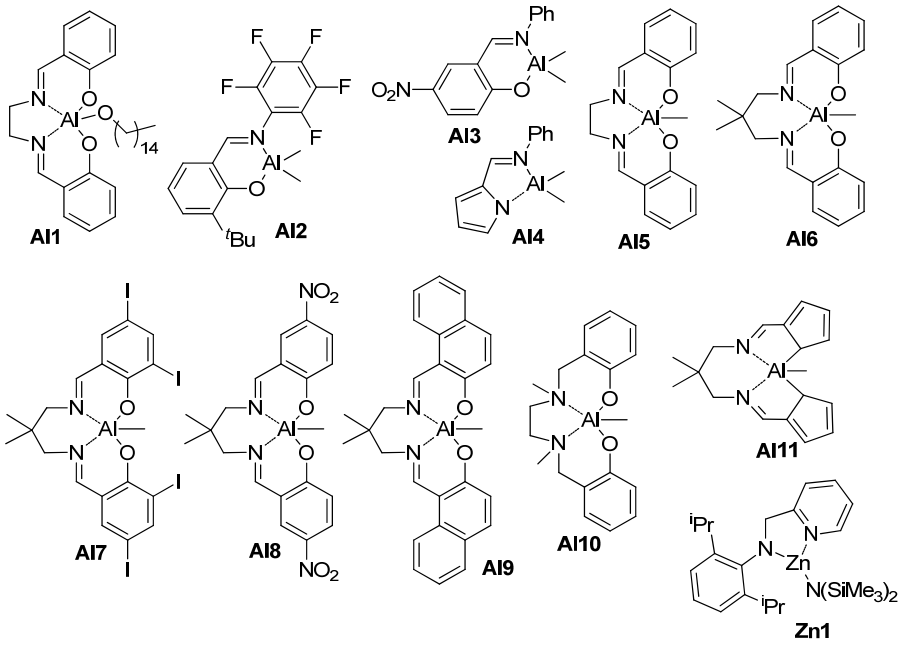

Scheme 24. The structures of coordination catalysts studied in ROTEP of UMs.

In 2013, Mecerreyes and coll. reported the results of their study of the acid-catalyzed polymerization of GL and AL with the use of BnOH as an initiator [151]. The rate of polymerization depended on the pK_a value (CF_3SO_3H > Dodecylbenzenesulfonic acid (DBSA) > $(PhO)_2P(O)OH$). In addition to bulk polymerization, mini-emulsion ROTEP was carried out, with the formation of latexes suitable for subsequent cross-linking with the use of benzoyl peroxide (BPO) [151].

The complex **Al1** (Scheme 24) was studied in the ROTEP of AL; homopolymers were characterized by a broadened MWD due to the partial formation of cyclic polymers with lower molecular weights [152]. One year later, the **Al1**-catalyzed synthesis of AL homopolymers and copolymers with PDL was described; the obtained (co)polymers had an M_w = 106–199 kDa and $Đ_M$ = 2.2–2.7 [153]. The less sterically hindered complex **Al2** was used in the polymerization of HL [154]; homopolymers with an M_n = 8.9–36.3 kDa were obtained. This catalyst was also used for the synthesis of block- and stat-copolymers of HL with εCL [154,155]. In 2020, Naddeo et al. proposed the use of the pyridylamido zinc(II) complex **Zn1** (Scheme 24) as a catalyst of the BnOH-initiated ROTEP of HL and its copolymerization with εCL and PDL [156]. Poly(HL) had a T_m = 55 °C. Poly(HL-*co*-εCL) containing 73 mol% of εCL units had a T_m = 42 °C. Very recently, Al complexes **Al3**–**Al12** were synthesized and studied in the (co)polymerization of HL; the complexes **Al5**, **Al6** and **Al11** (Scheme 24) demonstrated higher activities [158].

The homopolymerization of RL, catalyzed by Me_3SiONa, yielded low-MW polymer; the same results were obtained when using a mixture of RL with cyclic dimer and trimer [157]. In the same work, the copolymerization of RL with LLA, catalyzed by Tin(II) 2-ethylhexanoate ($Sn(Oct)_2$), resulted in the formation of random copolymers containing 6.3–17 wt% of RA (melting point T_m = 105–130 °C).

3.2. Alternative Approaches to Unsaturated Polyesters

Evidently, UMs may also be subjected to ring-opening metathesis polymerization (ROMP), with the formation of polymers with a similar structure. GL and its homologs remain virtually unexplored in ROMP, because alkenyl alkenoates can be introduced to ADMET with the same results. However, if there is an efficient approach to UMs that does not use non-conjugated dienes as a raw materials, the use of ROMP makes more sense. The classic example of a similar synthetically available macrolactone is RL.

(Co)polymers of RA could be obtained by the polycondensation of RA or RA esters [159–163] and by the ROTEP [157] or ROMP [164,165] of RL. As was mentioned in Section 3.1, the ROTEP of RL was found to be ineffective in the synthesis of high-MW poly(RA). In 2020, hetero-dimeric monomers of RA and 4-hydroxycinnamic acid were prepared and introduced to polycondensation in the presence of *N*,*N*-dimethyleminopyridine (DMAP) or its tosylate; the highest M_n was 24.3 kDa [160]. Recently, high-MW poly(RA) was synthesized via the solution polycondensation of methyl ricinoleate in 1-alkyl-3-methylimidazolium bis(trifluoromethanesulfonyl)imide ILs with the retaining of a (*Z*)-configuration; homopolymers with an M_n up to 64.7 kDa were obtained [163]. Poly(RA) had a T_g = −72.8 °C and decomposition temperature T_d = 319 °C; the authors considered poly(RA) as a degradable elastomer. Catalytic ROMP (**Ru6**) was successfully applied in the synthesis of the copolymer of RA with bile acid monomer (Scheme 25); copolymers with an M_w up to 530 kDa were obtained [164].

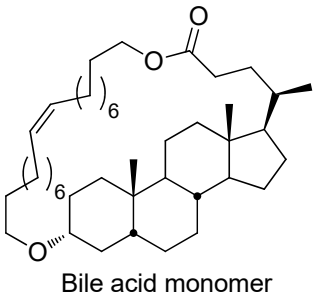

Scheme 25. The structure of bile acid monomer used in co-ROMP with RL [164].

The ROMP of UMs starts to make sense when synthetically available cycloolefin is introduced into the copolymer backbone at a high ratio. In 2012, Duchateau and coll. synthesized a series of copolymers of AL and (*Z*)-cyclooctene (Scheme 26), used for the preparation of polar analogs of polyethylene (PE, see Section 3.3.3) [166]. The copolymerization of HL and norbornene in the presence of **Ru2**, **Ru6** or **Ru14** resulted in copolymers with an M_n up to 134 kDa; their elasticity increased with the increase in HL content [167]. The homopolymerization of HL (**Ru2**, **Ru6** or **Ru14**) was conducted by Martínez and coll. in 2018; the highest M_n of 155 kDa was achieved in $C_2H_4Cl_2$ (0.1 mol% **Ru14**) [168].

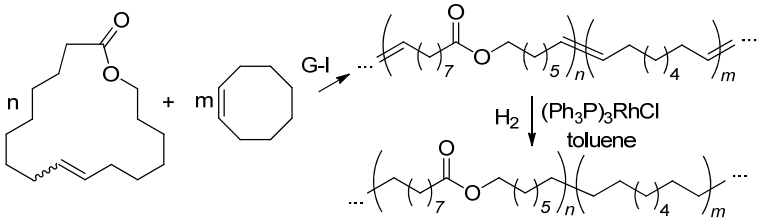

Scheme 26. Ring-opening metathesis polymerization of AL and (*Z*)-cyclooctene and subsequent hydrogenation [166].

3.3. Post-Modification of Unsaturated Polyesters and Application Prospects

3.3.1. Post-Modification of Unsaturated Polyesters

A homopolymer of AL was subjected to thermal cross-linking with the use of dicumyl peroxide (DCP), which resulted in the complete disappearance of T_m and T_c peaks [129]. Poly(GL-*co*-MeCL) (75:25) had a T_m = 35.5 °C and represented opaque material; thermal cross-linking (DCP) resulted in the formation of transparent films (Figure 11). Poly(GL-*co*-DXO) had an enhanced biodegradability due to higher hydrophilicity [131].

Figure 11. Poly(Gl-*co*-4MeCl) (75:25) before (**left**) and after (**right**) thermal cross-linking with dicumyl peroxide. Reprinted with permission from [131]. Copyright (2011) American Chemical Society.

The common methods of the post-functionalization of unsaturated polyesters are based on thiol-ene click chemistry. In 2011, poly(GL) was functionalized by the reaction with 6-mercapto-1-hexanol, butyl-3-mercapto propionate and N-acetylcysteamine, with the formation of polymers with a saturated backbone [169]. An attempt at pre-functionalization (by the AIBN-induced reaction of GL with N-acetylcysteamine) resulted in a cyclic substrate that was found to be inert in ROTEP [170]. However, the cyclic monomers obtained by the reaction of AL with $^{n}C_5H_{11}SH$ or $HO(CH_2)_6SH$, were active in a copolymerization with PDL, initiated by **Al1**, that resulted in functionalized PE-like copolymers [153]. Poly(GL-*co*-εCL) was cross-linked using $EtC(CH_2OC(O)CH_2CH_2SH)_3$, but in contrast with DCP cross-linking, more than 2 wt% of sol fraction was detected in copolymer containing 47 mol% of GL [132].

An efficient method of cross-linking with the use of thiol-ene chemistry was proposed by Heise and coll. in 2017: the reactions of poly(GL) with $HS(CH_2)_5SH$ or $(CH_2OC(O)CH_2CH_2SH)_2$ linkers were created using UV irradiation directly during the electrospinning (ES) [134]. Another non-standard approach was proposed by Mosnáček and coll.; transparent polymeric gels were obtained by the UV-initiated interaction of poly(GL) with a homopolymer of PEG-substituted SH-functionalized succinic acid [136]. The interaction of poly(GL) with $^{t}BuOC(O)NHCH_2CH_2SH$ resulted in a grafted polymer containing *N*-Boc substituents in side chains; after deprotection, derivatives of *L*-glutamic acid [139,171] and *L*-lysine [139] were obtained via condensation, with corresponding cyclic anhydride (Scheme 27). A similar synthetic strategy was used for the synthesis of poly(GL) containing oligo(*L*-alanine) fragments [172].

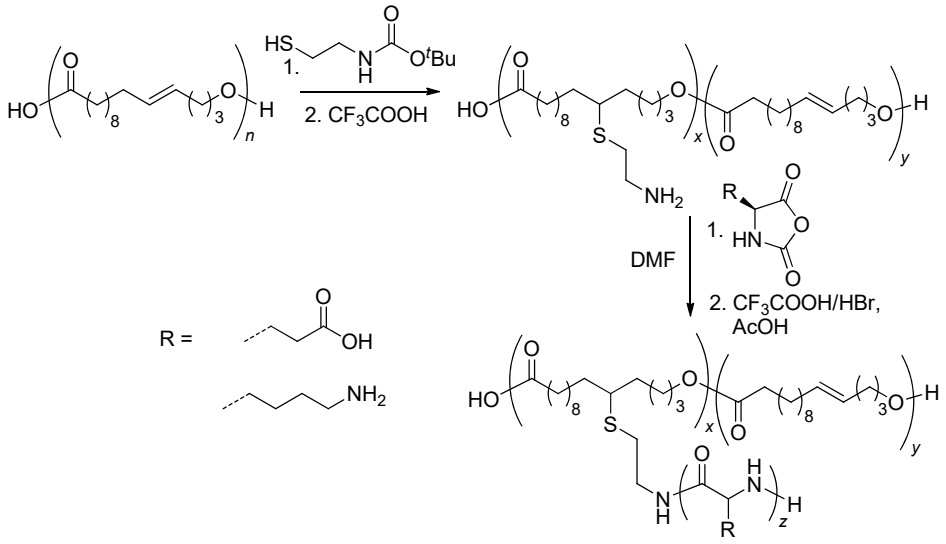

Scheme 27. Synthesis of poly[$(GL_{20}$-*g*-$(AA)_z$] copolymers (AA—amino acid fragment). An 11-ene isomer of GL is depicted for simplicity [139,171].

Another approach to the functionalization of poly(GL) was based on the reaction with triazolinediones [138]. Cross-linking was performed during ES molding (Figure 12); non-crosslinked and crosslinked fibers had different filament and surface morphologies. To increase poly(GL) biocompatibility, the polymer was functionalized by $HS(CH_2)_6OP(O)(OR)_2$ (R = Et, Ph); the ES of a 1:1 *w*/*w* mixture of functionalized poly(GL) and poly(PDL) resulted in the obtaining of scaffolds with an excellent morphology [173].

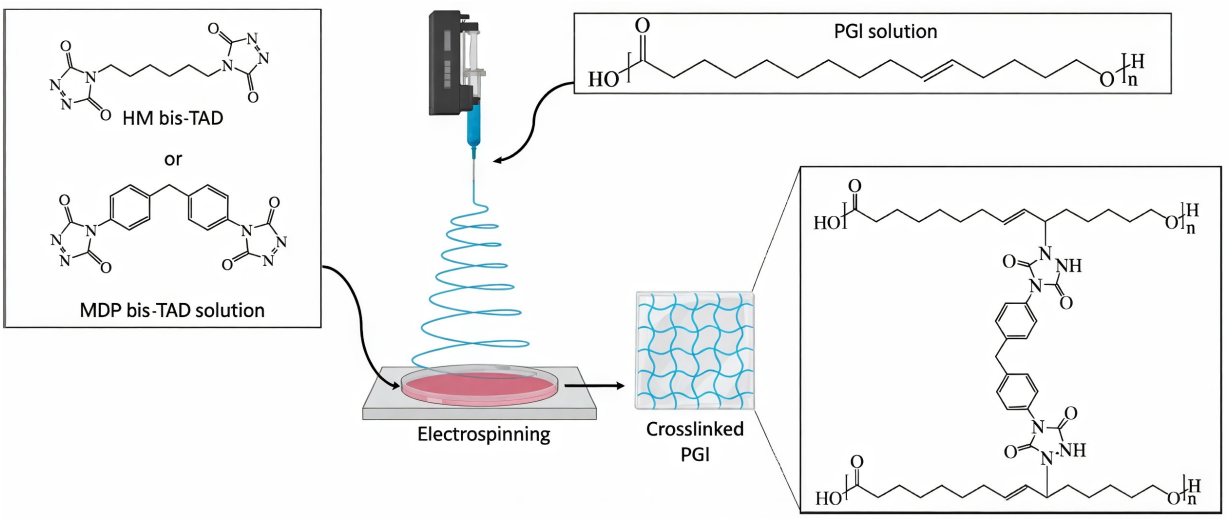

Figure 12. Electrospinning of poly(GL) into bis(triazolinedione) solutions. Reprinted with permission from [138]. Copyright (2019) MDPI AG.

The thiol-ene reaction was used for the introduction of reactive –S(CH_2)$_6$OH fragments at the surface of poly(GL) films, with a subsequent reaction with a-bromoisobutyryl bromide [133]. Functionalized films were used as a substrate for the atom transfer radical polymerization (ATRP) of ^{t}Bu acrylate, followed by deprotection with the formation of polyacids. The surface modification of poly(GL-*co*-εCL) nanoparticles by *N*-acetylcysteine (model reactant) and bovine serum albumine (BSA) was described in [143]. Functionalization of poly(GL-*co*-εCL) by *N*-acetylcysteine in solution was carried out in [144,174] the degree of functionalization was 40–80 mol% depending on the GL/εCL ratio. Poly(GL-*co*-εCL) was also functionalized by a thiol-ene reaction with *L*-cysteine; copolymer was used for the preparation of non-toxic superparamagnetic iron oxide nanoparticles containing reactive –COOH groups [175]. Poly(GL-*co*-PDL) ES mats were used for *L*-cysteine grafting followed by chemical binding with gelatin via EDC/NHS chemistry to increase the hydrophilicity and biocompatibility of fibrous scaffolds [176].

Poly(HL) was transformed to corresponding polyoxirane (3-chlorobenzoperoxoic acid (mCPBA) in CH_2Cl_2) with subsequent cross-linking by a reaction with Na(CN)BH_3/BF_3·Et_2O that resulted in an increase in the T_m from 57.6 to 65.8 °C [154].

The exhaustive hydrogenation of copolymers obtained by the co-ROMP of AL and (*Z*)-cyclooctene (Scheme 26) resulted in the formation of PE-like materials with promising characteristics (see Section 3.2) [166].

3.3.2. Cytotoxicity, Biocompatibility and Prospects of Biomedical Applications

A standard MTT test (3T3 mouse fibroblast cell line) revealed the absence of the cytotoxicity of AL and HL homopolymers [129]. ES-molded mats prepared from cross-linked poly(GL) showed a good biocompativility with mesenchymal stem cells (MSCs); the presence of S-containing linkers had no effect on cell viability [134].

In 2014, Heise and coll. synthesized poly(–COOH) functionalized films based on poly(GL) (see Section 3.3.2) and used these materials for the immobilization of proteins (fluorescent protein eGFP, Chitobiase enzyme) [133]. The obtained material demonstrated a high activity in the hydrolysis of N-acetylglucosamine.

BSA–poly(GL-*co*-εCL) nanoparticle conjugates were studied for cell uptake; a reduced internalization of the nanoparticles by Hela cells and macrophages was detected [143]. *N*-Acetylcysteine-functionalized poly(GL-*co*-εCL) demonstrated moderate antioxidant activity in both DPPH (EC_{50} = 4065 ± 157 μg·mL^{-1}) and ABTS (EC_{50} = 1553 ± 22 μg·mL^{-1}) assays

(for *N*-acetylcysteine, the EC_{50} = 4.31 ± 0.03 μg·mL^{-1} (DPPH) and EC_{50} = 137 ± 3 μg·mL^{-1} (ABTS)) [144].

Poly(GL) was simultaneously functionalized by HS-containing antimicrobal dyes and cross-linked with $(CH_2OCH_2CH_2SH)_2$ via the thiol-ene reaction [140]. The resulting organogels showed excellent antimicrobial activity against *S. aureus* and *E. coli*.

The colloidal behavior of functionalized poly(GL)s containing ~20 GL fragments and ~5 fragments of *L*-glutamic acid or ~12 fragments of *L*-lysine was studied in [139]. In aqueous media, they formed pH-responsive micelles; derivatives of *L*-glutamic acid were studied as doxorubicin delivery articles, whereas *L*-lysine derivatives demonstrated an ability to form polyplexes with salmon testes DNA [139]. Experiments on gene delivery were not conducted during this study.

Based on poly(GL) (M_n = 51 kDa, T_m = 44 °C), bilayered films with regenerated cellulose nanofibers were prepared via layer-by-layer casting [177]. The bilayered films showed a keratinocyte growth far superior in comparison with pristine poly(globalide), demonstrating the high potential of these materials in skin tissue engineering.

Introducing RGD peptide to improve the cell-adhesive and proliferative characteristics of poly(GL) was performed by Heise and coll. [178]. ES mats were cross-linked by $HS(CH_2)_5SH$, functionalized by $^tBuOC(O)NH(CH_2)_2SH$ and, after deprotection, coupled with RGD peptide via 1-ethyl-3-(3-dimethylaminopropyl)carbodiimide and N-hydroxysuccinimide (EDC/NHS) chemistry (Figure 13). RGD-functionalized ES material showed a similar tensile strength as compared with non-functionalized cross-linked fibers but a higher elasticity. An in vitro test revealed the increased adhesion and proliferation of human mesenchymal stem cells.

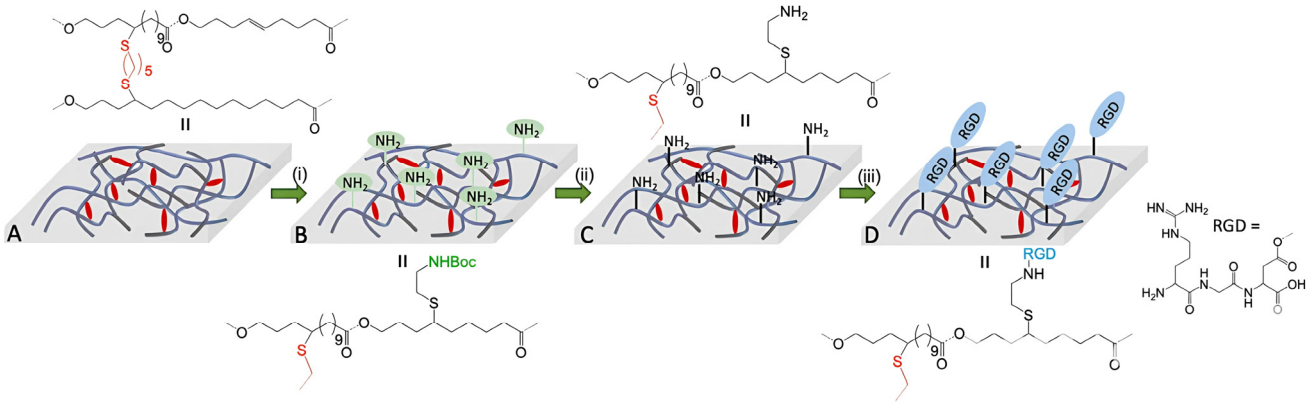

Figure 13. Reaction steps to produce RGD-functional electrospun fibers from crosslinked poly(globalide): (**A**) dithiol crosslinked PGL; (**B**) functionalization of crosslinked fibers with 2-(Boc-amino) ethanethiol (i); (**C**) Boc deprotection to produce amino functional fibers by TFA (ii); (**D**) coupling of RGD to amino functional fibers by EDC/NHS coupling (iii). Reprinted with permission from [178]. Copyright (2022) Wiley-VCH Verlag GmbH and Co.

Poly(LLA-*b*-GL-*b*-LLA) and poly(DLLA-*b*-GL-*b*-DLLA) with different ratios of lactate and GL fragments were used for the preparation of porous scaffolds for bone regeneration [150]. Chain-end functionalization using NHS, followed by binding with RGD peptide, increased the adhesion and proliferation of BM-MSCs and MC3T3-E1 cells.

3.3.3. Other Possible Applications of Unsaturated (Co)Polyesters

Hydrogenated copolymers of AL and (*Z*)-cyclooctene with methylene-to-ester ratios (M/E) of 15–223 had a T_m ranging from 132.1 °C (hydrogenated (*Z*)-cyclooctene homopolymer) to 91.5 °C (M/E = 15) [166] (Figure 14). Hydrogenated HL homopolymer had a T_m = 47.6 °C [168]. Introducing ester groups into the PE backbone, besides reducing the T_m

(and consequently molding temperature), may affect the biodegradability of the material. The results of these studies were used in further investigations of PE-like materials obtained from renewable feedstocks [179–181].

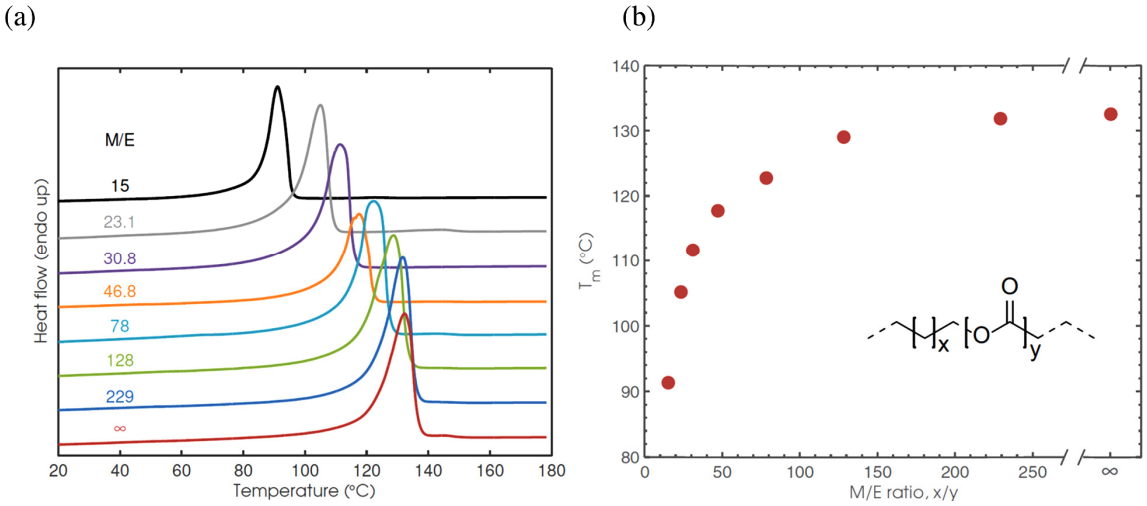

Figure 14. DSC thermograms of the saturated copolymers of AL and (Z)-cyclooctene (**a**) and a plot of the T_m as a function of M/E (**b**). Reprinted with permission from [166]. Copyright (2013) American Chemical Society.

Copolymers of PDL with $HO(CH_2)_6S$-functionalized AL, containing both short- and long-chain branches, have demonstrated elastomeric behavior [153].

4. Conclusions

The RCM of alkenyl alkenoates, including derivatives of renewable raw materials and derivatives of undec-10-enoic and dec-9-enoic acids, represent an efficient method for the synthesis of UMs. Obvious progress has been made in the development of highly selective RCM catalysts that provide the formation of UMs with a given ring size and position and configuration of C=C bonds. Recent studies on the optimization of the synthesis of NHC Ru complexes (G-II, HG-II and their analogs) with the use of mechanochemical methods [81] improve the availability of the Ru catalysts of RCM and therefore RCM products. It is possible to expect that scalable approaches to newly discovered highly active and selective catalysts (CAAC, dithiolate derivatives and others) will also be developed in the near future.

The structural variety of UMs potentially entails the differences in their chemical properties. The ROTEP of Ums, with the formation of unsaturated polyesters that are capable of post-modification, appears a promising approach to new materials; however, numerous MUs with different structures are still unexplored. One possible reason is the unavailability of synthetic MUs in preparative amounts, but quite recently Grela and coll. Proposed an efficient method for the preparation of UMs, based on the shift of oligomer/UM equilibria by the separation of the reaction product by vacuum distillation [31,99,111]. Further improvement of this method requires the rational design of the catalysts and the optimization of the processes.

Solutions to these problems will allow the use of UMs as a starting compound in the synthesis of new materials with a variety of potential advanced applications, including the development of composite scaffolds, polymeric vehicles for drug and gene delivery and others.

Author Contributions: Conceptualization, I.N. and P.I.; methodology, P.I.; software, P.I.; validation, A.A., A.V. and P.I.; formal analysis, P.I.; investigation, I.N., A.A., A.V. and P.I.; resources, I.N.; data curation, P.I.; writing—original draft preparation, A.A. and P.I.; writing—review and editing, I.N. and P.I.; visualization, P.I.; supervision, I.N. and P.I.; project administration, I.N. and P.I.; funding acquisition, P.I. All authors have read and agreed to the published version of the manuscript.

Funding: This research was funded by the Russian Science Foundation, grant number 24-43-20016.

Conflicts of Interest: The authors declare no conflicts of interest.

Abbreviations

The following abbreviations are used in this manuscript:

ADMET	Acyclic diene metathesis
AIBN	α,α′-Azoisobutyronitrile, 2,2′-azobis(2-methylpropionitrile)
AL	Ambrettolide (oxacycloheptadec-10-en-2-one)
BPO	Benzoyl peroxide
CAAC	Cyclic alkyl amino carbene
εCL	ε-Caprolactone
DCP	Dicumyl peroxide
DOSY	Diffusion ordered spectroscopy
EDC	1-ethyl-3-(3-dimethylaminopropyl)carbodiimide
ES	Electrospinning
FAMEs	Fatty acid methyl esters
G-I	First-generation Grubbs catalyst
G-II	Second-generation Grubbs catalyst
GC	Gas chromatography
GL	Globalide (oxacyclohexadec-12-en-2-one)
HG-II	Second-generation Hoveyda–Grubbs catalyst
HL	ω-6-Hexadecenlactone (oxacycloheptadec-7-en-2-one)
LA	Lactide
LLA	*L*-lactide
mCPBA	3-Chlorobenzoperoxoic acid
MO	Methyl oleate
MS	Mass spectrometry
NHC	N-heterocyclic carbene
NHS	*N*-hydroxysuccinimide
PDL	ω-Pentadecalactone (oxacyclohexadecan-2-one)
PE	Polyethylene
RA	Ricinoleic acid
RCM	Ring-closing metathesis
RL	Ricinoleic lactone ((*R*,*Z*)-13-hexyloxacyclotridec-10-en-2-one)
ROMP	Ring-opening metathesis polymerization
ROTEP	Ring-opening transesterification polymerization
$Sn(Oct)_2$	Tin(II) 2-ethylhexanoate
TFQ	2,3,5,6-Tetrafluorocyclohexa-2,5-diene-1,4-dione
TMC	1,3-Dioxan-2-one (trimethylene carbonate)
TON	Turnover number, the molar ratio of the converted reactant and the catalyst
T_c	Crystallization temperature
T_m	Melting temperature
UM	Unsaturated macrolactone

References

1. Engel, J.; Cordellier, A.; Huang, L.; Kara, S. Enzymatic Ring-Opening Polymerization of Lactones: Traditional Approaches and Alternative Strategies. *ChemCatChem* **2019**, *11*, 4983–4997. [CrossRef]
2. Wilson, J.A.; Ates, Z.; Pflughaupt, R.L.; Dove, A.P.; Heise, A. Polymers from macrolactones: From pheromones to functional materials. *Prog. Polym. Sci.* **2019**, *91*, 29–50. [CrossRef]
3. Parenty, A.; Moreau, X.; Campagne, J.-M. Macrolactonizations in the Total Synthesis of Natural Products. *Chem. Rev.* **2006**, *106*, 911–939. [CrossRef] [PubMed]
4. Parenty, A.; Moreau, X.; Neil, G.; Campagne, J.-M. Update 1 of: Macrolactonizations in the Total Synthesis of Natural Products. *Chem. Rev.* **2013**, *113*, PR1–PR40. [CrossRef] [PubMed]
5. Syed, N.; Singh, S.; Chaturvedi, S.; Nannaware, A.D.; Khare, S.K.; Rout, P.K. Production of lactones for flavoring and pharmacological purposes from unsaturated lipids: An industrial perspective. *Crit. Rev. Food Sci. Nutr.* **2023**, *63*, 10047–10078. [CrossRef]
6. Gradillas, A.; Pérez-Castells, J. Macrocyclization by Ring-Closing Metathesis in the Total Synthesis of Natural Products: Reaction Conditions and Limitations. *Angew. Chem. Int. Ed.* **2006**, *45*, 6086–6101. [CrossRef]
7. Sytniczuk, A.; Milewski, M.; Kajetanowicz, A.; Grela, K. Preparation of macrocyclic musks via olefin metathesis: Comparison with classical syntheses and recent advances. *Russ. Chem. Rev.* **2020**, *89*, 469–490. [CrossRef]
8. Ivchenko, P.V.; Nifant'ev, I.E. The Chemistry of Oleates and Related Compounds in 2020s. *Green Chem.* **2025**, *27*, 41–95. [CrossRef]
9. Monfette, S.; Fogg, D.E. Equilibrium Ring-Closing Metathesis. *Chem. Rev.* **2009**, *109*, 3783–3816. [CrossRef]
10. Dutra, A.C.; Mayer, D.A.; Silva, A.; Rebelatto, E.A.; Oliveira, J.V. High-pressure phase equilibrium data for the ternary and quaternary systems containing carbon dioxide, globalide, ε-caprolactone dichloromethane. *Fluid Phase Equilibria* **2023**, *570*, 113791. [CrossRef]
11. Kerschbaum, M. Über Lactone mit großen Ringen—die Träger des vegetabilischen Moschus-Duftes. *Ber. Dtsch. Chem. Ges.* **1927**, *60*, 902–909. [CrossRef]
12. Nee, T.Y.; Cartt, S.; Pollard, M.R. Seed coat components of Hibiscus abelmoschus. *Phytochemistry* **1986**, *25*, 2157–2161. [CrossRef]
13. Mookherjee, B.D.; Trenkle, R.W.; Patel, R.R. Synthesis of Δ^9-isoambrettolide and its isomers from 1,9-cyclohexadecadiene. *J. Org. Chem.* **1972**, *37*, 3846–3848. [CrossRef]
14. Villemin, D. Synthese de macrolides par methathese. *Tetrahedron Lett.* **1980**, *21*, 1715–1718. [CrossRef]
15. Rodefeld, L.; Tochtermann, W. A new approach to (9*Z*)-dodec-9-en-12-olide (Yuzu lactone) via phase transfer catalysis cyclization. *Tetrahedron* **1998**, *54*, 5893–5898. [CrossRef]
16. Lehmann, J.; Tochtermann, W. Synthesis and olfactory properties of regioisomeric alkynolides and (*Z*)-alkenolides. *Tetrahedron* **1999**, *55*, 2639–2658. [CrossRef]
17. Voss, G.; Gerlach, H. Orthocarbonsäure-ester mit 2,4,10-Trioxaadamantanstruktur als Carboxylschutzgruppe; Verwendung zur Synthese von substituierten Carbonsäuren mit Hilfe von Grignard-Reagenzien. *Helv. Chim. Acta* **1983**, *66*, 2294–2307. [CrossRef]
18. Fortunati, T.; D'Acunto, M.; Caruso, T.; Spinella, A. Chemoenzymatic preparation of musky macrolactones. *Tetrahedron* **2015**, *71*, 2357–2362. [CrossRef]
19. Guerrero-Morales, J.; Collins, S.K. Biocatalysis as a versatile tool for macrolactonization: Comparative evaluation of catalytic and stoichiometric approaches. *Green Chem.* **2024**, *26*, 10404–10410. [CrossRef]
20. Force, G.; Perfetto, A.; Mayer, R.J.; Ciofini, I.; Lebœuf, D. Macrolactonization Reactions Driven by a Pentafluorobenzoyl Group. *Angew. Chem. Int. Ed.* **2021**, *60*, 19843–19851. [CrossRef]
21. Shiina, I.; Hashizume, M. Synthesis of (9*E*)-isoambrettolide, a macrocyclic musk compound, using the effective lactonization promoted by symmetric benzoic anhydrides with basic catalysts. *Tetrahedron* **2006**, *62*, 7934–7939. [CrossRef]
22. Sanz-Navarro, S.; Garnes-Portolés, F.; López-Cruz, C.; Espinós-Ferri, E.; Corma, A.; Leyva-Pérez, A. Radical α–alkylation of ketones with unactivated alkenes under catalytic and sustainable industrial conditions. *Appl. Catal. A Gen.* **2021**, *613*, 118021. [CrossRef]
23. Meijer, J.; Gerritsen, R.; Fischer, B. Process for Preparing Unsaturated Lactones. U.S. Patent 8383834B2, 26 February 2013.
24. Wang, Y.; Ying, S.; Zhu, J.; Mao, S.; Wang, L.; He, L.; Hu, S.; Liu, Z.; Liu, C.; Ying, D. A Preparation Method of Harbanolide and Its Intermediates. Chin. Patent 118619914A, 22 November 2024.
25. Singh, S.; Sharma, S.; Sarma, S.J.; Brar, S.K. A comprehensive review of castor oil-derived renewable and sustainable industrial products. *Environ. Prog. Sustain. Energy* **2023**, *42*, e14008. [CrossRef]
26. Sytniczuk, A.; Kajetanowicz, A.; Grela, K. "Inverted" cyclic(alkyl)(amino)carbene ligands allow olefin metathesis with ethylene at parts-per-billion catalyst loading. *Chem Catal.* **2023**, *3*, 100713. [CrossRef]
27. Gawin, R.; Tracz, A.; Krajczy, P.; Kozakiewicz-Piekarz, A.; Martínez, J.P.; Trzaskowski, B. Inhibition of the Decomposition Pathways of Ruthenium Olefin Metathesis Catalysts: Development of Highly Efficient Catalysts for Ethenolysis. *J. Am. Chem. Soc.* **2023**, *145*, 25010–25021. [CrossRef]

28. Afanaseva, A.V.; Vinogradov, A.A.; Vinogradov, A.A.; Minyaev, M.E.; Pyatakov, D.A.; Tavtorkin, A.N.; Bagrov, V.V.; Ivchenko, P.V.; Nifant'ev, I.E. The Impact of Ligand Structure and Reaction Temperature on Ethenolysis of Fatty Acid Methyl Esters Catalyzed by Spirocyclic Alkyl Amino Carbene Ru Complexes. *ChemSusChem* **2025**, *18*, e202402190. [CrossRef]
29. Mol, J.C. Industrial applications of olefin metathesis. *J. Mol. Catal. A Chem.* **2004**, *213*, 39–45. [CrossRef]
30. Fürstner, A.; Langemann, K. Macrocycles by Ring-Closing Metathesis. *Synthesis* **1997**, *1997*, 792–803. [CrossRef]
31. Sytniczuk, A.; Dąbrowski, M.; Banach, Ł.; Urban, M.; Czarnocka-Śniadała, S.; Milewski, M.; Kajetanowicz, A.; Grela, K. At Long Last: Olefin Metathesis Macrocyclization at High Concentration. *J. Am. Chem. Soc.* **2018**, *140*, 8895–8901. [CrossRef]
32. Fürstner, A.; Langemann, K. Total Syntheses of (+)-Ricinelaidic Acid Lactone and of (−)-Gloeosporone Based on Transition-Metal-Catalyzed C−C Bond Formations. *J. Am. Chem. Soc.* **1997**, *119*, 9130–9136. [CrossRef]
33. Higman, C.S.; Nascimento, D.L.; Ireland, B.J.; Audörsch, S.; Bailey, G.A.; McDonald, R.; Fogg, D.E. Chelate-Assisted Ring-Closing Metathesis: A Strategy for Accelerating Macrocyclization at Ambient Temperatures. *J. Am. Chem. Soc.* **2018**, *140*, 1604–1607. [CrossRef] [PubMed]
34. Fürstner, A. Teaching Metathesis "Simple" Stereochemistry. *Science* **2013**, *341*, 1229713. [CrossRef] [PubMed]
35. Montgomery, T.P.; Johns, A.M.; Grubbs, R.H. Recent Advancements in Stereoselective Olefin Metathesis Using Ruthenium Catalysts. *Catalysts* **2017**, *7*, 87. [CrossRef]
36. Nascimento, D.L.; Foscato, M.; Occhipinti, G.; Jensen, V.R.; Fogg, D.E. Bimolecular Coupling in Olefin Metathesis: Correlating Structure and Decomposition for Leading and Emerging Ruthenium−Carbene Catalysts. *J. Am. Chem. Soc.* **2021**, *143*, 11072–11079. [CrossRef]
37. Jawiczuk, M.; Marczyk, A.; Trzaskowski, B. Decomposition of Ruthenium Olefin Metathesis Catalyst. *Catalysts* **2020**, *10*, 887. [CrossRef]
38. van Lierop, B.J.; Lummiss, J.A.M.; Fogg, D.E. Ring-Closing Metathesis. In *Olefin Metathesis: Theory and Practice*; Grela, K., Ed.; John Wiley & Sons, Inc.: Hoboken, NJ, USA, 2014; pp. 85–152. [CrossRef]
39. Nascimento, D.L.; Fogg, D.E. Origin of the Breakthrough Productivity of Ruthenium–Cyclic Alkyl Amino Carbene Catalysts in Olefin Metathesis. *J. Am. Chem. Soc.* **2019**, *141*, 19236–19240. [CrossRef]
40. Fürstner, A.; Thiel, O.R.; Ackermann, L.; Schanz, H.-J.; Nolan, S.P. Ruthenium Carbene Complexes with *N*,*N*′-Bis(mesityl)imidazol-2-ylidene Ligands: RCM Catalysts of Extended Scope. *J. Org. Chem.* **2000**, *65*, 2204–2207. [CrossRef]
41. Dumas, A.; Colombel-Rouen, S.; Curbet, I.; Forcher, G.; Tripoteau, F.; Caijo, F.; Queval, P.; Rouen, M.; Baslé, O.; Mauduit, M. Highly selective macrocyclic ring-closing metathesis of terminal olefins in non-chlorinated solvents at low dilution. *Catal. Sci. Technol.* **2019**, *9*, 436–443. [CrossRef]
42. Sytniczuk, A.; Leszczyn'ska, A.; Kajetanowicz, A.; Grela, K. Preparation of Musk-Smelling Macrocyclic Lactones from Biomass: Looking for the Optimal Substrate Combination. *ChemSusChem* **2018**, *11*, 3157–3166. [CrossRef]
43. Sytniczuk, A.; Forcher, G.; Grotjahn, D.B.; Grela, K. Sequential Alkene Isomerization and Ring-Closing Metathesis in Production of Macrocyclic Musks from Biomass. *Chem. Eur. J.* **2018**, *24*, 10403–10408. [CrossRef]
44. Jiang, A.J.; Zhao, Y.; Schrock, R.R.; Hoveyda, A.H. Highly *Z*-Selective Metathesis Homocoupling of Terminal Olefins. *J. Am. Chem. Soc.* **2009**, *131*, 16630–16631. [CrossRef] [PubMed]
45. Yu, M.; Wang, C.; Kyle, A.F.; Jakubec, P.; Dixon, D.J.; Schrock, R.R.; Hoveyda, A.H. Synthesis of macrocyclic natural products by catalyst-controlled stereoselective ring-closing metathesis. *Nature* **2011**, *479*, 88–93. [CrossRef] [PubMed]
46. Wang, C.; Yu, M.; Kyle, A.F.; Jakubec, P.; Dixon, D.J.; Schrock, R.R.; Hoveyda, A.H. Efficient and Selective Formation of Macrocyclic Disubstituted Z Alkenes by Ring-Closing Metathesis (RCM) Reactions Catalyzed by Mo- or W-Based Monoaryloxide Pyrrolide (MAP) Complexes: Applications to Total Syntheses of Epilachnene, Yuzu Lactone, Ambrettolide, Epothilone C, and Nakadomarin A. *Chem. Eur. J.* **2013**, *19*, 2726–2740. [CrossRef]
47. Rosebrugh, L.E.; Herbert, M.B.; Marx, V.M.; Keitz, B.K.; Grubbs, R.H. Highly Active Ruthenium Metathesis Catalysts Exhibiting Unprecedented Activity and *Z*-Selectivity. *J. Am. Chem. Soc.* **2013**, *135*, 1276–1279. [CrossRef]
48. Marx, V.M.; Herbert, M.B.; Keitz, B.K.; Grubbs, R.H. Stereoselective Access to *Z* and *E* Macrocycles by Ruthenium-Catalyzed *Z*-Selective Ring-Closing Metathesis and Ethenolysis. *J. Am. Chem. Soc.* **2013**, *135*, 94–97. [CrossRef]
49. Conrad, J.C.; Eelman, M.D.; Duarte Silva, J.A.; Monfette, S.; Parnas, H.H.; Snelgrove, J.L.; Fogg, D.E. Oligomers as Intermediates in Ring-Closing Metathesis. *J. Am. Chem. Soc.* **2007**, *129*, 1024–1025. [CrossRef] [PubMed]
50. Fürstner, A.; Langemann, K. Conformationally Unbiased Macrocyclization Reactions by Ring Closing Metathesis. *J. Org. Chem.* **1996**, *61*, 3942–3943. [CrossRef]
51. Litinas, K.E.; Salteris, B.E. Unsaturated macrocyclic lactone synthesis via catalytic ring-closing metathesis. *J. Chem. Soc. Perkin Trans. I* **1997**, 2869–2872. [CrossRef]
52. Goldring, W.P.D.; Hodder, A.S.; Weiler, L. Synthesis of macrocyclic lactams and lactones via ring-closing olefin metathesis. *Tetrahedron Lett.* **1998**, *39*, 4955–4958. [CrossRef]
53. Allinger, N.L.; Yuh, Y.H.; Lii, J.H. Molecular mechanics. The MM3 force field for hydrocarbons. 1. *J. Am. Chem. Soc.* **1989**, *111*, 8551–8566. [CrossRef]

54. Ackermann, L.; Fürstner, A.; Weskamp, T.; Kohl, F.J.; Herrmann, W.A. Ruthenium carbene complexes with imidazolin-2-ylidene ligands allow the formation of tetrasubstituted cycloalkenes by RCM. *Tetrahedron Lett.* **1999**, *40*, 4787–4790. [CrossRef]
55. Lee, C.W.; Grubbs, R.H. Stereoselectivity of Macrocyclic Ring-Closing Olefin Metathesis. *Org. Lett.* **2000**, *2*, 2145–2147. [CrossRef] [PubMed]
56. Fürstner, A.; Ackermann, L.; Beck, K.; Hori, H.; Koch, D.; Langemann, K.; Liebl, M.; Six, C.; Leitner, W. Olefin Metathesis in Supercritical Carbon Dioxide. *J. Am. Chem. Soc.* **2001**, *123*, 9000–9006. [CrossRef] [PubMed]
57. Hon, Y.-S.; Wong, Y.-C.; Chang, C.-P.; Hsieh, C.-H. Tishchenko reactions of aldehydes promoted by diisobutylaluminum hydride and its application to the macrocyclic lactone formation. *Tetrahedron* **2007**, *63*, 11325–11340. [CrossRef]
58. Ekeli, J.B.; Foscato, M.; Blanco, C.O.; Occhipinti, G.; Fogg, D.E.; Jensen, V.R. Enabling Automation of de Novo Catalyst Design: An Experimentally Validated, Multifactor Design Metric for Olefin Metathesis. *ACS Catal.* **2024**, *14*, 16731–16747. [CrossRef]
59. Gawin, R.; Tracz, A.; Chwalba, M.; Kozakiewicz, A.; Trzaskowski, B.; Skowerski, K. Cyclic Alkyl Amino Ruthenium Complexes—Efficient Catalysts for Macrocyclization and Acrylonitrile Cross Metathesis. *ACS Catal.* **2017**, *7*, 5443–5449. [CrossRef]
60. Ablialimov, O.; Kędziorek, M.; Malińska, M.; Woźniak, K.; Grela, K. Synthesis, Structure, and Catalytic Activity of New Ruthenium(II) Indenylidene Complexes Bearing Unsymmetrical N-Heterocyclic Carbenes. *Organometallics* **2014**, *33*, 2160–2171. [CrossRef]
61. Kadyrov, R. Low Catalyst Loading in Ring-Closing Metathesis Reactions. *Chem. Eur. J.* **2013**, *19*, 1002–1012. [CrossRef]
62. Blanco, C.O.; Sims, J.; Nascimento, D.L.; Goudreault, A.Y.; Steinmann, S.N.; Michel, C.; Fogg, D.E. The Impact of Water on Ru-Catalyzed Olefin Metathesis: Potent Deactivating Effects Even at Low Water Concentrations. *ACS Catal.* **2021**, *11*, 893–899. [CrossRef]
63. Tracz, A.; Matczak, M.; Urbaniak, K.; Skowerski, K. Nitro-Grela-type complexes containing iodides—robust and selective catalysts for olefin metathesis under challenging conditions. *Beilstein J. Org. Chem.* **2015**, *11*, 1823–1832. [CrossRef]
64. Nascimento, D.L.; Gawin, A.; Gawin, R.; Guńka, P.A.; Zachara, J.; Skowerski, K.; Fogg, D.E. Integrating Activity with Accessibility in Olefin Metathesis: An Unprecedentedly Reactive Ruthenium-Indenylidene Catalyst. *J. Am. Chem. Soc.* **2019**, *141*, 10626–10631. [CrossRef]
65. Del Vecchio, A.; Talcik, J.; Colombel-Rouen, S.; Lorkowski, J.; Serrato, M.R.; Roisnel, T.; Vanthuyne, N.; Bertrand, G.; Jazzar, R.; Mauduit, M. Highly Robust and Efficient Blechert-Type Cyclic(alkyl)(amino)carbene Ruthenium Complexes for Olefin Metathesis. *ACS Catal.* **2023**, *13*, 6195–6202. [CrossRef]
66. Gawin, R.; Kozakiewicz, A.; Guńka, P.A.; Dąbrowski, P.; Skowerski, K. Bis(Cyclic Alkyl Amino Carbene) Ruthenium Complexes: A Versatile, Highly Efficient Tool for Olefin Metathesis. *Angew. Chem. Int. Ed.* **2017**, *56*, 981–986. [CrossRef] [PubMed]
67. Milewski, M.; Kajetanowicz, A.; Grela, K. Improved preparation of an olefin metathesis catalyst bearing quaternary ammonium tag (FixCat) and its use in ethenolysis and macrocyclization reactions after immobilization on metal-organic framework (MOF). *ARKIVOC Online J. Org. Chem.* **2021**, *2021*, 73–84. [CrossRef]
68. Blanco, C.O.; Nascimento, D.L.; Fogg, D.E. Routes to High-Performing Ruthenium–Iodide Catalysts for Olefin Metathesis: Ligand Lability Is Key to Efficient Halide Exchange. *Organometallics* **2021**, *40*, 1811–1816. [CrossRef] [PubMed]
69. Pederson, R.L.; Johns, A.M. Reactions of Olefin Derivatives in the Presence of Methathesis Catalysts. U.S. Patent 11161104B2, 2 November 2021.
70. Monfette, S.; Eyholzer, M.; Roberge, D.M.; Fogg, D.E. Getting Ring-Closing Metathesis off the Bench: Reaction-Reactor Matching Transforms Metathesis Efficiency in the Assembly of Large Rings. *Chem. Eur. J.* **2010**, *16*, 11720–11725. [CrossRef]
71. Morvan, J.; McBride, T.; Curbet, I.; Colombel-Rouen, S.; Roisnel, T.; Crévisy, C.; Browne, D.L.; Mauduit, M. Continuous Flow *Z*-Stereoselective Olefin Metathesis: Development and Applications in the Synthesis of Pheromones and Macrocyclic Odorant Molecules. *Angew. Chem. Int. Ed.* **2021**, *60*, 19685–19690. [CrossRef]
72. Phatake, R.S.; Nechmad, N.B.; Reany, O.; Lemcoff, N.G. Highly Substrate-Selective Macrocyclic Ring Closing Metathesis. *Adv. Synth. Catal.* **2022**, *364*, 1465–1472. [CrossRef]
73. Monfette, S.; Crane, A.K.; Duarte Silva, J.A.; Facey, G.A.; dos Santos, E.N.; Araujo, M.H.; Fogg, D.E. Monitoring ring-closing metathesis: Limitations on the utility of ^{1}H NMR analysis. *Inorg. Chim. Acta* **2010**, *363*, 481–486. [CrossRef]
74. Hagiwara, H.; Nakamura, T.; Okunaka, N.; Hoshi, T.; Suzuki, T. Catalytic Performance of Ruthenium-Supported Ionic-Liquid Catalysts in Sustainable Synthesis of Macrocyclic Lactones. *Helv. Chim. Acta* **2010**, *93*, 175–182. [CrossRef]
75. Morin, É.; Sosoe, J.; Raymond, M.; Amorelli, B.; Boden, R.M.; Collins, S.K. Synthesis of a Renewable Macrocyclic Musk: Evaluation of Batch, Microwave, and Continuous Flow Strategies. *Org. Process Res. Dev.* **2019**, *23*, 283–287. [CrossRef]
76. Rana, R.; Shreya; Upadhyay, R.; Maurya, S.K. Synthesis of Macrocyclic Lactones and Dilactones Using Olive Oil. *ACS Omega* **2021**, *6*, 25381–25388. [CrossRef] [PubMed]
77. Yelchuri, V.; Azmeera, T.; Karuna, M.S.L. Synthesis of lactones from fatty acids by ring-closing metathesis and their biological evaluation. *Eur. J. Chem.* **2023**, *14*, 273–279. [CrossRef]
78. Zhang, H.; Yu, E.C.; Torker, S.; Schrock, R.R.; Hoveyda, A.H. Preparation of Macrocyclic Z-Enoates and (*E*,*Z*)-or (*Z*,*E*)-Dienoates through Catalytic Stereoselective Ring-Closing Metathesis. *J. Am. Chem. Soc.* **2014**, *136*, 16493–16496. [CrossRef] [PubMed]

79. Menke, M.; Peram, P.S.; Starnberger, I.; Hödl, W.; Jongsma, G.F.M.; Blackburn, D.C.; Rödel, M.-O.; Vences, M.; Schulz, S. Identification, synthesis and mass spectrometry of a macrolide from the African reed frog *Hyperolius cinnamomeoventris*. *Beilstein J. Org. Chem.* **2016**, *12*, 2731–2738. [CrossRef]
80. Skowerski, K.; Białecki, J.; Tracz, A.; Olszewski, T.K. An attempt to provide an environmentally friendly solvent selection guide for olefin metathesis. *Green Chem.* **2014**, *16*, 1125–1130. [CrossRef]
81. Mukherjee, N.; Marczyk, A.; Szczepaniak, G.; Sytniczuk, A.; Kajetanowicz, A.; Grela, K. A Gentler Touch: Synthesis of Modern Ruthenium Olefin Metathesis Catalysts Sustained by Mechanical Force. *ChemCatChem* **2019**, *11*, 5362–5369. [CrossRef]
82. Grela, K.; Gzarnocka-Gniadla, S.; Gytniczuk, A.; Milewski, M.; Urban, M.; Banach, L.; Dabrowski, M. Production Method of Cyclic Compounds by Olefin Metathesis Reaction and Use of Ruthenium Catalysts in Production of Cyclic Olefines by Olefin Metathesis Reaction. U.S. Patent Application 20200140470A1, 7 May 2020.
83. Grzesiński, Ł.; Milewski, M.; Nadirova, M.; Kajetanowicz, A.; Grela, K. Unexpected Latency of *Z*-Stereoretentive Ruthenium Olefin Metathesis Catalysts Bearing Unsymmetrical *N*-heterocyclic Carbene or Cyclic(alkyl)(amino)carbene Ligands. *Organometallics* **2023**, *42*, 2453–2459. [CrossRef]
84. Ahmed, T.S.; Grubbs, R.H. A Highly Efficient Synthesis of *Z*-Macrocycles Using Stereoretentive, Ruthenium-Based Metathesis Catalysts. *Angew. Chem. Int. Ed.* **2017**, *56*, 11213–11216. [CrossRef]
85. Ahmed, T.S.; Montgomery, T.P.; Grubbs, R.H. Using stereoretention for the synthesis of *E*-macrocycles with ruthenium-based olefin metathesis catalysts. *Chem. Sci.* **2018**, *9*, 3580–3583. [CrossRef]
86. Xu, C.; Shen, X.; Hoveyda, A.H. In Situ Methylene Capping: A General Strategy for Efficient Stereoretentive Catalytic Olefin Metathesis. The Concept, Methodological Implications, and Applications to Synthesis of Biologically Active Compounds. *J. Am. Chem. Soc.* **2017**, *139*, 10919–10928. [CrossRef] [PubMed]
87. Illuminati, G.; Mandolini, L. Ring closure reactions of bifunctional chain molecules. *Acc. Chem. Res.* **1981**, *14*, 95–102. [CrossRef]
88. Doss, R.P.; Gould, S.J.; Johnson, K.J.R.; Flath, R.A.; Kohnert, R.L. (*Z*)-oxacyclotridec-10-en-2-one, an alfalfa weevil feeding deterrent from Medicago rugosa. *Phytochemistry* **1989**, *28*, 3311–3315. [CrossRef]
89. Breen, C.P.; Parrish, C.; Shangguan, N.; Majumdar, S.; Murnen, H.; Jamison, T.F.; Bio, M.M. A Scalable Membrane Pervaporation Approach for Continuous Flow Olefin Metathesis. *Org. Process Res. Dev.* **2020**, *24*, 2298–2303. [CrossRef]
90. Teo, P.; Grubbs, R.H. Facile Synthesis of Effcient and Selective Ruthenium Olefin Metathesis Catalysts with Sulfonate and Phosphate Ligands. *Organometallics* **2010**, *29*, 6045–6050. [CrossRef]
91. Endo, K.; Grubbs, R.H. Chelated Ruthenium Catalysts for *Z*-Selective Olefin Metathesis. *J. Am. Chem. Soc.* **2011**, *133*, 8525–8527. [CrossRef]
92. Keitz, B.K.; Endo, K.; Patel, P.R.; Herbert, M.B.; Grubbs, R.H. Improved Ruthenium Catalysts for *Z*-Selective Olefin Metathesis. *J. Am. Chem. Soc.* **2012**, *134*, 693–699. [CrossRef] [PubMed]
93. Khan, R.K.M.; Torker, S.; Hoveyda, A.H. Readily Accessible and Easily Modifiable Ru-Based Catalysts for Efficient and *Z*-Selective Ring-Opening Metathesis Polymerization and Ring-Opening/Cross-Metathesis. *J. Am. Chem. Soc.* **2013**, *135*, 10258–10261. [CrossRef]
94. Ahmed, T.S.; Grubbs, R.H. Highly Efficient Synthesis of Z-Macrocycles Using Stereoretentive, Ruthenium-Based Metathesis Catalysts. U.S. Patent 11053209B2, 6 July 2021. Available online: https://patents.google.com/patent/US11053209B2 (accessed on 6 April 2025).
95. Fürstner, A.; Guth, O.; Rumbo, A.; Seidel, G. Ring Closing Alkyne Metathesis. Comparative Investigation of Two Different Catalyst Systems and Application to the Stereoselective Synthesis of Olfactory Lactones, Azamacrolides, and the Macrocyclic Perimeter of the Marine Alkaloid Nakadomarin A. *J. Am. Chem. Soc.* **1999**, *121*, 11108–11113. [CrossRef]
96. Chołuj, A.; Krzesiński, P.; Ruszczyńska, A.; Bulska, E.; Kajetanowicz, A.; Grela, K. Noncovalent Immobilization of Cationic Ruthenium Complex in a Metal–Organic Framework by Ion Exchange Leading to a Heterogeneous Olefin Metathesis Catalyst for Use in Green Solvents. *Organometallics* **2019**, *38*, 3397–3405. [CrossRef]
97. Clavier, H.; Grela, K.; Kirschning, A.; Mauduit, M.; Nolan, S.P. Sustainable Concepts in Olefin Metathesis. *Angew. Chem. Int. Ed.* **2007**, *46*, 6786–6801. [CrossRef] [PubMed]
98. Kamau, S.D.; Hodge, P.; Hall, A.J.; Dad, S.; Ben-Haida, A. Cyclo-depolymerization of olefin-containing polymers to give macrocyclic oligomers by metathesis and the entropically-driven ROMP of the olefin-containing macrocyclic esters. *Polymer* **2007**, *48*, 6808–6822. [CrossRef]
99. Grzesiński, Ł.; Nadirova, M.; Guschlbauer, J.; Brotons-Rufes, A.; Poater, A.; Kajetanowicz, A.; Grela, K. Preserving precise choreography of bonds in *Z*-stereoretentive olefin metathesis by using quinoxaline-2,3-dithiolate ligand. *Nat. Commun.* **2024**, *15*, 8981. [CrossRef]
100. Jee, J.-E.; Cheong, J.L.; Lim, J.; Chen, C.; Hong, S.H.; Lee, S.S. Highly Selective Macrocycle Formations by Metathesis Catalysts Fixated in Nanopores. *J. Org. Chem.* **2013**, *78*, 3048–3056. [CrossRef] [PubMed]
101. Lim, J.; Lee, S.S.; Ying, J.Y. Mesoporous silica-supported catalysts for metathesis: Application to a circulating flow reactor. *Chem. Commun.* **2010**, *46*, 806–808. [CrossRef]

102. Ziegler, F.; Teske, J.; Elser, I.; Dyballa, M.; Frey, W.; Kraus, H.; Hansen, N.; Rybka, J.; Tallarek, U.; Buchmeiser, M.R. Olefin Metathesis in Confined Geometries: A Biomimetic Approach toward Selective Macrocyclization. *J. Am. Chem. Soc.* **2019**, *141*, 19014–19022. [CrossRef]
103. Tallarek, U.; Hochstrasser, J.; Ziegler, F.; Huang, X.; Kübel, C.; Buchmeiser, M.R. Olefin Ring-closing Metathesis under Spatial Confinement: Morphology−Transport Relationships. *ChemCatChem* **2021**, *13*, 281–292. [CrossRef]
104. Ziegler, F.; Roider, T.; Pyschik, M.; Haas, C.P.; Wang, D.; Tallarek, U.; Buchmeiser, M.R. Olefin Ring-closing Metathesis under Spatial Confinement and Continuous Flow. *ChemCatChem* **2021**, *13*, 2234–2241. [CrossRef]
105. Emmerling, S.T.; Ziegler, F.; Fischer, F.R.; Schoch, R.; Bauer, M.; Plietker, B.; Buchmeiser, M.R.; Lotsch, B.V. Olefin Metathesis in Confinement: Towards Covalent Organic Framework Scaffolds for Increased Macrocyclization Selectivity. *Chem. Eur. J.* **2022**, *28*, e202104108. [CrossRef]
106. Tsuji, J.; Hashiguchi, S. Metathesis reactions of unsaturated esters catalyzed by homogenous tungsten complexes. Syntheses of civetone and macrolides. *J. Organomet. Chem.* **1981**, *218*, 69–80. [CrossRef]
107. Schrock, R.R.; Hoveyda, A.H. Molybdenum and Tungsten Imido Alkylidene Complexes as Efficient Olefin-Metathesis Catalysts. *Angew. Chem. Int. Ed.* **2003**, *42*, 4592–4633. [CrossRef] [PubMed]
108. Mu, Y.; Hartrampf, F.W.W.; Yu, E.C.; Lounsbury, K.E.; Schrock, R.R.; Romiti, F.; Hoveyda, A.H. *E*- and *Z*-trisubstituted macrocyclic alkenes for natural product synthesis and skeletal editing. *Nat. Chem.* **2022**, *14*, 640–649. [CrossRef]
109. Shen, X.; Nguyen, T.T.; Koh, M.J.; Xu, D.; Speed, A.W.H.; Schrock, R.R.; Hoveyda, A.H. Kinetically *E*-selective macrocyclic ring-closing metathesis. *Nature* **2017**, *541*, 380–385. [CrossRef]
110. Ziegler, F.; Kraus, H.; Benedikter, M.J.; Wang, D.; Bruckner, J.R.; Nowakowski, M.; Weißer, K.; Solodenko, H.; Schmitz, G.; Bauer, M.; et al. Confinement Effects for Efficient Macrocyclization Reactions with Supported Cationic Molybdenum Imido Alkylidene *N*-Heterocyclic Carbene Complexes. *ACS Catal.* **2021**, *11*, 11570–11578. [CrossRef]
111. Sytniczuk, A.; Milewski, M.; Dąbrowski, M.; Grela, K.; Kajetanowicz, A. Schrock molybdenum alkylidene catalyst enables selective formation of macrocyclic unsaturated lactones by ring-closing metathesis at high-concentration. *Green Chem.* **2023**, *25*, 2299–2304. [CrossRef]
112. Worch, J.C.; Dove, A.P. 100th Anniversary of Macromolecular Science Viewpoint: Toward Catalytic Chemical Recycling of Waste (and Future) Plastics. *ACS Macro Lett.* **2020**, *9*, 1494–1506. [CrossRef]
113. Chen, X.; Wang, Y.; Zhang, L. Recent Progress in the Chemical Upcycling of Plastic Wastes. *ChemSusChem* **2021**, *14*, 4137–4151. [CrossRef] [PubMed]
114. Payne, J.; Jones, M.D. The Chemical Recycling of Polyesters for a Circular Plastics Economy: Challenges and Emerging Opportunities. *ChemSusChem* **2021**, *14*, 4041–4070. [CrossRef]
115. Zheng, J.; Arifuzzaman, M.d.; Tang, X.; Chen, X.C.; Saito, T. Recent development of end-of-life strategies for plastic in industry and academia: Bridging their gap for future deployment. *Mater. Horiz.* **2023**, *10*, 1608–1624. [CrossRef]
116. Schade, A.; Melzer, M.; Zimmermann, S.; Schwarz, T.; Stoewe, K.; Kuhn, H. Plastic Waste Recycling—A Chemical Recycling Perspective. *ACS Sustain. Chem. Eng.* **2024**, *12*, 12270–12288. [CrossRef]
117. Sathe, D.; Yoon, S.; Wang, Z.; Chen, H.; Wang, J. Deconstruction of Polymers through Olefin Metathesis. *Chem. Rev.* **2024**, *124*, 7007–7044. [CrossRef] [PubMed]
118. Garnes-Portolés, F.; Leyva-Pérez, A. Macrocyclization Reactions at High Concentration (≥0.2 M): The Role of Catalysis. *ACS Catal.* **2023**, *13*, 9415–9426. [CrossRef]
119. Foster, J.C.; Dishner, I.T.; Damron, J.T.; Kertesz, V.; Popovs, I.; Saito, T. Toward Efficient Entropic Recycling by Mastering Ring–Chain Kinetics. *Macromolecules* **2025**, *58*, 2694–2700. [CrossRef]
120. Davey, P.N. Preparation of Macrocyclic Lactones. U.S. Patent 10633359B2, 28 April 2020.
121. Gallin, C.F.; Lee, W.-W.; Byers, J.A. A Simple, Selective, and General Catalyst for Ring Closing Depolymerization of Polyesters and Polycarbonates for Chemical Recycling. *Angew. Chem. Int. Ed.* **2023**, *62*, e202303762. [CrossRef]
122. Anastas, P.; Eghbali, N. Green Chemistry: Principles and Practice. *Chem. Soc. Rev.* **2010**, *39*, 301–312. [CrossRef]
123. Younes, M.; Aquilina, G.; Castle, L.; Engel, K.-H.; Fowler, P.; Fürst, P.; Gürtler, R.; Gundert-Remy, U.; Husøy, T.; Mennes, W.; et al. Re-evaluation of name of hydrogenated poly-1-decene (E 907) as food additive. *EFSA J.* **2020**, *18*, e06034. [CrossRef]
124. Lecomte, P.; Jérôme, C. Recent Developments in Ring-Opening Polymerization of Lactones. *Adv. Polym. Sci.* **2012**, *245*, 173–217. [CrossRef]
125. Li, Z.; Shen, Y.; Li, Z. Ring-Opening Polymerization of Lactones to Prepare Closed-Loop Recyclable Polyesters. *Macromolecules* **2024**, *57*, 1919–1940. [CrossRef]
126. Hodge, P. Entropically Driven Ring-Opening Polymerization of Strainless Organic Macrocycles. *Chem. Rev.* **2014**, *114*, 2278–2312. [CrossRef]
127. Namekawa, S.; Suda, S.; Uyama, H.; Kobayashi, S. Lipase-catalyzed ring-opening polymerization of lactones to polyesters and its mechanistic aspects. *Int. J. Biol. Macromol.* **1999**, *25*, 145–151. [CrossRef]

128. Wang, K.; Li, C.; Man, L.; Zhang, M.; Jia, Y.-G.; Zhu, X.X. Lipase-catalyzed ring-opening polymerization of natural compound-based cyclic monomers. *Chem. Commun.* **2023**, *59*, 9182–9194. [CrossRef] [PubMed]
129. Van der Meulen, I.; de Geus, M.; Antheunis, H.; Deumens, R.; Joosten, E.A.J.; Koning, C.E.; Heise, A. Polymers from Functional Macrolactones as Potential Biomaterials: Enzymatic Ring Opening Polymerization, Biodegradation, and Biocompatibility. *Biomacromolecules* **2008**, *9*, 3404–3410. [CrossRef]
130. Van Der Meulen, I.; Deumens, R.; Heise, A.; Koning, C.E.; Marcus, M.A.E.; Joosten, E.A.J. Process for Preparing Copolyesters, Copolyesters and Their Medical Uses. PCT Patent Application WO2012065745A1, 24 May 2012.
131. Van der Meulen, I.; Li, Y.; Deumens, R.; Joosten, E.A.J.; Koning, C.E.; Heise, A. Copolymers from Unsaturated Macrolactones: Toward the Design of Cross-Linked Biodegradable Polyesters. *Biomacromolecules* **2011**, *12*, 837–843. [CrossRef] [PubMed]
132. Claudino, M.; Van der Meulen, I.; Trey, S.; Jonsson, M.; Heise, A.; Johansson, M. Photoinduced thiol–ene crosslinking of globalide/ε-caprolactone copolymers: Curing performance and resulting thermoset properties. *J. Polym. Sci. A Polym. Chem.* **2012**, *50*, 16–24. [CrossRef]
133. Ates, Z.; Audouin, F.; Harrington, A.; O'Connor, B.; Heise, A. Functional Brush-Decorated Poly(globalide) Films by ARGET-ATRP for Bioconjugation. *Macromol. Biosci.* **2014**, *14*, 1600–1608. [CrossRef]
134. De Oliveira, F.C.S.; Olvera, D.; Sawkins, M.J.; Cryan, S.-A.; Kimmins, S.D.; da Silva, T.E.; Kelly, D.J.; Duffy, G.P.; Kearney, C.; Heise, A. Direct UV-Triggered Thiol–ene Cross-Linking of Electrospun Polyester Fibers from Unsaturated Poly(macrolactone)s and Their Drug Loading by Solvent Swelling. *Biomacromolecules* **2017**, *18*, 4292–4298. [CrossRef]
135. Chiaradia, V.; Polloni, A.E.; de Oliveira, D.; de Oliveira, J.V.; Araújo, P.H.H.; Sayer, C. Polyester nanoparticles from macrolactones via miniemulsion enzymatic ring-opening polymerization. *Coll. Polym. Sci.* **2018**, *296*, 861–869. [CrossRef]
136. Savin, C.L.; Peptu, C.; Kroneková, Z.; Sedlačík, M.; Mrlik, M.; Sasinková, V.; Peptu, C.A.; Popa, M.; Mosnáček, J. Polyglobalide-Based Porous Networks Containing Poly(ethylene glycol) Structures Prepared by Photoinitiated Thiol–Ene Coupling. *Biomacromolecules* **2018**, *19*, 3331–3342. [CrossRef]
137. Polloni, A.E.; Chiaradia, V.; Figura, E.M.; De Paoli, J.P.; de Oliveira, D.; de Oliveira, J.V.; de Araujo, P.H.H.; Sayer, C. Polyesters from Macrolactones Using Commercial Lipase NS 88011 and Novozym 435 as Biocatalysts. *Appl. Biochem. Biotechnol.* **2018**, *184*, 659–672. [CrossRef]
138. Chiaradia, V.; Hanay, S.B.; Kimmins, S.D.; de Oliveira, D.; Araújo, P.H.H.; Sayer, C.; Heise, A. Crosslinking of Electrospun Fibres from Unsaturated Polyesters by Bis-Triazolinediones (TAD). *Polymers* **2019**, *11*, 1808. [CrossRef]
139. Tinajero-Díaz, E.; de Ilarduya, A.M.; Cavanagh, B.; Heise, A.; Muñoz-Guerra, S. Poly(amino acid)-grafted polymacrolactones. Synthesis, self-assembling and ionic coupling properties. *React. Funct. Polym.* **2019**, *143*, 104316. [CrossRef]
140. Rowley, J.V.; Wall, P.; Yu, H.; Tronci, G.; Devine, D.A.; Vernon, J.J.; Thornton, P.D. Antimicrobial Dye-Conjugated Polyglobalide-Based Organogels. *ACS Appl. Polym. Mater.* **2020**, *2*, 2927–2933. [CrossRef]
141. Guindani, C.; Jaramillo, W.A.G.; Candiotto, G.; Rebelatto, E.A.; Tavares, F.W.; Pinto, J.C.; Ndiaye, P.M.; Nele, M. Synthesis of polyglobalide by enzymatic ring opening polymerization using pressurized fluids. *J. Supercrit. Fluids* **2022**, *186*, 105588. [CrossRef]
142. Guindani, C.; Dozoretz, P.; Veneral, J.G.; da Silva, D.M.; Araújo, P.H.H.; Ferreira, S.R.S.; de Oliveira, D. Enzymatic ring opening copolymerization of globalide and ε-caprolactone under supercritical conditions. *J. Supercrit. Fluids* **2017**, *128*, 404–411. [CrossRef]
143. Guindani, C.; Frey, M.-L.; Simon, J.; Koynov, K.; Schultze, J.; Ferreira, S.R.S.; Araújo, P.H.H.; de Oliveira, D.; Wurm, F.R.; Mailänder, V.; et al. Covalently Binding of Bovine Serum Albumin to Unsaturated Poly(Globalide-co-ε-Caprolactone) Nanoparticles by Thiol-Ene Reactions. *Macromol. Biosci.* **2019**, *19*, 1900145. [CrossRef]
144. Guindani, C.; Dozoretz, P.; Araújo, P.H.H.; Ferreira, S.R.S.; de Oliveira, D. N-acetylcysteine side-chain functionalization of poly(globalide-co-ε-caprolactone) through thiol-ene reaction. *Mater. Sci. Eng. C* **2019**, *94*, 477–483. [CrossRef]
145. Vaida, C.; Keul, H.; Moeller, M. Tailor-made polyesters based on pentadecalactone via enzymatic catalysis. *Green Chem.* **2011**, *13*, 889–899. [CrossRef]
146. Gupta, A.C.; Guindani, C.; Beltrame, J.M.; da Silva, A.; Mayer, D.A.; Rebelatto, E.A.; Oliveira, J.V. High-pressure phase equilibrium data for systems involving carbon dioxide, globalide, ε-caprolactone, poly(globalide-co-ε-caprolactone) and dichloromethane. *Fluid Phase Equilibria* **2023**, *576*, 113932. [CrossRef]
147. Santos, R.D.; Rebelatto, E.A.; Guindani, C.; Madalosso, H.B.; Scorsin, L.; Mayer, D.A.; Oliveira, J.V. Lipase-catalyzed synthesis of poly(ω-pentadecalactone-co-globalide) in supercritical carbon dioxide. *J. Supercrit. Fluids* **2025**, *215*, 106409. [CrossRef]
148. Cupaja, M.N.H.; Guindani, C.; Tavares, F.W.; Ndiaye, P.M. Effect of pressure and monomer concentration on ring-opening enzymatic polymerization of globalide in pressurized propane. *J. Supercrit. Fluids* **2025**, *220*, 106508. [CrossRef]
149. Martínez-Cutillas, A.; León, S.; Oh, S.; Martínez de Ilarduya, A. Enzymatic recycling of polymacrolactones. *Polym. Chem.* **2022**, *13*, 1586–1595. [CrossRef]
150. Martínez Cutillas, A.; Sanz-Serrano, D.; Oh, S.; Ventura, F.; Martínez de Ilarduya, A. Synthesis of Functionalized Triblock Copolyesters Derived from Lactic Acid and Macrolactones for Bone Tissue Regeneration. *Macromol. Biosci.* **2023**, *23*, 2300066. [CrossRef] [PubMed]

151. Pascual, A.; Leiza, J.R.; Mecerreyes, D. Acid catalyzed polymerization of macrolactones in bulk and aqueous miniemulsion: Ring opening vs. condensation. *Eur. Polym. J.* **2013**, *49*, 1601–1609. [CrossRef]
152. Pepels, M.P.F.; Souljé, P.; Peters, R.; Duchateau, R. Theoretical and Experimental Approach to Accurately Predict the Complex Molecular Weight Distribution in the Polymerization of Strainless Cyclic Esters. *Macromolecules* **2014**, *47*, 5542–5550. [CrossRef]
153. Pepels, M.P.F.; Koeken, R.A.C.; van der Linden, S.J.J.; Heise, A.; Duchateau, R. Mimicking (Linear) Low-Density Polyethylenes Using Modified Polymacrolactones. *Macromolecules* **2015**, *48*, 4779–4792. [CrossRef]
154. Fuoco, T.; Meduri, A.; Lamberti, M.; Venditto, V.; Pellecchia, C.; Pappalardo, D. Ring-opening polymerization of ω-6-hexadecenlactone by a salicylaldiminato aluminum complex: A route to semicrystalline and functional poly(ester)s. *Polym. Chem.* **2015**, *6*, 1727–1740. [CrossRef]
155. Sorrentino, A.; Gorrasi, G.; Bugatti, V.; Fuoco, T.; Pappalardo, D. Polyethylene-like macrolactone-based polyesters: Rheological, thermal and barrier properties. *Mater. Today Commun.* **2018**, *17*, 380–390. [CrossRef]
156. Naddeo, M.; D'Auria, I.; Viscusi, G.; Gorrasi, G.; Pellecchia, C.; Pappalardo, D. Tuning the thermal properties of poly(ethylene)-like poly(esters) by copolymerization of ε-caprolactone with macrolactones, in the presence of a pyridylamidozinc(II) complex. *J. Polym. Sci.* **2020**, *58*, 528–539. [CrossRef]
157. Slivniak, R.; Domb, A.J. Macrolactones and Polyesters from Ricinoleic Acid. *Biomacromolecules* **2005**, *6*, 1679–1688. [CrossRef]
158. Nakornkhet, C.; Kamavichanurat, S.; Joopor, W.; Hormnirun, P. Controlled ring-opening (co)polymerization of macrolactones: A pursuit for efficient aluminum-based catalysts. *Polym. Chem.* **2024**, *15*, 1660–1679. [CrossRef]
159. Ebata, H.; Toshima, K.; Matsumura, S. Lipase-Catalyzed Synthesis and Curing of High-Molecular-Weight Polyricinoleate. *Macromol. Biosci.* **2007**, *7*, 798–803. [CrossRef]
160. Yamamoto, A.; Nemoto, K.; Yoshida, M.; Tominaga, Y.; Imai, Y.; Ata, S.; Takenaka, Y.; Abe, H.; Sato, K. Improving thermal and mechanical properties of biomass-based polymers using structurally ordered polyesters from ricinoleic acid and 4-hydroxycinnamic acids. *RSC Adv.* **2020**, *10*, 36562–36570. [CrossRef] [PubMed]
161. Tonta, M.M.; Sezer, U.A.; Olmez, H.; Gurek, A.G.; Sezer, S. Cost-effective synthesis of polyricinoleate: Investigation of coating characteristics, in vitro degradation, and antibacterial activity. *J. Appl. Polym. Sci.* **2019**, *136*, 48172. [CrossRef]
162. Vadgama, R.N.; Odaneth, A.A.; Lali, A.M. New synthetic route for polyricinoleic acid with Tin(II) 2-ethylhexanoate. *Heliyon* **2019**, *5*, e01944. [CrossRef]
163. Wang, L.; Yuan, H.; Ma, X.; Li, Z.; Sun, H.; Zhang, X.; Huang, X.; Peng, Q.; Tan, Y. Synthesis of high molecular weight poly(ricinoleic acid) via direct solution polycondensation in hydrophobic ionic liquids. *RSC Sustain.* **2024**, *2*, 2541–2548. [CrossRef]
164. Gautrot, J.E.; Zhu, X.X. High molecular weight bile acid and ricinoleic acid-based copolyesters via entropy-driven ring-opening metathesis polymerisation. *Chem. Commun.* **2008**, 1674–1676. [CrossRef]
165. Ogawa, R.; Hillmyer, M.A. High molar mass poly(ricinoleic acid) via entropy-driven ring-opening metathesis polymerization. *Polym. Chem.* **2021**, *12*, 2253–2257. [CrossRef]
166. Pepels, M.P.F.; Hansen, M.R.; Goossens, H.; Duchateau, R. From Polyethylene to Polyester: Influence of Ester Groups on the Physical Properties. *Macromolecules* **2013**, *46*, 7668–7677. [CrossRef]
167. Martínez, A.; Zárate-Saldaña, D.; Vargas, J.; Santiago, A.A. Unsaturated Copolyesters from Macrolactone/Norbornene: Toward Reaction Kinetics of Metathesis Copolymerization Using Ruthenium Carbene Catalysts. *Int. J. Mol. Sci.* **2022**, *23*, 4521. [CrossRef]
168. Martínez, A.; Tlenkopatchev, M.A.; Gutiérrez, S. The Unsaturated Polyester Via Ring-Opening Metathesis Polymerization (ROMP) of ω-6-Hexadecenlactone. *Curr. Org. Synth.* **2018**, *15*, 566–571. [CrossRef]
169. Ates, Z.; Thornton, P.D.; Heise, A. Side-chain functionalisation of unsaturated polyesters from ring-opening polymerisation of macrolactones by thiol–ene click chemistry. *Polym. Chem.* **2011**, *2*, 309–312. [CrossRef]
170. Ates, Z.; Heise, A. Functional films from unsaturated poly(macrolactones) by thiol–ene cross-linking and functionalisation. *Polym. Chem.* **2014**, *5*, 2936–2941. [CrossRef]
171. Tinajero-Díaz, E.; de Ilarduya, A.M.; Muñoz-Guerra, S. Copolymacrolactones Grafted with l-Glutamic Acid: Synthesis, Structure, and Nanocarrier Properties. *Polymers* **2020**, *12*, 995. [CrossRef]
172. Tinajero-Díaz, E.; de Ilarduya, A.M.; Muñoz-Guerra, S. Block and Graft Copolymers Made of 16-Membered Macrolactones and l-Alanine: A Comparative Study. *Macromol. Chem. Phys.* **2019**, *220*, 1900214. [CrossRef]
173. Polloni, A.E.; Chiaradia, V.; do Amaral, R.J.F.C.; Kearney, C.; Gorey, B.; de Oliveira, D.; de Oliveira, J.V.; de Araújo, P.H.H.; Sayer, C.; Heise, A. Polyesters with main and side chain phosphoesters as structural motives for biocompatible electrospun fibres. *Polym. Chem.* **2020**, *11*, 2157–2165. [CrossRef]
174. Guindani, C.; Candiotto, G.; Araújo, P.H.H.; Ferreira, S.R.S.; de Oliveira, D.; Wurm, F.R.; Landfester, K. Controlling the biodegradation rates of poly(globalide-co-ε-caprolactone) copolymers by post polymerization modification. *Polym. Degrad. Stab.* **2020**, *179*, 109287. [CrossRef]
175. Beltrame, J.M.; Ribeiro, B.B.P.; Guindani, C.; Candiotto, G.; Felipe, K.B.; Lucas, R.; D'Agostini Zottis, A.; Isoppo, E.; Sayer, C.; de Araújo, P.H.H. Coating of SPIONs with a Cysteine-Decorated Copolyester: A Possible Novel Nanoplatform for Enzymatic Release. *Pharmaceutics* **2023**, *15*, 1000. [CrossRef]

176. Madalosso, H.B.; Guindani, C.; Maniglia, B.C.; de Araújo, P.H.H.; Sayer, C. Collagen-decorated electrospun scaffolds of unsaturated copolyesters for bone tissue regeneration. *J. Mater. Chem. B* **2024**, *12*, 3047–3062. [CrossRef]
177. Amaral, H.R.; Wilson, J.A.; do Amaral, R.J.F.C.; Pasçu, I.; de Oliveira, F.C.S.; Kearney, C.J.; Freitas, J.C.C.; Heise, A. Synthesis of bilayer films from regenerated cellulose nanofibers and poly(globalide) for skin tissue engineering applications. *Carbohydr. Polym.* **2021**, *252*, 117201. [CrossRef]
178. Sales de Oliveira, F.C.; Correa do Amaral, R.J.F.; Cardoso dos Santos, L.E.; Cummins, C.; Morris, M.M.; Kearney, C.J.; Heise, A. Versatility of unsaturated polyesters from electrospun macrolactones: RGD immobilization to increase cell attachment. *J. Biomed. Mater Res. A* **2022**, *110*, 257–265. [CrossRef]
179. Marxsen, S.F.; Häußler, M.; Mecking, S.; Alamo, R.G. Unlayered–Layered Crystal Transition in Recyclable Long-Spaced Aliphatic Polyesters. *ACS Appl. Polym. Mater.* **2021**, *3*, 5243–5256. [CrossRef]
180. Häußler, M.; Eck, M.; Rothauer, D.; Mecking, S. Closed-loop recycling of polyethylene-like materials. *Nature* **2021**, *590*, 423–427. [CrossRef] [PubMed]
181. Eck, M.; Mecking, S. Closed-Loop Recyclable and Nonpersistent Polyethylene-like Polyesters. *Acc. Chem. Res.* **2024**, *57*, 971–980. [CrossRef] [PubMed]